HUMAN DNA HELICASE B FUNCTIONS IN DNA DAMAGE RESPONSE AND HOMOLOGOUS RECOMBINATION

By

Hanjian Liu

Dissertation

Submitted to the Faculty of the

Graduate School of Vanderbilt University

in partial fulfillment of the requirements

for the degree of

DOCTOR OF PHILOSOPHY

in

Biological Sciences

December, 2007

Nashville, Tennessee

Approved:

Professor James Patton

Professor David Cortez

Professor Ellen Fanning

Professor Eugene Oltz

Professor Jennifer Pietenpol

ACKNOWLEDGEMENTS

I wish to express my gratitude to all those who gave me the possibility to complete this thesis. First, I would like to thank my advisor, Dr. Ellen Fanning, for her continuous support throughout my studies. Ellen was always there to listen and to give advice. She taught me how to ask questions and express my ideas. She showed me different ways to approach a research problem and the need to be persistent to accomplish any goal. I would also like to thank the rest of my thesis committee, Dr. James Patton, Dr. David Cortez, Dr. Eugene Oltz and Dr. Jennifer Pietenpol for their advice and encouragement. Their insightful comments and questions on my work greatly inspired me to improve the quality of my dissertation.

I could not have finished this dissertation without the love and support of my family members. I own a lot to my parents for their generous support to my graduate studies. My wife gave me her great love and encouragement for me to continue to proceed on my projects. I cannot express enough gratitude for their love and support.

I would like to thank both the past and present members of the lab who has been working together with me and also good friends of mine. I wish to acknowledge Dr. Peijun Yan for his supportive work and discussion on my projects. Thanks to Gulfem Guler for her explorations on ToBP1/HDHB and her generous supply of HDHB protein. Thanks to Dr. Haijiang Zhang and Kun Zhao for their supply of RPA protein. Thanks to Dr. Xiaorong Zhao for confocal microscopy. I would like to thank Haleh Kadivar, Nilesh Kashikar, Shi Meng and Amanda Hafer for their efforts on this project. Thanks to Dr. Jinming Gu for the supply of shRNA constructs. This work is also benefited from

discussions with Dr. Jeannie Gerhardt and Xiaohua Jiang.

I should also acknowledge our colleagues outside of our lab. I would like to thank Elisabeth Kremmer for the monoclonal HDHB antibodies, Dr. Walter Chazin for hRad51 construct, Dr. Mark Meuth for SW480/SN.3 cells. I appreciate our collaborations with the Vanderbilt flow cytometry facility. Without their efforts, my dissertation could not be finished.

This work was supported by grants from the NIH (GM52948 to EF and P30 CA68485 to the Vanderbilt-Ingram Cancer Center), HHMI Professors Program (52003905), and by Vanderbilt University.

TABLE OF CONTENTS

Page

ACKNOWLEDGEMENTS ii

LIST OF FIGURES vi

LIST OF ABBREVIATIONS viii

Chapter

I. INTRODUCTION 1

DNA Replication 1
Restart of Stalled Replication Forks 7
DNA Damage Signaling and Repair 9
DNA Damage Signaling and Checkpoints 10
DNA Repair 14
Helicases 18
Biochemical Activities of Helicases 21
Biological Functions of Helicases 23
Human DNA Helicase B 26

II. DNA DAMAGE-INDUCED RECRUITMENT OF HUMAN DNA HELICASE B TO CHROMATIN STIMULATES TOPBP1 FOCUS FORMATION 30

Introduction 30
Materials and Methods 32
Protein Purification 32
Production of Monoclonal Antibodies 33
Other Antibodies 33
Cell Culture, Synchronization and Flow Cytometry 34
Subcellular Fractionation 35
Radiation and Drug Treatment 36
ShRNA-directed Gene Silencing 37
Co-immunoprecipitation 38
Fluorescence Microscopy 38
CHK1 Phosphorylation 39
Results 40
HDHB Associates with Chromatin Throughout the Cell Cycle 40
Genotoxins Induce Accumulation of HDHB on Chromatin, Most Prominently in S Phase Cells 45

Soluble Nuclear HDHB Redistributes to Chromatin in Response to DNA Damage....47
Damage-induced Recruitment of HDHB to Chromatin does not Require Checkpoint Kinase Activity....50
The Chromatin-associated Fraction of HDHB Functions Together with RPA, Rad9, and TopBP1 in the Early Steps of the Intra-S Phase DNA Damage Response....52
DNA-damage Induced CHK1 phosphorylation is Impaired in HDHB-depleted cells....63
Discussion....65

III. HUMAN DNA HELICASE B PROMOTES HOMOLOGOUS RECOMBINATION BY STIMULATING 5'-3' HETERODUPLEX EXTENSTION....68
Introduction....68
Materials and Methods....69
Cell Culture and Plasmids....69
Clonogenic Survival Assay....70
Aphidicolin-induced Chromosome Breaks and Sister Chromatid Exchange Assay....70
In Vivo Recombination Assay....72
Flow Cytometry and Cell Sorting....73
Fluorescence Microscopy....73
DNA Substrates....73
Proteins....74
Strand Exchange Assay and Helicase Assay....77
Co-immunoprecipitation....78
Results....78
HDHB-depleted Cells are Sensitive to DNA Damaging Agents and Replication Fork Uncoupling....78
HDHB Facilitates Homologous Recombination....82
Delayed Formation of RPA Damage Foci after Ionizing Radiation of HDHB-depleted Cells....88
Physical Interaction of HDHB with Rad51....89
HDHB Stimulates Rad51-mediated 5'-3' Heteroduplex Extension....93
Discussion....99

IV. CONCLUSIONS AND FUTURE DIRECTIONS....107

Appendix

PHOSPHORYLATION OF HDHB AFTER DNA DAMAGE....112

REFERENCES....116

LIST OF FIGURES

Figure		Page
I-1.	Structure of pre-replicative complex	2
I-2.	Control of the initiation of DNA synthesis in budding yeast	5
I-3.	Restart of stalled replication forks with a lesion on the leading strand template	8
I-4.	Pathways of DNA damage response in mammalian cells	11
I-5.	The classification of helicases by their primary structures	20
I-6.	The polarity of helicases	22
II-1.	A small fraction of HDHB resides on chromatin	41
II-2.	Chromatin association of HDHB is independent of the cell cycle in unperturbed cells	42
II-3.	UV, camptothecin and hydroxyurea stimulate HDHB chromatin association	46
II-4.	Damage-induced accumulation of HDHB on chromatin varies in the cell cycle	48
II-5.	Soluble nuclear HDHB migrates to chromatin in response to UV irradiation	49
II-6.	Genotoxin–induced accumulation of HDHB on chromatin does not require checkpoint signaling	51
II-7.	Time course of HDHB, RPA, TopBP1, and Rad9 chromatin association in UV-treated S phase cells	54
II-8.	HDHB partially co-localizes with TopBP1 and Rad9 foci and interacts directly with TopBP1	55

II-9. Silencing of endogenous HDHB in human cells does not significantly perturb cell cycle distribution 57
II-10. HDHB silencing diminishes UV-induced TopBP1 focus formation 58
II-11. HDHB-depleted Cells show less CHK1 phosphorylation after DNA damage ... 64
III-1. Clonogenic survival assay with HDHB-depleted cells 80
III-2. Frequency of aphidicolin-induced chromosome damage is greater in HDHB-depleted cells 81
III-3. Sister chromatid exchange (SCE) in HCT116 cells 83
III-4. *In vivo* recombination assay 85
III-5. Ionizing radiation-induced Rad51, H2AX or RPA34 foci in HCT116 cells 90
III-6. Ionizing radiation-induced RPA34 foci in U2OS cells 91
III-7. Colocalization and interaction of HDHB with Rad51 92
III-8. hRad51-mediated strand exchange reaction 95
III-9. HDHB promotes the heteroduplex extension of hRad51-catalyzed strand exchange 97
III-10. Walker B mutant HDHB did not promote the heteroduplex extension 98
III-11. HDHB promotes heteroduplex extension but not joint molecule formation 100
III-12. T-antigen does not promote heteroduplex extension 101
III-13. A model for the function of HDHB in stimulating heteroduplex extension during homologous recombination 105
IV-1. DNA damage induces phosphorylation of HDHB 114

LIST OF ABBREVIATIONS

53BP1	p53 binding protein 1
9-1-1	Rad9-Rad1-Hus1
ACS	ARS consensus sequence
AP	abasic
APE	AP endonuclease
APH	aphidicolin
ARS	autonomously replicating sequences
A-T	ataxia telangiectasia
ATM	ataxia telangiectasia mutated
ATP	adenosine triphosphate
ATR	ATM and Rad3 related
ATRIP	ATR-interacting protein
BLM	Bloom’s syndrome helicase
BrdU	bromodeoxyuridine
BSA	bovine serum albumin
CDK	cyclin-dependent kinases
CHK1	checkpoint kinase 1
CHK2	checkpoint kinase 2
Chr	chromatin fraction
CPT	camptothecin
Cyto	cytosol

DMEM	Dulbecco-modified Eagle medium
DMSO	dimethyl sulfoxide
DNA	deoxyribonucleic acid
DNA-PK	DNA-dependent protein kinase
dsDNA	double-stranded DNA
DTT	dithiothreitol
EDTA	ethylenediamine tetraacetic acid
EGTA	ethylene glycol tetreaacetic acid
ExoI	exonuclease I
FBS	fetal bovine serum
GFP	green fluorescence protein
GST	glutathione-S-transferase
Gy	gray
HDHB	human DNA helicase B
HR	homologous recombination
hRad51	human Rad51
HU	hydroxyurea
i.p	intraperitoneally
IP	immunoprecipitation
IR	ionizing radiation
jm	joint molecules
MCM	minichromosome maintenance
MDC1	mediator of DNA damage checkpoint 1

MMR	mismatch repair
MNase	micrococcal nuclease
MRN	Mre11/Rad50/NBS1
Mut B	Walker B mutant HDHB
nc	nicked-circular DNA
NES	nuclear export signal
NHEJ	nonhomologous end-joining
NTP	nucleotide triphosphate
ORC	origin recognition complex
PAGE	polyacrylamide gel electrophoresis
PBS	phosphate-buffered saline
PCNA	proliferating cell nuclear antigen
PIKK	phosphoinositide 3-kinase-like kinase
PMSF	phenylmethylsulfonyl fluoride
pol-prim	polymerase α-primase
pre-RC	pre-replicative complex
PSLD	phospho-subcellular localization domain
RFC	replication factor C
RIPA	radioimmunoprecipitation assay
RNA	ribonucleic acid
RPA	replication protein A
s.c	subcutaneously
SCE	sister chromatid exchange

SDS	sodium dodecyl sulfate
shRNA	small hairpin RNA
siRNA	small interfering RNA
Sol Nu	soluble nuclear
SSA	single-strand annealing
SSB	single-stranded DNA binding protein
SSC	saline sodium citrate
ssDNA	single-stranded DNA
TAE	Tris-Acetate-EDTA
T-antigen	tumor antigen
TBE	Tris-Borate-EDTA
TopBP1	DNA topoisomerase II binding protein 1
UV	ultraviolet
WCE	whole cell extract
WRN	Werner’s syndrome helicase

CHAPTER I

INTRODUCTION

DNA Replication

The primary structure of DNA contains important genetic information that is transmitted from one generation of cells to the next by precisely replicated DNA molecules. Genomic DNA usually contains two strands. In the semi-conservative replication process, which was proposed by Watson and Crick (Watson and Crick, 1953) soon after the publication of their paper on the structure of DNA, each strand serves as a template for the synthesis of a new strand. Two new DNA molecules will result, each with one new strand and one old strand. The fundamental properties of the DNA replication process and the underlying mechanisms have proven to be essentially identical in all organisms. DNA replication usually begins at an origin and progresses bidirectionally. A new strand of DNA is always synthesized in the 5'-3' direction. One strand, the leading strand, is synthesized continuously. The other strand, the lagging strand, is synthesized discontinuously in the short pieces, called Okazaki fragments.

In prokaryotes, the DNA replication process is well defined (Kaguni, 2006). *E. coli* chromosomal DNA replication initiates at a specific sequence (*ori*C) located at 84 min on the genetic map (Oka et al., 1980) (Figure I-1A). The minimal *ori*C is 245 bp and highly conserved among enteric bacteria (Zyskind et al., 1983). It has four copies of highly conserved short sequences in the form of two inverted repeats, known for DnaA protein binding (Fuller and Kornberg, 1983) and referred as a DnaA box. The replication

A

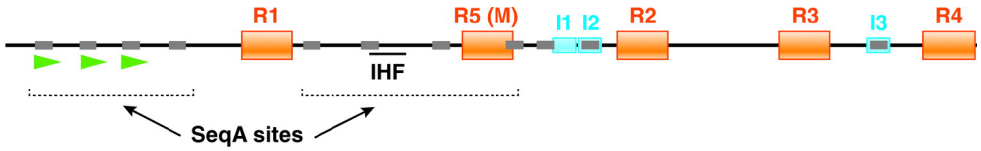

(Kaguni, *Annu Rev Microbiol*, 2006)

B

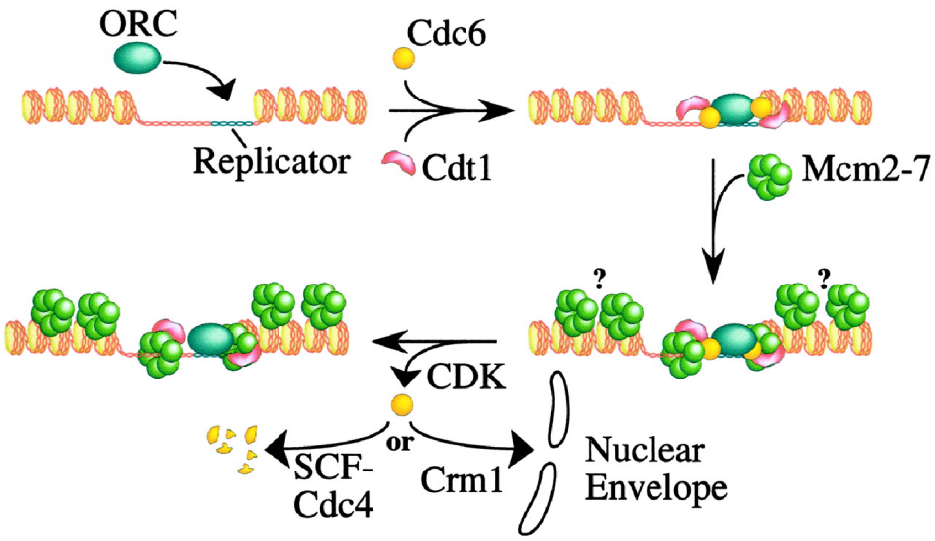

(Bell and Dutta, *Annu Rev Biochem*, 2002)

Figure I-1. **Structure of pre-replicative complex.** A, DNA motifs of the *E. Coli oriC*. The orange boxes represent DnaA box sequences. Blue boxes correspond to I sites bound by DnaA-ATP complex. Green arrowheads on the left represent the 13-mer regions unwound by DnaA. Gray boxes represent GATC sequences recognized by DNA adenine methyltransferase. B, Assembly of eukaryotic pre-replicative (pre-RC) complex. The origin recognition complex (ORC) is loaded to the origin first. Subsequently, Cdc6 and Cdt1 are recruited to the origin. ORC, Cdc6 and Cdt1 together are required for the loading of MCM2-7 proteins, which are the replicative helicases, to the origin during G1.

initiation starts with the binding of the DnaA protein to the DnaA box. On *ori*C region, three A+T-rich 13mers are directly to the left of the DnaA boxes. Sequential melting from right to left of the 13mers follows the DnaA binding and opens the duplex (Bramhill and Kornberg, 1988). DnaA then loads DnaB protein to the denatured bubble, forming a prepriming complex. With the help of SSB (single-stranded DNA binding protein) and DNA gyrase, a DNA topoisomerase, DnaB will unwind the template DNA bidirectionally from *ori*C (Baker et al., 1986). The DnaB protein is the replication-fork helicase with a 5'-3' polarity (LeBowitz and McMacken, 1986). In the presence of DnaB, DnaG, a primase, will synthesize RNA primers on ssDNA, which can be used to initiate subsequent DNA synthesis by the DNA polymerase III (Arai and Kornberg, 1979).

In *E. coli*, DNA polymerase III, which consists of at least 10 subunits (Maki and Kornberg, 1988), was identified as the cellular replicative polymerase (Nusslein et al., 1971). The catalytic core of polymerase III is composed of a heterotrimer of α, ε, and θ subunits (McHenry and Crow, 1979). It has a DNA polymerase activity and a proofreading 3'-5' exonuclease activity (Scheuermann and Echols, 1984; Spanos et al., 1981). At the replication fork, the DNA polymerases for both the leading strand synthesis and the Okazaki fragment synthesis can interact with each other and form a dimeric structure (McHenry, 1982). The leading strand product is a long, continuous nascent DNA strand. The Okazaki fragment synthesis is a repeated cycle which includes: synthesis of a new RNA primer, transit of the polymerase from the terminus of the previously completed Okazaki fragment to the new primer 3' terminus, nascent lagging-strand DNA synthesis, and termination of Okazaki fragment synthesis. Finally, the RNA primers are replaced by DNA and the mature Okazaki fragments need to be ligated.

DNA replication in eukaryotic cells is much more complicated and requires more proteins than in *E. coli*. The sequences required for an origin of replication vary significantly between different eukaryotic species. In *Saccharomyces cerevisiae*, many regions were identified as replication origins, which usually contain three to four sequences of 10-15 base pairs spread over 100-150 nucleotides (Newlon and Theis, 1993). These regions were identified initially as autonomously replicating sequences (ARS) that are able to confer extrachromosomal maintenance to yeast plasmids. Then subsequent studies showed that these elements served as chromosomal DNA replicators. ARS has a highly conserved and essential A-element or ARS consensus sequence (ACS) and less well conserved elements called B-elements, which are the DNA unwinding element of the origin (Bell, 1995). The origins in other eukaryotic organisms have no consensus sequences but appear to consist of several modular elements (Aladjem and Fanning, 2004).

Eukaryotic DNA replication is initiated by the formation of a pre-replicative complex (pre-RC) at an origin of replication in G1 (Figure I-1B). Several proteins were shown to be involved in this process. The origin recognition complex (ORC) is a six-subunit complex that initiates the assembly of pre-RC by associating with the replication origin (Rowles et al., 1996). Subsequently, Cdc6 and Cdt1 are recruited to the origins. ORC, Cdc6 and Cdt1 together are required for the loading of MCM2-7 proteins, which are the replicative helicases, to the origin during G1 (Coleman et al., 1996; Nishitani et al., 2000; Romanowski et al., 1996). When cells begin to enter S phase, a lot of regulatory factors are activated and act to initiate DNA synthesis (Figure I-2). MCM10, Cdc45, Dpb11 (TopBP1), GINS associate with the origin and are required for the

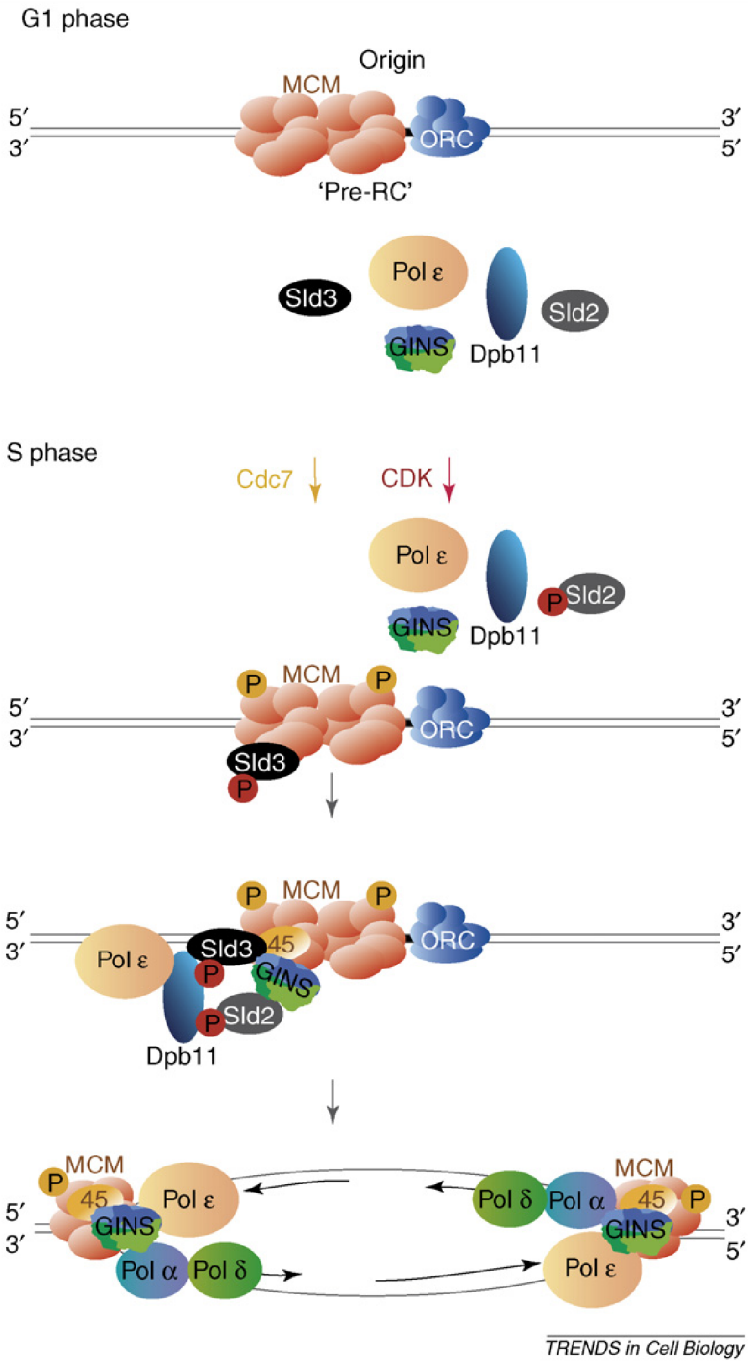

(Labib and Gambus, *Trends Cell Biol*, 2007)

Figure I-2. **Control of the initiation of DNA synthesis in budding yeast.** When cells enter S phase, CDK phosphorylates Sld2 and Sld3, which can then bind to Dpb11 and promote loading of other factors, such as GINS, Cdc45 and DNA polymerase. The Cdc7 kinase also phosphorylates target proteins, such as MCM, to facilitate this transition. The combined action of CDK and Cdc7 results in the formation of an active MCM complex that initiates the unwinding of the origin duplex.

transition to DNA synthesis (Araki et al., 1995; Labib et al., 2000; Merchant et al., 1997; Mimura and Takisawa, 1998). The origin duplex is unwound by MCM (minichromosome maintenance) proteins. Finally, DNA polymerase α-primase, RPA, PCNA, DNA polymerase δ, and polymerase ε assemble at the origins and start DNA replication (Bell and Dutta, 2002). The transition to DNA synthesis is also tightly controlled by at least two kinases: Cdc7/Dbf4 and Cyclin-dependent kinases (CDK). ORC, MCM2-7, and Cdc6 are some of the targets of CDK (Drury et al., 2000; Findeisen et al., 1999; Nguyen et al., 2001). Sld2 and Sld3 were reported to be the minimal set of S phase CDK targets required for DNA replication (Zegerman and Diffley, 2007).

Eukaryotic DNA replication starts with the RNA-DNA primer synthesis by DNA polymerase α-primase (Bullock et al., 1991). Once the RNA-DNA primer is synthesized, replication factor C (RFC) binds to the 3'-end of the primer, displaces polymerase α-primase, and loads proliferating cell nuclear antigen (PCNA) onto the DNA (Tsurimoto and Stillman, 1991). PCNA has a trimeric, ring-like structure and functions as a processivity factor for polymerase δ during DNA replication (Bravo et al., 1987). DNA polymerase δ is a heterotetramer composed of p125, p66, p50, and p12 subunits (Podust et al., 2002; Zhang et al., 2007a). p125 is the catalytic subunit for the DNA polymerase activity. It also has a proofreading, 3'-5' exonuclease activity. Polymerase δ is required for the lagging strand synthesis (Garg and Burgers, 2005). DNA polymerase ε is also essential in DNA replication, probably for leading strand synthesis, although its precise role in DNA replication remains to be determined. Recent studies show polymerase ε may be involved in DNA translesion synthesis (Lehmann, 2005). During the lagging strand synthesis, the short Okazaki fragments synthesized discontinuously are converted

into long, ungapped DNA products. This maturation requires several distinct steps including removal of RNA primers, gap filling, and ligation of two adjacent DNA fragments. Two different nucleases, RNase HI and FEN1, are involved in the removal of RNA primers (Ishimi et al., 1988; Turchi et al., 1994). In yeast, Dna2 helicase has been shown to be involved in removal of RNA primers (Bambara et al., 1997). Dna2 can unwind the RNA primer from the template DNA and create a flap-like substrate for FEN1 endonuclease.

Restart of Stalled Replication Forks

During normal cell growth, endogenous and exogenous DNA damage can inactivate replication forks (Heller and Marians, 2006). If DNA synthesis is prevented by a lesion on the template or by depleting dNTP pools, the replication fork will stall. To ensure that DNA replication is completed, cells use specialized restart pathways to enable fork reactivation.

Restart of stalled replication forks has been studied extensively in prokaryotes (Figure I-3). In *E. coli*, when the replisome encounters a lesion on the leading-strand template, the nascent lagging strand will pass the lesion and leave a gap on the leading-strand template. The two nascent strands can undergo regression to form a four-way, Holliday-junction structure. Replication can be restarted by a few distinct mechanisms (Heller and Marians, 2006). In the recombination-dependent replication pathway, the Holliday-junction will be resolved by branch-migration helicase and endonuclease RuvABC. After the lesion is removed by excision, a D-loop structure can be created by the recombination between the broken chromosome and the intact duplex, and restart the

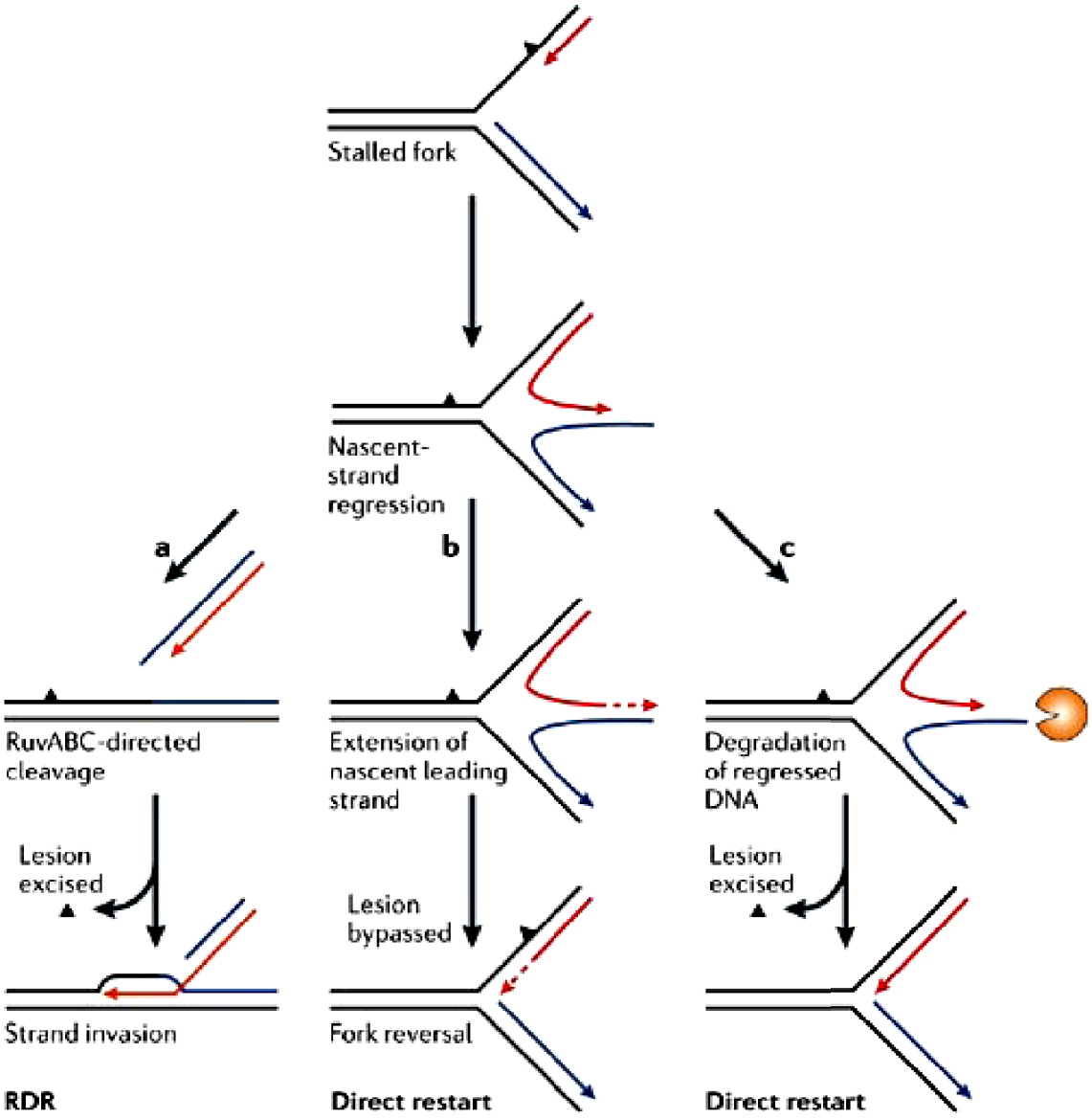

(Heller and Marians, *Nat Rev Mol Cell Bio*, 2006)

Figure I-3. **Restart of stalled replication forks with a lesion on the leading strand template.** When the replisome encounters a lesion on the leading-strand template, the two nascent strands undergo regression to form a four-way, Holliday-junction structure. In the recombination-dependent replication (RDR) pathway, the Holliday-junction will be resolved by RuvABC. After the lesion is removed by excision, the broken chromosome invades into another intact duplex and restart the replication. In the direct restart model, the nascent leading strand can be extended by using the pairing lagging strand as template on the Holliday-junction, thus bypass the lesion and restart replication. Another way for the direct restart involves partial degradation of both the nascent leading and lagging strands on the four-way junction. After removal of the lesion on the template, replication restart takes place.

replication. In the direct restart model, the nascent leading strand can be extended by using the paired lagging strand as template on the Holliday-junction. After the reversal of the Holliday-junction, the lesion can be bypassed and replication restarts. Another way for the direct restart is to degrade both the nascent leading and lagging strands on the regressed junction. After removal of the lesion on the template, replication restart takes place (Heller and Marians, 2006).

Restart of stalled replication forks requires the reloading of replisome. PriA, a 3'-5' DNA helicase, can direct replisome assembly during recombination-dependent restart (Liu and Marians, 1999). In another replisome-loading system, PriC loads the replicative helicase DnaB to the lagging-strand template of stalled fork structures for the assembly of replisome (Heller and Marians, 2005).

DNA Damage Signaling and Repair

DNA molecules are constantly exposed to alterations by exogenous DNA-damaging agents and cellular metabolites. Because the primary structure of DNA contains important genetic information, to repair damaged DNA is extremely essential for all organisms. Sophisticated machineries have evolved in different species to respond to DNA damage.

Abnormal DNA structures are induced by the following mechanisms (Sancar et al., 2004). Treatments by chemicals, such as large polycyclic hydrocarbons or alkylating agents, can form various base adducts. Ultraviolet (UV) radiation produces cyclobutane pyrimidime dimers and photoproducts. Damage on DNA backbone gives rise to single- and double-strand DNA breaks. Double-strand breaks also form after exposure to

ionizing radiation and other DNA-damaging agents. Single-strand breaks are produced by DNA-damaging agents or as intermediates of excision repair. Some agents, such as cisplatin, mitomycin C, or etoposide, can induce inter-strand cross-links and DNA-protein cross-links. Holliday-junctions, fork structures, single- and double-strand breaks, and other abnormal DNA structures are formed during the processing of stalled replication forks or DNA recombination.

DNA Damage Signaling and Checkpoints

Cellular responses to DNA damage are initiated with the recognition of DNA damage by sensor proteins. DNA damage signals are subsequently transmitted to downstream effectors to induce DNA repair, DNA damage checkpoints, transcriptional response, or apoptosis (Figure I-4).

ATM (ataxia telangiectasia mutated) and ATR (ATM and Rad3 related) proteins are two important phosphoinositide 3-kinase-like kinase (PIKK) family members that signal in cellular responses to DNA damage. Mutations in ATM cause ataxia telangiectasia (A-T) in humans with the symptoms of genome instability, clinical radiosensitivity, immunodeficiency, cerebellar degeneration, and cancer predisposition (Shiloh, 1997). ATM is a 350-kDa oligomeric protein containing many HEAT motifs (Perry and Kleckner, 2003). Exposing cells to ionizing radiation converts ATM dimers into monomers and triggers ATM autophosphorylation at serine 1981 (Bakkenist and Kastan, 2003). Activated ATM phosphorylates many downstream substrates, including CHK2, p53, NBS1, BRCA1 (Banin et al., 1998; Canman et al., 1998; Cortez et al., 1999;

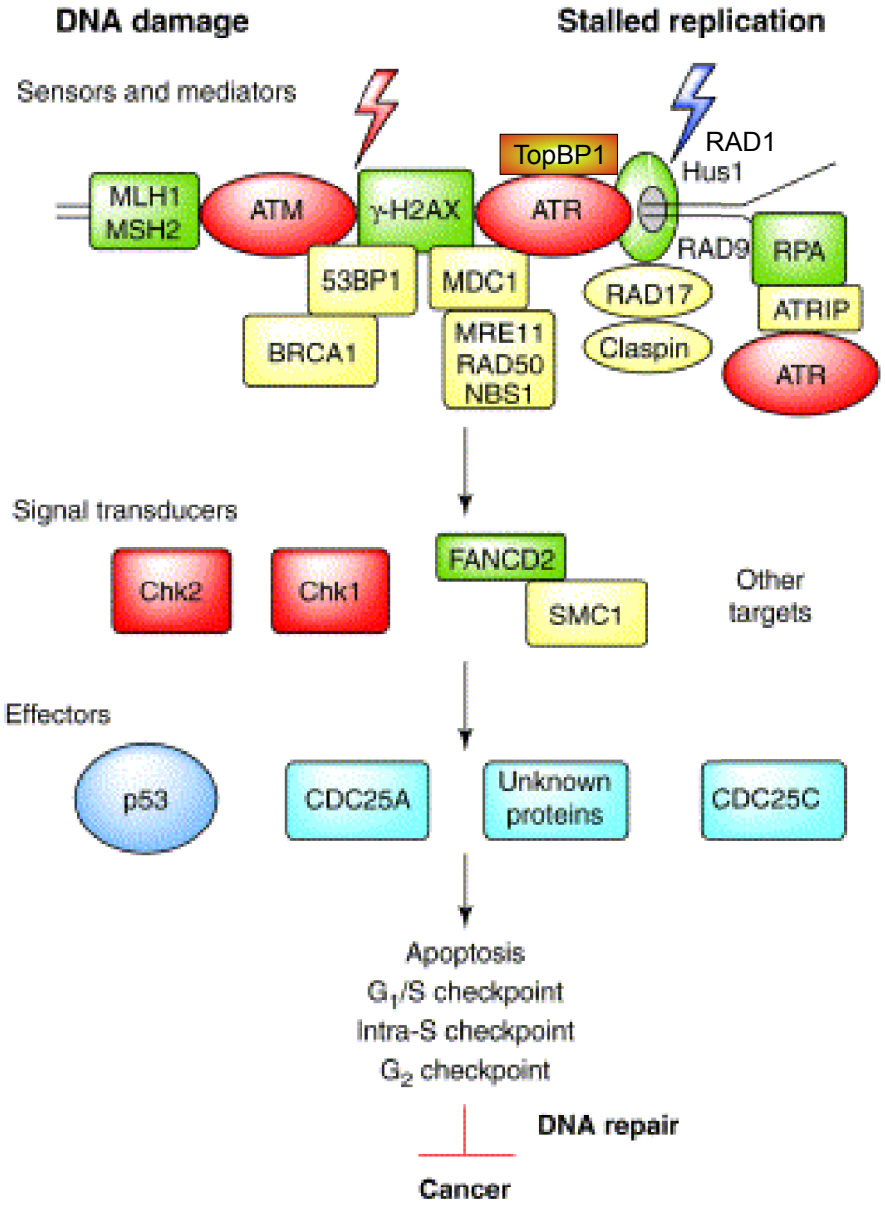

(Adapted from Motoyama and Naka, *Curr Opin Genet Dev*,.2004)

Figure I-4. **Pathways of DNA damage responses in mammalian cells.** DNA damage or stalled replication forks are detected by sensor proteins. Recognition of DNA damage by Mre11/Rad50/NBS1 (MRN) activates ATM. ATR is activated by RPA-ssDNA, Rad9/Rad1/Hus1 and TopBP1. ATM and ATR phosphorylate downstream targets such as CHK1 and CHK2, and transduce the damage signal. Effector proteins promote checkpoint control and damage repair in response to DNA damage.

Lim et al., 2000; Matsuoka et al., 1998). Sites phosphorylated by ATM and ATR usually have the conserved SQ/TQ sequence motif (Kim et al., 1999).

Mre11/Rad50/NBS1 (MRN) is a protein complex involved in checkpoint signaling, meiosis, homologous recombination, non-homologous end joining, and telomere maintenance (D'Amours and Jackson, 2002). Mutations of Mre11 and NBS1 cause ataxia-telangiectasia-like disease and Nijmegen breakage syndrome, respectively, with similar symptoms as A-T disease (Carney et al., 1998; Stewart et al., 1999). MRN has 3'-5' exonuclease and endonuclease activity (Paull and Gellert, 1998; Paull and Gellert, 1999). MRN is required for the activation of ATM after DNA damage (Uziel et al., 2003). *In vitro* studies show that ATM can be directly activated by MRN and DNA (Lee and Paull, 2004; Lee and Paull, 2005). The rapid relocalization of MRN to DNA damage sites after ionizing radiation suggests it is one of the earliest protein complexes that associates with DNA double-strand breaks after ionizing radiation (Mirzoeva and Petrini, 2001).

ATR was discovered in the human genome database as a gene with sequence homology to ATM and Rad3 (Cimprich et al., 1996). Knockout of ATR in mice results in embryonic lethality (Brown and Baltimore, 2000). In contrast to ATM, ATR is activated *in vivo* to higher levels by UV and DNA synthesis inhibitors than by ionizing radiation (Abraham, 2001). After DNA damage, RPA-coated ssDNA is required for ATR activation (Zou and Elledge, 2003). However, RPA-ssDNA is not sufficient for ATR activation (Ball et al., 2007; Ball et al., 2005; Kim et al., 2005). When a DNA replication fork is stalled by UV or aphidicolin treatment, DNA primer synthesis by polymerase α-primase is required for ATR activation (Byun et al., 2005). DNA stretches composed of

both single-stranded and double-stranded DNA are very effective at triggering the activation of *Xenopus* ATR (Kumagai et al., 2004). TopBP1, a protein involved in DNA replication initiation and checkpoint signaling, directly activates ATR complex (Hashimoto et al., 2006; Kumagai et al., 2006; Yan et al., 2006). ATR phosphorylates many proteins, one important target of ATR is CHK1, a checkpoint regulating kinase (Liu et al., 2000). The ATR-dependent phosphorylation of CHK1 requires ATRIP, a binding partner of ATR (Cortez et al., 2001). There is also a crosstalk between ATM and ATR. ATM and MRN are required for the activation of ATR after ionizing radiation, while ATR activates ATM after UV or replication fork stalling (Adams et al., 2006; Jazayeri et al., 2006; Myers and Cortez, 2006; Stiff et al., 2006).

The Rad17-RFC and 9-1-1 (Rad9-Rad1-Hus1) are two complexes involved in DNA damage signaling. The Rad17-RFC complex has a very similar structure as the replicative RFC complex: a heteropentamer with a globular "C" shape (Griffith et al., 2002). Although the 9-1-1 proteins have little sequence homology to PCNA, they form a PCNA-like heterotrimeric ring (Griffith et al., 2002). *In vitro*, Rad17-RFC loads 9-1-1 complex onto DNA in a similar manner as RFC loading PCNA (Bermudez et al., 2003). Rad17 is also required for loading 9-1-1 to chromatin after DNA damage *in vivo* (Zou et al., 2002). In *Xenopus*, single-stranded DNA and polymerase α-primase are required for Hus1 chromatin association after replication inhibition (You et al., 2002). Recent study in yeast shows that Rad17-RFC and 9-1-1 activates Mec1 (ATR homolog) during the initiation of the DNA damage checkpoint (Majka et al., 2006).

During DNA damage signaling, some proteins play the roles as mediators. The p53 binding protein, 53BP1 and the mediator of DNA damage checkpoint 1, MDC1, can

affect the phosphorylation of ATM/ATR substrates and checkpoint control after DNA damage (Goldberg et al., 2003; Lou et al., 2003; Schultz et al., 2000; Stewart et al., 2003; Wang et al., 2002).

In mammalian cells, CHK1 and CHK2 are two kinases with a signal transduction function in cell cycle regulation and checkpoint responses (Melo and Toczyski, 2002). The double-strand break signal is mainly transduced by CHK2 through ATM-dependent phosphorylation and UV damage is transduced by CHK1 through ATR-dependent phosphorylation (Liu et al., 2000; Matsuoka et al., 1998). CHK1 (-/-) causes embryonic lethality in mice (Lupardus et al., 2002). Activated CHK1 and CHK2 phosphorylate many downsteam effectors, such as p53, Cdc25A, Wee1, and regulate G1/S, intra-S, and G2/M checkpoints after DNA damage (Chehab et al., 1999; Falck et al., 2001; O'Connell et al., 1997; Ryan et al., 2001; Xiao et al., 2003). CHK1 and CHK2 pathways are not absolutely separated from each other, in fact, there is some overlap between these two pathways.

DNA Repair

One of the cellular responses to DNA damage is to repair the damaged DNA molecule. DNA repair pathways can be divided into distinct categories: direct repair, base excision repair, nucleotide excision repair, double-strand break repair, and mismatch repair.

Direct repair utilizes unique enzymes to removal DNA lesions. The DNA photolyase can reverse UV-induced pyrimidine dimer (Sancar, 1994). The O^6-methyl

group from O^6-methylguanine (O^6MeGua) in DNA can be removed by DNA methyltransferase (Daniels and Tainer, 2000).

In base excision repair, a DNA glycosylase removes the damaged base to form an abasic (AP) site in the DNA (Memisoglu and Samson, 2000). The 3'-sugar residue can be removed by an AP endonuclease (APE) and result in a one-nucleotide gap. In mammalian cells, DNA polymerase β, APE1, and DNA ligase III-XRCC1 are required for the gap repair (Matsumoto and Kim, 1995). In some other cases, APE1 makes a 5' incision to the AP site, generating a nick on DNA molecule. Then under the combinational function of DNA polymerase δ/ε and PCNA, a flap of 2-10 nucleotides is produced from the nick. The flap is cut at the junction of the single strand and the duplex by FEN1 endonuclease and the gap is ligated by DNA ligase I (Klungland and Lindahl, 1997).

Nucleotide excision repair is the major repair system to remove DNA lesions formed by radiation, chemicals, or by protein-DNA cross-link, on one strand of the duplex. In *E. coli*, nucleotide excision repair is carried out by three proteins, UvrA, UvrB, and UvrC. In mammalian cells, the nucleotide excision repair system involves more proteins (Sancar et al., 2004). The DNA damage is recognized by DNA-binding proteins: RPA, XPA and XPC (Mu et al., 1997). Then TFIIH is recruited to form a pre-excision complex. ATP hydrolysis by XPB and XPD, two helicases in TFIIH complex, unwinds the lesion region on the duplex by about 20 bp. XPG then replaces XPC to form a more stable pre-excision complex. Finally XPF-ERCC1 is recruited to excise and release the DNA lesion. The resulting gap can be filled by the DNA replication machinery including polymerase δ/ε, PCNA, and RFC.

During DNA replication, mispaired nucleotides are occasionally inserted into the duplex. The DNA mismatch repair (MMR) system corrects DNA base-pairing errors in newly replicated DNA. The human MMR system consists of a protein family termed hMSH (Kunkel and Erie, 2005). hMSH2/6 is a heterodimer and recognizes base/base mismatch and short insertion/deletion loops, while hMSH2/3 recognizes larger insertion/deletion loops. The DNA-MSH-ATP complex recruits the hMLH1/hPMS2 heterodimer, which displaces the DNA polymerase and PCNA from the nascent daughter strand. Then exonuclease I (ExoI) is recruited to excise the mismatch. The resulting gap is filled with resynthesized DNA (Constantin et al., 2005).

Double-strand breaks can be induced by ionizing radiation and reactive oxygen species. They are also formed during V(D)J recombination, immunoglobulin class-switching processes, and replication fork arrest. Double-strand breaks are repaired by either nonhomologous end-joining (NHEJ), single-strand annealing (SSA) or homologous recombination (HR) mechanisms.

In NHEJ, Ku 70/80 heterodimer binds to the ends of a double-strand break. DNA-PK and ligase IV-XRCC4 are then recruited and ligate the two duplex termini (Ma et al., 2004; Ramsden and Gellert, 1998).

In single-strand annealing (SSA) mechanism, the two ends of the break are digested by an exonuclease to generate two single strands. Once the two single strands are paired at regions with sequence homology, the nonhomologous tails are trimmed off and the two duplex ends are ligated. Rad52 and RPA are involved in the SSA pathway (Fishman-Lobell et al., 1992; Shinohara et al., 1998; Sugawara and Haber, 1992).

The DNA duplex recovered by both NHEJ and SSA pathways will lose genetic information, due to the shortening of the broken ends during repair. In contrast, homologous recombination (HR) repairs DNA by using a homologous duplex as the template thus the broken DNA will be precisely repaired. HR only occurs in S and G2 phase cells. HR is initiated by the 5'-3' nuclease digestion of the ends of a double-strand break, resulting in a 3'-single-stranded (ss) DNA (Dudas and Chovanec, 2004). In *E. coli,* this process is done by RecBCD holoenzyme. The RecBCD complex contains two helicases, RecB and RecD, with opposite polarities (Dillingham et al., 2003; Taylor and Smith, 2003). RecBCD complex binds to the end of a double-stranded DNA, unwinds processively and degrades the 3'-end strand until it reaches a Chi sequence, the recombination hot spot (Bianco and Kowalczykowski, 1997). After interaction with the Chi site, the nuclease activity is switched and starts to produce a 3'-ssDNA tail (Anderson and Kowalczykowski, 1997). The enzyme responsible for creating the 3'-ssDNA in eukaryotes is not clear yet, although Mre11/Rad50/NBS1 complex has been suggested to be involved in this process (Nairz and Klein, 1997).

During HR, the 3'-ssDNA is coated with recombinases, which are the RecA protein in *E. coli* and the Rad51 protein in eukaryotes. Single-stranded DNA binding proteins can help the nucleoprotein filament formation by removing DNA secondary structures (Roman et al., 1991; Sugiyama et al., 1997). In eukaryotes, Rad52 can overcome the inhibitory effect of RPA on Rad51 filament formation when RPA binds to the ssDNA first (New and Kowalczykowski, 2002). The recombinase-coated ssDNA then invades into an intact homologous duplex and generates a D-loop structure. In eukaryotes, Rad54 protein stimulates this pairing process (Petukhova et al., 2000; Van Komen et al.,

2000; Zhang et al., 2007b). New DNA synthesis then initiates at the 3'-end of the invading strand, using the homologous duplex as a template. After DNA synthesis, the ligation of DNA ends leads to the formation of two Holliday junctions, which then undergo branch migration and are resolved by a resolvase. Bloom's syndrome helicase has been suggested to help to resolve the Holliday junctions and prevent the formation of crossover products (Wu and Hickson, 2003).

Helicases

The sequence of polynucleotide bases contains important genomic information. In a typical double-stranded polynucleotide, specific hydrogen bonds form between the pairing bases of the paralleling two strands. To access genomic information for many important biological processes, the two complementary strands have to be separated. DNA unwinding is involved in many aspects of DNA metabolism, such as DNA replication, recombination, repair, and transcription. For RNA, in some processes it is important to remove unwanted RNA secondary structure or to dissociate RNA-DNA hybrids. Therefore, a diverse class of enzymes has evolved, known as "helicases", to be able to unwind duplex polynucleotides.

Helicase was first discovered in E. *coli* as a "DNA unwinding enzyme" in 1976 (Abdel-Monem et al., 1976). The first eukaryotic DNA helicase was reported in 1978 (Hotta and Stern, 1978). The first bacteriophage protein reported as DNA helicase was T4 gene 41 protein (Venkatesan et al., 1982). In 1986, SV40 large tumor antigen was reported as the first viral encoded DNA helicase (Stahl et al., 1986). Since the discovery of the first helicase, a large number of these enzymes have been identified and

characterized in different organisms. These helicases were classified into distinct superfamilies based on their primary structures (Gorbalenya and Koonin, 1993). The majority of helicases belong to superfamilies I and II. These two superfamilies include proteins in a diversified spectrum of organisms ranging from virues, bacteria, to human, and include both DNA and RNA helicases. Superfamily III is much smaller and consists of helicases from small DNA and RNA virues. Other helicases can be divided into two small subfamilies, DnaB-like and Rho-like helicases (Figure I-5).

The proteins of superfamilies I and II contain seven conserved motifs, while helicases of superfamily III and the two small subfamilies only have three or five motifs, respectively. No matter which superfamily they belong to, all helicases contain NTP-binding motifs that are characterized as Walker A and Walker B motifs (Walker et al., 1982). Walker A motif has a sequence of G-X-X-X-X-G-K(T)X-X-X-X-X-X-I/V additionally preceded by a basic amino acid. The sequence of Walker B motif contains the common sequence R/K-XXX-G-XXX-L-hydrophobic-hydrophobic-hydrophobic-hydrophobic followed by an aspartic acid residue (Walker et al., 1982). Mutations in Walker motifs result in losing the function of NTPase and abolishing the activity of helicases.

The active form varies among helicases: they can be grouped as monomeric or multimeric helicases (Tuteja and Tuteja, 2004). A lot of oligomeric helicases show hexameric structures, such as MCM2-7 (minichromosome maintenance) protein complex (Masai et al., 2005), or SV40 large T (tumor)-antigen protein (Bullock, 1997). Hexameric helicases have a ring-shape structure that encircles the oligonucleotides and slides along the oligonucleotides, thus preventing local reannealing. The bacterial helicase priA and

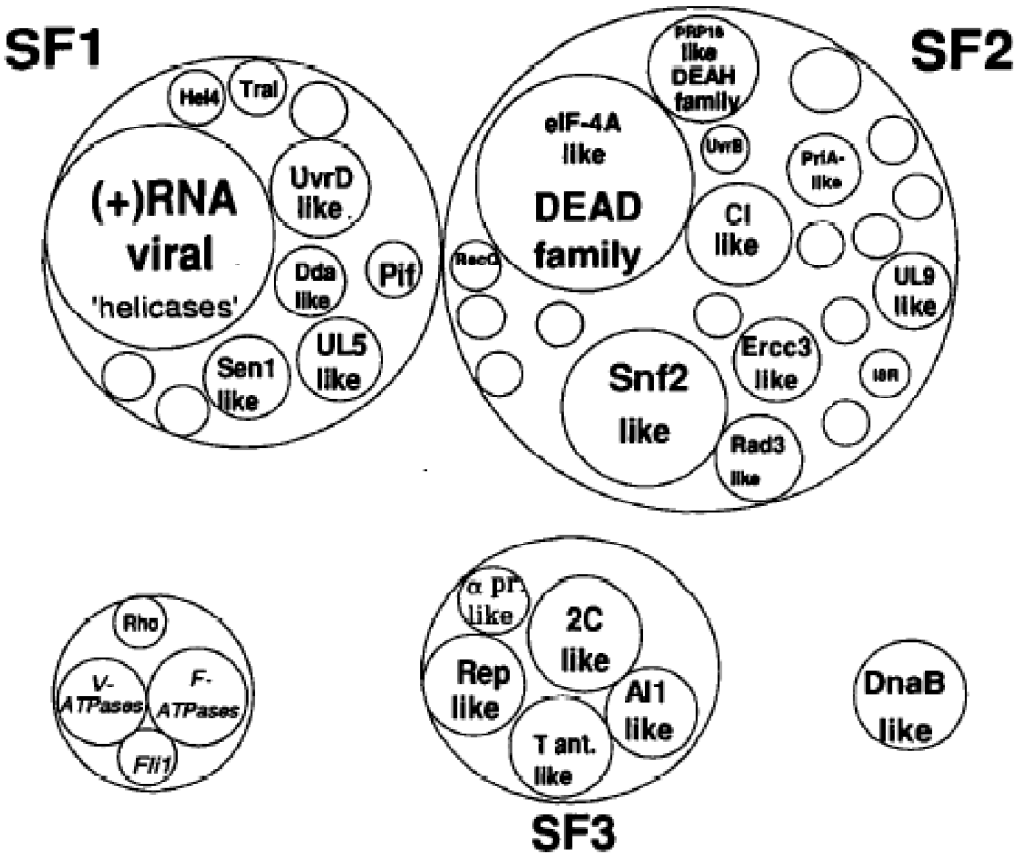

(Gorbalenya and Koonin, *Curr Opin Struc Biol*, 1993)

Figure I-5. **The classification of helicases by their primary structures.** Superfamily 1 (SF1) and superfamily 2 (SF2) are two large superfamilies including proteins in a diversified spectrum of organisms ranging from virues, bacteria, to human, and include both DNA and RNA helicases. Supefamily 3 (SF3) and DnaB-like family are much smaller groups of helicases.

bacteriophage T4 dda helicase are examples of monomeric helicases. Some complexes of the multimeric helicases contain different subunits. RecBCD protein complex has RecB, RecC and RecD subunits and MCM hexamer consists of MCM 2-7 proteins except in Archaea.

Biochemical Activities of Helicases

All helicases share common biochemical properties. In order to unwind duplex oligonucleotides, they have both ss (single-stranded) and ds (double-stranded) polynucleotide binding abilities. In addition, all helicases bind NTP and exhibit nucleic acid-dependent NTPase activity required for duplex unwinding. The unwinding activity of helicases can be measured by an *in vitro* assay (Venkatesan et al., 1982). Helicases unwind a duplex substrate obtained by annealing a ^{32}P-labeled oligonucleotide to a longer single-stranded oligonucleotide and yield two single-stranded oligonucleotides, which are then resolved from the starting duplex by native electrophoresis, allowing direct visualization of the unwound products.

When unwinding duplexes, helicases exhibit specific directional polarity, either 5'-3' or 3'-5', which is defined as the direction of helicase translocating along one of the two strands of the duplex (Figure I-6) (Soultanas and Wigley, 2001). While most helicases have unique polarities, some have bipolar enzyme activity. In RecBCD complex, RecB and RecD components of the complex unwind DNA from 3'-5' and 5'-3' directions, respectively (Dillingham et al., 2003). HerA protein from thermophilic archaea is able to utilize either 3' or 5' ssDNA extensions for DNA duplex unwinding (Constantinesco et al., 2004).

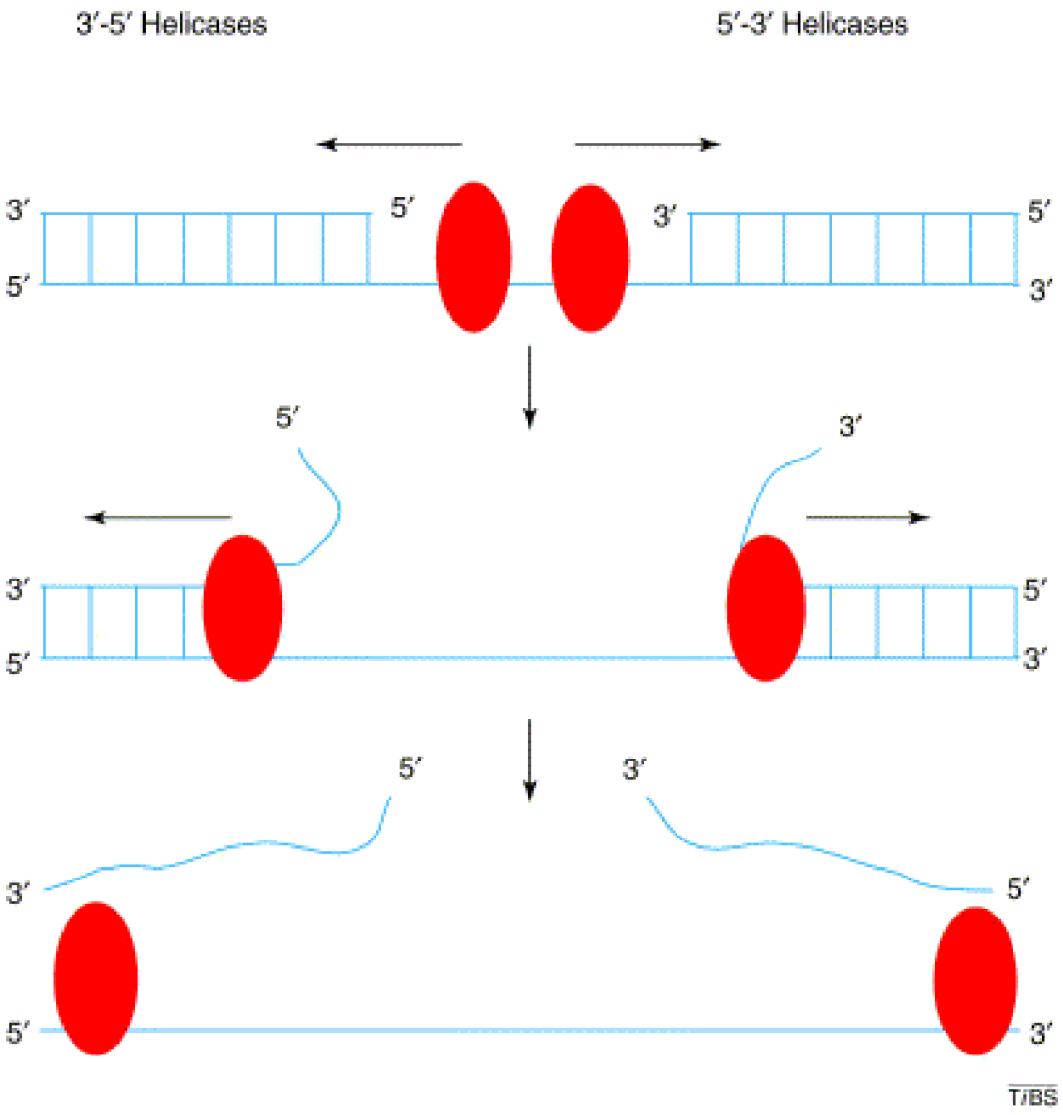

(Soultanas and Wigley,Trends Biochem Sci, 2001)

Figure I-6. **The polarity of helicases.** The polarity of helicases is defined as the direction of helicases translocating along one of the two strands of the duplex.

Studies on many superfamily I and II DNA helicases suggested an “inchworm” mechanism for the translocation of helicases along DNA strand (Mackintosh and Raney, 2006). In this model, the functional unit of the helicase contains two different nucleic acid binding sites. ATP binding and hydrolysis induce conformational changes within the DNA-binding sites. Alternative binding of DNA at two DNA-binding sites drives the translocation of the helicase on DNA molecule. In the case of dda protein, a cooperative inchworm model was proposed (Byrd and Raney, 2004). In this model, multiple dda monomers loaded to ssDNA could cooperatively increase the rate of unwinding. In terms of melting the duplex, two different models have been proposed (Soultanas and Wigley, 2001). Passive mechanism suggests the helicase only contacts with the ssDNA and unwinds the duplex by trapping ssDNA at a thermally fraying fork. In the active mechanism, helicases bind with the duplex and destablize it, thus separating the two strands.

When helicases are translocating along DNA or RNA molecules, they could displace proteins bound on nucleic acid (Mackintosh and Raney, 2006). DnaB can dissociate proteins from dsDNA to facilitate DNA branch migration in DNA repair or recombination (Kaplan and O'Donnell, 2002). Dda helicase can remove RNA polymerase from DNA-protein complex,-thereby allowing DNA repair to occur (Salinas and Kodadek, 1994).

Biological Functions of Helicases

DNA helicases participate in nearly every aspect of DNA metabolism. MCM proteins, originally identified from the screening for yeast mutants which cannot stably

maintain ARS (automously replicating sequence) plasmid, are required in the initiation and elongation steps of eukaryotic chromosome replication (Labib et al., 2000; Tye, 1999). MCM protein complex contains 6 protein subunits (MCM2-7) that interact with each other and form a stable hexmer structure (Lei et al., 1996). MCM4-6-7, which was shown to have DNA-dependent ATPase as well as 3'-5' DNA helicase activities, is the catalytic core of the MCM complex (Ishimi, 1997). However, until now no helicase activiy was found for the MCM2-7 heterohexamer. In fact, introducing MCM2 or MCM3-5 to MCM4-6-7 disassembles MCM4-6-7 dimeric structure and inhibits its helicase activity (Lee and Hurwitz, 2000). During G1 phase, MCM proteins are loaded to pre-RC (pre-replicative complex) by Cdc6 and Cdt1. In G1, its helicase activity must be carefully regulated so that it is only activated at the onset of DNA replication. At the beginning of S phase, the complex is activated and triggers the initiation of DNA replication. MCM2, MCM4, and MCM6 are phosphorylated by Cdk (cyclin-dependent kinases) and Cdc7 in S phase (Masai et al., 2000). However, the precise role of this phosphorylation needs further studies.

RecQ helicases are superfamily II helicases involved in processes related to DNA replication, DNA recombination, and gene silencing. The RecQ family is highly conserved in evolution from bacteria to human. It was discovered during a search for genes that contribute to *E. coli* thymine-starvation resistance and participate in RecF recombination pathway (Nakayama et al., 1984). All RecQ helicases share seven central helicase motifs and have 3'-5' DNA unwinding activity (Khakhar et al., 2003). Sgs1 is a RecQ helicase found in *S. cerevisiae*. In humans, the BLM, WRN, and RecQ4 helicases are defective in Bloom's syndrome, Werner's syndrome, and Rothmund-Thompson

syndrome, respectively (Ellis et al., 1995; Kitao et al., 1999; Yu et al., 1996). RecQ helicases are required for the maintenance of genome stability. Patients with Bloom's syndrome and Werner's syndrome show predisposition to cancer. Werner's syndrome patients also show significant features of premature aging. Rothmund-Thompson syndrome is characterized by skin pigmentation change, short stature, and predisposition to cancer (Hickson, 2003).

RecQ helicases show clear links to DNA homologous recombination and replication fork restart. In cells from Bloom's syndrome patients, there is a great increase of sister chromatid exchange events (Chaganti et al., 1974). WRN helicase can help to resolve intermediates of homologous recombination (Saintigny et al., 2002). Excessive homologous recombination was reported to be responsible for cell death in the absence of the Sgs1 and Srs2 helicases (Gangloff et al., 2000). Together with Topoisomerase III, BLM could dissolve the double-junction formed during the late stage of homologous recombination and suppress crossing over (Wu and Hickson, 2003). WRN helicase has a 3'-5' exonuclease activity in addition to its 3'-5' helicase activity (Huang et al., 1998). The premature aging feature of Werner's syndrome suggests that WRN may have functions in telomere maintenance. In fact, telomere lagging strand synthesis was shown to be defective in cells lacking WRN helicase activity (Crabbe et al., 2004).

The Simian virus 40 large T-antigen is a viral helicase required for viral DNA replication (Fanning and Knippers, 1992). Large T-antigen has a helicase domain ranging from residues 251-627 (Li et al., 2003). The N-terminal region of T-antigen (residues 1-130) has a J-domain, which interacts with heat shock protein 70 (Campbell et al., 1997). The N-terminal region contributes to the transforming function of T-antigen, at least in

part by binding to the ubiquitin ligase subunit Cul7 (Ahuja et al., 2005). Furthermore, this region contains a binding site for Rb family members. The interaction of Rb family members with T-antigen is necessary for stimulating the transcription of E2F-dependent genes. The amino acids 131-259 of T-antigen constitute the origin DNA-binding domain. The origin-binding domain of T-antigen is essential for origin-specific DNA unwinding, but not for T-antigen's helicase function (Arthur et al., 1988; Li et al., 2003). T-antigen interacts with many cellular proteins to carry out its biological functions. It associates with replication proteins such as replication protein A, DNA polymerase α-primase and topoisomerase I (Dornreiter et al., 1993; Dornreiter et al., 1992; Dornreiter et al., 1990; Fairman and Stillman, 1988; Simmons et al., 1996). T-antigen also interacts with a group of proteins that play roles in regulating cell cycle and DNA damage responses, such as p53, Rb, and transforms cells (DeCaprio et al., 1988; Linzer and Levine, 1979). T-antigen interacts with DNA damage responding protein NBS1 to disrupt DNA replication control (Wu et al., 2004).

In the presence of ATP, T-antigen assembles as a double hexamer at the SV40 origin (Parsons et al., 1991). T-antigen is an ATP-dependent DNA helicase that translocates along the leading-strand template in a 3'-5' direction (Goetz et al., 1988). In the presence of topoisomerase I, replication protein A, and ATP, T-antigen can unwind SV40 origin and recruit the human or monkey initiation proteins (Dodson et al., 1987). The duplex DNA is then unwound bidirectionally and results in two single-stranded loops that serve as the templates for replication (Wessel et al., 1992).

Human DNA Helicase B

Mouse DNA helicase B was initially discovered as a DNA-dependent ATPase during the biochemical purification of proteins from mouse FM3A cells (Tawaragi et al., 1984). Further characterization showed that this protein also has a DNA helicase activity (Seki et al., 1987). Mouse cells with temperature-sensitive DNA helicase B have an impaired DNA synthesis when exposed to non-permissive temperature (Seki et al., 1995). It was also shown to promote DNA synthesis in an *in vitro* system composed of mouse extract and a plasmid with a yeast autonomously replicating sequence (ARS) (Matsumoto et al., 1995). A point mutation in mouse DNA helicase B that causes temperature-sensitive DNA replication was identified (Tada et al., 2001). A human DNA helicase B has been cloned according to the sequence homology with mouse helicase B (Taneja et al., 2002). Both mouse and human DNA helicase B (HDHB) can interact with DNA polymerase α-primase and stimulate the activity of DNA primase *in vitro* (Saitoh et al., 1995; Taneja et al., 2002). Mouse cells with temperature-sensitive DNA helicase B showed impaired overall DNA synthesis but normal strand elongation during replication at non-permissive temperature (Seki et al., 1995). Upon a shift to non-permissive temperature, these cells arrested at the G1/S transition. When the Walker B mutant of HDHB protein was injected into the nucleus of cells in early G1, it inhibited DNA synthesis, while injection of mutant HDHB into cells at G1/S or S phase did not prevent DNA synthesis (Taneja et al., 2002), suggesting that HDHB may regulate DNA synthesis *in vivo*, possibly by directly controlling the firing of DNA replication origins or regulating G1/S or intra-S checkpoints.

Endogenous HDHB localizes in both the cytoplasm and nucleus in asynchronously growing cells, with more nuclear localization during G1 and more

cytoplasmic localization during S phase (Gu et al., 2004). A nuclear localization and a nuclear export signal (NES) have been identified in the carboxy-terminal domain of HDHB (PSLD). NES is activated by phosphorylation of HDHB at G1/S. Ectopically expressed GFP- or FLAG-tagged HDHB can also form nuclear foci on chromatin, and their appearance is altered in Walker A and B mutants (Gu et al., 2004). The number of GFP-HDHB foci per nucleus can be stimulated by different DNA damaging agents such as topoisomerase II inhibitor etoposide, or topoisomerase I inhibitor camptothecin (Gu et al., 2004). Sites of DNA damage and repair appear to localize in nuclear foci (Nelms et al., 1998) that contain DNA repair and signaling proteins such as Mre11, Rad51, Rad52, and RPA. This suggests that HDHB nuclear foci are associated with DNA damage response. However, how HDHB is involved is still not clear.

The primary goal of the reseach presented in this dissertation is to define the potential role of HDHB in DNA damage response. In the first part of this dissertation, we show that the chromatin-associated fraction of HDHB increases in cells exposed to a variety of DNA damaging agents. HDHB chromatin accumulation is most prominent in S phase cells exposed to agents that cause replication fork stalling or collapse. Inhibition of checkpoint kinases does not prevent damage-induced accumulation of HDHB on chromatin, suggesting that HDHB associates directly with DNA lesions or with other proteins recruited to the lesions. Silencing of HDHB does not affect UV-induced RPA focus formation, but diminishes the induction of TopBP1 foci. HDHB-depleted cells show less CHK1 phosphorylation after DNA damage. These results identify HDHB as a novel factor that associates with damaged chromatin and promotes intra-S phase damage response.

In the second part of this dissertation, we further investigated the potential function of HDHB in homologous recombination. HDHB-depleted cells have less sister chromatid exchange than control-depleted cells. *In vivo* recombination assay showed that homologous recombination is impaired in HDHB-depleted cells. *In vitro*, recombinant HDHB stimulates Rad51-mediated 5'-3' heteroduplex extension. These results suggest a function of HDHB in generating ssDNA/duplex structure and recruiting DNA damage signaling factors during DNA damage response.

CHAPTER II

DNA DAMAGE-INDUCED RECRUITMENT OF HUMAN DNA HELICASE B TO CHROMATIN STIMULATES TOPBP1 FOCUS FORMATION

Hanjian Liu, Peijun Yan, Gulfem D. Guler, Xiaorong Zhao,

Jinming Gu, Haleh Kadivar, Elisabeth Kremmer, Hao Huang, and Ellen Fanning

Submitted to Experimental Cell Research

Introduction

DNA helicases unwind duplex DNA to expose the single strands for replication or repair and are crucial for the maintenance of genomic integrity (Boule and Zakian, 2006; Glover et al., 2005; Lehmann, 2005; Singleton and Wigley, 2002; Takahashi et al., 2005; Taniguchi and D'Andrea, 2006; Wu and Hickson, 2006). On the other hand, DNA helicase activity is potentially destructive and subject to tight regulation in vivo. Mechanisms to limit helicase level and localization, and to direct each helicase to the proper substrate in a timely manner must exist. These regulatory mechanisms are thought to rely on proteins that interact with helicases and on the ability of helicases to recognize different DNA structures. However, the physiological substrates of DNA helicases and the biochemical pathways in which they operate in vivo have been notoriously difficult to identify, particularly in vertebrates. Genetic analysis of human diseases, including xeroderma pigmentosum, Fanconi's anemia, Werner's and Bloom's syndromes, have identified several helicases essential for genomic integrity, and biochemical and structural studies are beginning to reveal their functions (Machwe et al., 2006; Rudolf et

al., 2006; Sharma et al., 2006; Sobeck et al., 2006; Wu and Hickson, 2006). However, the functions of many helicases not currently associated with human disease remain to be determined.

DNA helicase B (Figure II-1A) is a robust 5'-3' superfamily I DNA-specific helicase that is conserved among the vertebrates whose genomes have been sequenced (Tada et al., 2001; Taneja et al., 2002). Mouse and human DNA helicase B display ssDNA-dependent ATPase activity, interact directly with purified DNA polymerase α-primase (pol-prim) and replication protein A (RPA), and stimulate primer synthesis on RPA-ssDNA template in vitro (Matsumoto et al., 1995; Saitoh et al., 1995; Seki et al., 1995; Taneja et al., 2002) (Guler and Fanning, unpublished). Murine cells that encode a temperature-sensitive DNA helicase B arrest at G1/S when shifted to the non-permissive temperature (Seki et al., 1995; Tada et al., 2001). Consistent with these findings, injection of purified recombinant human DNA helicase B (HDHB) protein containing a Walker B point mutation into the nucleus of human cells in early G1 inhibited S phase entry, but injection later in G1/S or S, or injection of the wild type protein had no effect on DNA synthesis (Taneja et al., 2002). These results suggested that DNA helicase B activity promotes the G1/S transition, possibly through its interactions with RPA and pol-prim, but did not reveal the mechanism(s) involved.

The subcellular localization of endogenous HDHB is regulated in the cell cycle (Collis et al., 2005). Nuclear localization and nuclear export signals were identified in the carboxy-terminal domain of HDHB (Figure II-1A). Nuclear export of HDHB at G1/S depends on CDK phosphorylation of at least one site (Ser967) in a cluster of potential CDK sites near the nuclear export signal. Ectopically expressed GFP-HDHB was

visualized in nuclear foci (Gu et al., 2004). The number of foci was greater in cells exposed to DNA damaging agents, suggesting that HDHB may function not only at the G1/S transition, but also in DNA damage signaling or repair.

Here, we demonstrate that a minor fraction of HDHB resides on chromatin in undamaged cells throughout the cell cycle, and that this fraction increases in cells treated with a variety of DNA damaging agents, particularly in S phase cells. Importantly, checkpoint kinase activity is not required for damage-induced HDHB accumulation on chromatin. HDHB partially co-localizes with TopBP1 and Rad9 foci in human cells and interacts directly with recombinant TopBP1. ShRNA-mediated silencing of HDHB does not affect RPA recruitment to chromatin in UV-irradiated human cells, but diminishes induction of TopBP1 foci. Damage-induced CHK1 phosphorylation is reduced in HDHB-depleted cells. Our results suggest that HDHB functions in an early step of the intra-S phase damage response.

Materials and Methods

Protein Purification

High Five insect cells (Invitrogen, Carlsbad, CA) (5×10^8) infected by recombinant baculovirus for 48 h were lysed in 10 ml of lysis buffer (20 mM Tris-HCl at pH 7.5, 50 mM NaCl, 0.2% (v/v) Nonidet P-40, 10% glycerol, 1 mM DTT, 1 mM phenylmethylsulfonyl fluoride (PMSF), 10 µg/ml aprotinin, 1 µM leupeptin). Lysate was cleared by centrifugation, and the supernatant was loaded on a 20-ml P11 column (Whatman, Florham Park, NJ) pre-equilibrated in Buffer A (20 mM Tris-HCl at pH 7.5,

50 mM NaCl, 0.02% (v/v) Nonidet P-40, 10% glycerol, 1 mM DTT, 1 mM phenylmethylsulfonyl fluoride, 10 µg/ml aprotinin, 1 µM leupeptin). Proteins were eluted from the column with a 200-ml gradient of NaCl from 50 to 600 mM in Buffer A. The eluate was diluted 10-fold with Buffer A and loaded onto a 1-ml MonoQ column (Amersham Biosciences, UK). Proteins were eluted with a 20-ml gradient of NaCl from 50 to 600 mM in Buffer A and collected in 0.5-ml fractions. Protein concentration was determined by densitometric scanning, using IPLabgel 1.5 (Signal Analytics Corp., Vienna, VA), of Coomassie-stained protein bands in SDS-polyacrylamide gels. As protein standards, known amounts of bovine serum albumin (BSA) were loaded onto the same gel. The yield was generally about 3 mg of purified HDHB.

Production of Monoclonal Antibodies against HDHB.

Purified recombinant T7-tagged HDHB protein (Taneja et al., 2002) (50 µg) was injected intraperitoneally (*i.p.*) and subcutaneously (*s.c.*) into LOU/C rats using CPG2006 (TIB MOLBIOL, Berlin, Germany) as adjuvant. After 8 weeks, a boost of antigen was given i.p and s.c. Three days later, fusion of P3X63-Ag8.653 myeloma cells with the rat spleen cells was performed according to standard procedures (Kremmer et al., 1995). Hybridoma supernatants were tested in a solid-phase immunoassay using T7-tagged HDHB protein adsorbed to polystyrene microtiter plates. Crude E. coli extract served as a negative control. mAb 4C11 (rat IgG1) and mAb 5C9 (rat IgG2b) were stably subcloned and used to produce antibodies for further analysis.

Other Antibodies

Rabbit polyclonal antibodies were generated against purified recombinant HDHB (Bethyl Laboratories, Montgomery, TX) and affinity purified on recombinant HDHB-coupled CNBr-activated Sepharose-4B (Amersham Biosciences). Monoclonal antibody 70C against hRPA was purified as described (Kenny et al., 1990). Commercial sources of antibody were as follows: mouse anti-PCNA antibody (PC-10, Santa Cruz Biotechnology, Santa Cruz, CA), mouse anti-tubulin antibody (Ab-3, NeoMarkers, Fremont, CA), mouse anti-CHK2 antibody (Upstate, Charlottesville, VA), rabbit anti-CHK2 phospho-T68 antibody (Cell Signaling, Beverly, MA), mouse anti-CHK1 antibody (G-4, Santa Cruz Biotechnology), rabbit anti-CHK1 phospho-S345 antibody (Cell Signaling, Beverly, MA), rabbit anti-TopBP1 antibody (Bethyl Laboratories), mouse anti-Rad9 antibody (Calbiochem, La Jolla, CA), mouse anti-RPA34 antibody (Calbiochem), goat anti-ATR antibody (Santa Cruz Biotechnology), mouse anti-Rad51 antibody (Novus, Littleton, CO). Rabbit polyclonal anti-Orc2 was a kind gift from A.K. Patten.

Cell Culture, Synchronization, and Flow Cytometry

Human osteosarcoma U2OS and colon carcinoma HCT116 cells were grown as monolayers in Dulbecco-modified Eagle medium (DMEM) (Gibco BRL Lifetechnologies, Carlsbad, CA) supplemented with 10% fetal bovine serum (FBS) (Atlanta Biologicals, Norcross, GA) at 37°C. Human 293 Phoenix retroviral packaging cells were grown in DMEM with 10% FBS at 37°C.

U2OS cells were synchronized at G1/S by using double thymidine block. Briefly, cells were incubated for 17 h in the presence of 2.5 mM thymidine (Sigma, St. Louis, MO), then washed 3 times with PBS, and incubated in fresh medium. After 12 h, cells

were blocked again with 2.5 mM thymidine for 17 h. To obtain cells synchronized at pro-metaphase, cells were blocked with 30 ng/ml nocodazole (Sigma) for 16 h. Rounded cells were gently shaken off and collected by centrifugation at 800 rpm for 5 min. For flow cytometric analysis, cells were collected by trypsin treatment, washed with PBS+2%FBS, and fixed in 70% ethanol for 1 h at 4°C. After a PBS wash, cells were incubated for 30 min with 10 μg/ml propidium iodide and 250 U/ml RNase A (Calbiochem) at 37°C. Cell cycle analysis was done on a FACScan (BD Biosciences, San Diego, CA) at Vanderbilt Flow Cytometry Services Facility.

Subcellular Fractionation

To obtain whole cell extract, cells were washed with PBS and lysed in RIPA buffer (50 mM Tris-HCl at PH 7.5, 150 mM NaCl, 1% NP-40, 0.5% deoxycholic acid, 0.1% SDS, 1 mM PMSF, 10 μg/ml aprotinin, 1 μM leupeptin) on ice for 30 min. Then cell extracts were cleared by centrifugation at 12,500 rpm for 15 min.

To separate cytosol and intact nuclei, cells were extracted using digitonin to permeabilize the plasma membrane, releasing cytosolic proteins as described previously (Gu et al., 2004). Nuclei were extracted as described below to obtain soluble nuclear and chromatin-bound proteins.

Chromatin fractionation was performed as described (Mendez and Stillman, 2000) with some modifications. Briefly, a total of $\sim 5 \times 10^6$ cells were collected by trypsin treatment and centrifugation, washed with PBS and resuspended in 300 μl solution A (10 mM HEPES at pH 7.9, 10 mM KCl, 1.5 mM $MgCl_2$, 0.34 M sucrose, 10% glycerol, 1 mM DTT, 10 mM NaF, 1 mM Na_3VO_4, 1 mM PMSF, 10 μg/ml aprotinin, 1 μM

leupeptin). Triton X-100 was added to a final concentration of 0.05%, and the cells were incubated on ice for 5 min. Cytoplasmic proteins (S1) were separated from nuclei by centrifugation at 1300 × *g* for 5 min. Isolated nuclei were washed once with solution A and resuspended in 300 µl solution B (3 mM EDTA at pH 8.0, 0.2 mM EGTA, 1 mM DTT). After a 30-min incubation on ice, soluble nuclear proteins (S2) were separated from chromatin (P2) by centrifugation at 1700 × *g* for 5 min. Isolated chromatin was washed once with solution B, resuspended in 300 µl SDS-PAGE sample buffer, and sheared by sonication. To digest chromatin with micrococcal nuclease, nuclei were resuspended in solution A containing 1 mM $CaCl_2$ and 20 units of micrococcal nuclease (Sigma). After 4 min of incubation at 37°C, nuclei were lysed and fractionated as above. 8.5% SDS-PAGE and immunoblotting were performed as previously described (Gu et al., 2004).

Radiation and Drug Treatment

Cells were exposed to ionizing radiation (IR) from a ^{137}Cs source at a dose rate of 1.84 Gy/min. For ultraviolet (UV) treatment, growth medium was removed and cells were exposed to 254-nm UV in a Stratalinker (Stratagene, La Jolla, CA), followed by growth medium replacement. Hydroxyurea (Sigma) was dissolved in water at 0.5 M, and stored at -20°C. Camptothecin (Sigma) was dissolved in DMSO at 10 mM, and stored frozen. Aphidicolin were dissolved in DMSO at 2 mM and stored at -20°C. Wortmannin (Sigma) was dissolved in DMSO as a stock of 20 mM and stored at -20°C. Cells were pre-incubated with 200 µM wortmannin for 30 min before genotoxin treatment.

ShRNA-directed Gene Silencing

The pSuper (pS) and pRetro-Super (pRS) vectors were kindly provided by R. Agami (The Netherlands Cancer Institute, Amsterdam, Netherlands) (Brummelkamp et al., 2002a; Brummelkamp et al., 2002b). Three sequences targeting HDHB gene exon 1, 2, and 4 (shRNA-1: 5'-GAG TCC GTG TTC ATC GAC G-3', shRNA-2: 5'- CAG GTG CTT GGT GGA GAG T –3', and shRNA-3: 5'- GAC CAC AAT CGT TAG CCG T-3') and one control sequence targeting a GFP gene (Control-2: 5'- GAC CCG CGC CGA GGT GAA G-3') were selected. The pSuper vector served as Control-1. pS-HDHB, pRS-HDHB, and control-knockdown plasmids were generated as described previously (Brummelkamp et al., 2002a; Brummelkamp et al., 2002b). In brief, a 64-bp linker was inserted into pRS using the BamHI and HindIII sites. Oligonucleotide linkers containing HDHB-specific sense and GFP-specific sense sequences, flanking a 6-base hairpin, were PAGE purified (Integrated DNA Technologies, Coralville, IA). The three HDHB targeting sequences and GFP control sequence were cloned into pSuper or pSuper-Retro, which contains retrovirus packaging elements (Brummelkamp et al., 2002a). The constructed pSuper-Retro plasmids were transfected into the retrovirus packaging cell line Phoenix 293 as described on the Nolan lab website (http://www.stanford.edu/group/nolan) with minor modifications. Briefly, cells were transfected with each pRS-derived plasmid and selected with 5 µg/ml puromycin (Sigma-Aldrich). To harvest virus, cells at 75% confluence were incubated for 16 h at 37°C. Collected media were passed through a 0.45-µm syringe filter (Pall Corporation, East Hills, NY) and either used immediately or stored at -80°C. To infect U2OS or HCT116 cells, 4 µg/ml polybrene (Sigma-Aldrich) was added to virus stock before overlaying

cells plated at 6 x 10^4 cells/60-mm dish or 1.8 x 10^5 cells/100-mm dish. Cells were incubated overnight, then replated in DMEM, and selected in 5 μg/ml puromycin for 7–10 days.

For transient expression of HDHB-shRNA, pSuper-HDHB-shRNA was transfected into U2OS cells with Lipofectamine 2000 (Invitrogen, Carlsbad, CA) according to the manufacturer's protocol. Cells were allowed to grow for 48 hours before replating.

Co-immunoprecipitation

Recombinant GST-tagged human TopBP1 was purified as described (Liu et al., 2006). Protein A beads pre-bound to polyclonal anti-HDHB antibody were incubated with or without 1.5 μg of purified recombinant HDHB for 1 h at 4 °C. Then 5 μg purified GST-TopBP1 was added and the incubation was continued for another 1 h. Beads were washed three times with wash buffer (30 mM K-Hepes pH 7.8, 75 mM KCl, 7 mM $MgCl_2$, 0.25% inositol, 0.01% NP-40, 10 μM $ZnCl_2$). The associated proteins were separated on 8.5% SDS-PAGE and detected by western blotting.

Fluorescence Microscopy

To visualize RPA and TopBP1 DNA damage foci in pSuper or pSuper-HDHB-shRNA transfected U2OS cells, the cells were replated on cover slips in 35 mm dishes and treated 24 hours later with 30 J/m^2 UV. At the indicated time points after UV, cells were extracted for 5 min on ice with 0.2% Triton X-100 in CSK buffer (10 mM HEPES, pH 7.4, 300 mM sucrose, 100 mM NaCl, 3 mM $MgCl_2$, supplemented with 1x protease

inhibitors) and then fixed with 3.7% paraformaldehyde at room temperature for 20 min. Cells were stained with anti-RPA34 antibody (1:500 dilution) or anti-TopBP1 antibody (1:100 dilution) in phosphate-buffered saline (PBS) with 10% FBS at room temperature for 2 hours. After washing with PBS, cells were incubated with Cy3-conjugated secondary antibody (Jackson ImmunoResearch Laboratories, West Grove, PA) (1:100 dilution) for 1 h at room temperature. After three washes, the cells were incubated for 10 min with To-Pro-3 iodide (Invitrogen) at a concentration of 3 μM in PBS. Coverslips were mounted in ProLong Antifade (Molecular Probes, Eugene, OR). Pictures were taken on a Zeiss LSM 510 confocal microscope with three lasers giving excitation lines at 633, 543, and 488 nm. The data from the channels were collected sequentially using the appropriate band-pass filters built into the instrument. Data were collected at a resolution of 1024 × 1024 pixels, using optical slices of between 0.8 and 1.2 μm. Data sets were processed using the LSM image browser.

For GFP-HDHB colocalization, U2OS cells were transiently transfected with pGFP-HDHB expression plasmid (Gu et al., 2004). 24 hours later, cells were extracted, fixed, and stained as described above, except that the anti-Rad9 primary antibody was diluted 1:100 in PBS containing 10% FBS.

CHK1 Phosphorylation

Stable control- and HDHB-depleted HCT116 cells were plated in 100 mm dishes and grown to 80% confluence. Cells were then treated with 5 Gy IR or 2 μM aphidicolin. To obtain whole cell extract, 500 μl ice-cold RIPA buffer (50 mM Tris-Cl pH7.4, 150 mM NaCl, 1% NP-40, 0.5% deoxycholic acid, 0.1% SDS, 10 mM NaF, 1 μM Na_3VO_4, 1 mM PMSF, 10 μg/ml aprotinin, 1 μM leupeptin) were applied to the dish and cells were

scrubbed into the buffer. Cells were then transferred to an Eppendorf tube and left on ice for 20 min. Cell debris was removed by centrifuging at 12500 rpm for 15 min. The supernatant were mixed with 4×SDS sample buffer, boiled at 95°C for 5 min, and applied to 8.5% SDS-PAGE and western blotting. All the phospho-primary antibodies were diluted with 5% BSA in TBST. Blocking buffer and the dilution buffer for the secondary antibodies were 5% non-fat milk in TBST.

Results

HDHB Associates with Chromatin Throughout the Cell Cycle.

To determine whether HDHB associates with chromatin, we first generated and characterized polyclonal and monoclonal antibodies against recombinant HDHB. Crude polyclonal rabbit antiserum detected a major protein band at ~170 kDa and multiple other bands in U2OS whole cell extract (Figure II-1B, lane 1). Affinity-purified polyclonal antiserum detected primarily the ~170 kDa band (lane 2). Two rat monoclonal antibodies also recognized the ~170 kDa band (lanes 3, 4) and one of them also detected a minor 54 kDa band (lane 4). Purified recombinant HDHB (Figure II-1C, lanes 1) co-migrated with the ~170 kDa band detected by these antibodies in whole cell extract (lane 2), arguing that the ~170 kDa band represents full-length endogenous HDHB. Moreover, the intensity of this band was reduced in extracts of human cells expressing three different shRNAs against HDHB (Figure II-1A, Figure II-9A, B), confirming that these antibodies detect endogenous HDHB.

These antibodies were used to visualize HDHB in subcellular fractions prepared from asynchronously growing U2OS cells. Fractions enriched in soluble cytoplasmic and

Figure II-1. **A small fraction of HDHB resides on chromatin**. A, Functional domains of HDHB and location of shRNA target sequences. The superfamily I helicase domain (residues 467-926) is indicated (Gu et al., 2004). The phospho-subcellular localization domain (PSLD) contains signals for nuclear import and export (SLD) that are regulated by 7 CDK sites (SP/TP) (Gu et al., 2004). B, HDHB detected in whole cell extract (WCE) of U2OS cells by western blotting using rabbit anti-HDHB antiserum, affinity-purified polyclonal antibody, 4c11 and 5c9 monoclonal antibody, as indicated. C, Purified recombinant HDHB (20 ng) (lane 1) and U2OS whole cell extract (lane 2) detected by western blotting using polyclonal antibody. D, Asynchronously growing U2OS cells were fractionated as described in materials and methods to obtain a cytoplasmic fraction (S1), soluble nuclear fraction (S2), and chromatin-enriched fraction (P2). After removal of the S2 fraction, the chromatin-enriched nuclei were treated with micrococcal nuclease (MNase). The S2' and P2' fractions were obtained by extracting the digested nuclei. Orc2, a chromatin-bound protein, tubulin, a cytoplasmic protein, and WCE served as controls for the fractionation.HDHB was detected with polyclonal antibody (left panel) or 4c11 monoclonal antibody (right panel).

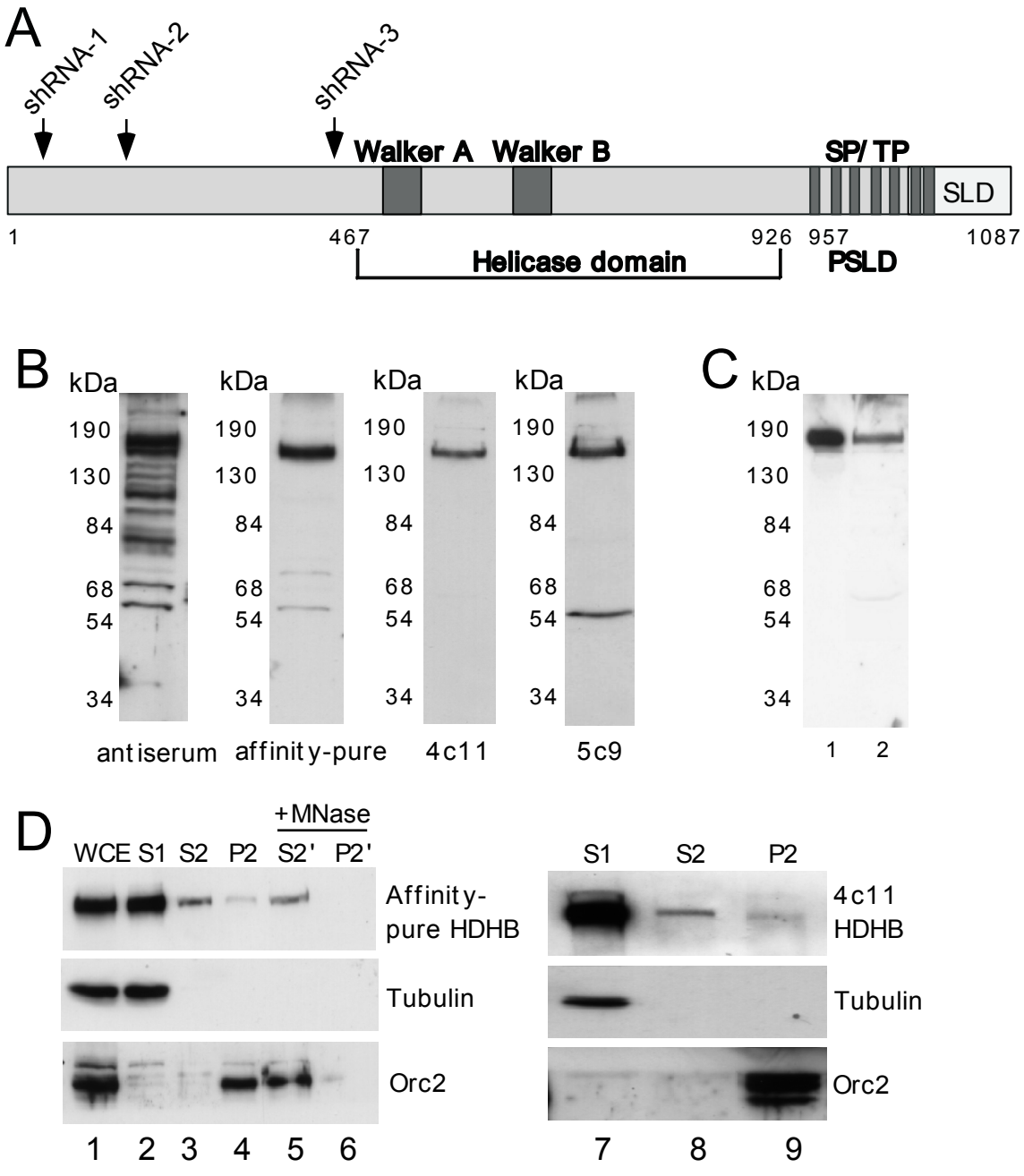
A
shRNA-1
shRNA-2
shRNA-3
Walker A
Walker B
SP/ TP
SLD
1
467
926
957
1087
Helicase domain
PSLD
B
kDa
190
130
84
68
54
34
antiserum
affinity-pure
4c11
5c9
C
1
2
D
+MNase
WCE S1 S2 P2 S2' P2'
Affinity-pure HDHB
Tubulin
Orc2
S1 S2 P2
4c11 HDHB
Tubulin
Orc2
1 2 3 4 5 6
7 8 9

Figure II-1

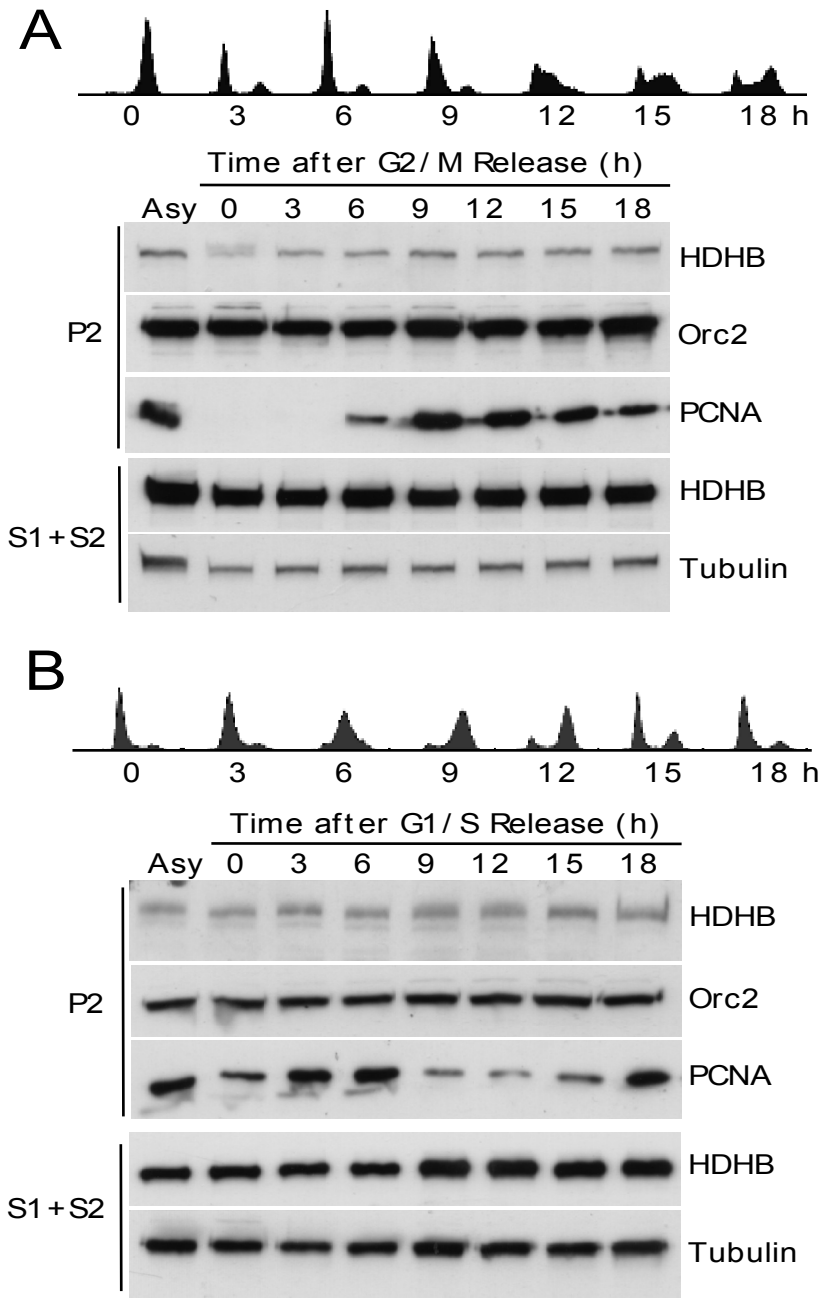

Figure II-2. **Chromatin association of HDHB is independent of the cell cycle in unperturbed cells**. A, U2OS cells were blocked at G2/M by nocodazole, and then released for the indicated times. Flow cytometry data is shown above. Proteins in the chromatin fraction (P2) and soluble fraction (S1+S2) were detected by western blotting with the indicated antibodies. Fractions from asynchronous cells (Asy) were analyzed in parallel. B, U2OS cells were released from a double thymidine block for the indicated times, fractionated, and analyzed as in panel A.

nuclear (S1, S2), and chromatin-bound proteins (P2) were analyzed by denaturing electrophoresis and western blotting (Figure II-1D). Tubulin and Orc2 served as controls for the fractionation. As expected, tubulin was found in the S1 fraction and Orc2, in the P2 fraction (Figure II-1D). Using the affinity-purified rabbit antibody, endogenous HDHB was found in all three fractions, with the greatest amount in the S1 fraction (Figure II-1D, lanes 2, 3). Similar results were obtained using HDHB monoclonal antibody 4c11 (lanes 7, 8). A small fraction of HDHB was detected in the P2 fraction (lanes 4, 9). To verify that the HDHB detected in P2 was not insoluble, but rather associated with chromatin, the isolated nuclei were treated with micrococcal nuclease to digest the chromatin, allowing solubilized chromatin-bound proteins (S2') to be separated from residual material (P2'). Both HDHB and Orc2 were released into S2' from the P2 fraction, confirming that they were in fact soluble proteins bound to chromatin in P2 (Figure II-1D, lanes 5, 6).

To investigate whether the level of chromatin-bound HDHB varies during the cell cycle, we arrested U2OS cells in pro-metaphase with a nocodazole block or in G1/S with a double thymidine block. Cells were collected at different times after release from the blocks, characterized by flow cytometry, and fractionated as in Figure II-1D. By 9 h after release from the nocodazole block, most of the cells were entering S phase, as indicated by flow cytometry (Figure II-2A, top), and the amount of PCNA associated with chromatin was maximal, as expected during S phase (Figure II-2A, bottom). At time 0 (G2/M), the level of chromatin-bound HDHB was reduced and the protein migrated as a diffuse band at slightly slower mobility. However, the amount of chromatin-bound HDHB remained nearly constant during G1 and S phase. Similarly, after release from the

G1/S block, the amount of chromatin-bound HDHB also remained approximately constant as cells progressed through S and G2/M phase (Figure II-2B). The level of soluble HDHB (S1+S2) also changed little during the cell cycle (Figure II-2A, B).

Genotoxins Induce Accumulation of HDHB on Chromatin, Most Prominently in S Phase Cells.

If HDHB participates in DNA damage signaling or repair, we might expect the level of HDHB on chromatin to increase in response to DNA damage. To test this prediction, asynchronously growing U2OS and HCT116 cells were exposed to UV, camptothecin, hydroxyurea, or ionizing radiation. Each of these agents led to increased amounts of HDHB in the chromatin fraction P2, while no increase in the soluble fractions S1+S2 was detectable (Figure II-3A, B, data not shown). The amount of chromatin-bound HDHB increased with the dosage of UV (10-100 J/m^2) or IR (4-24 Gy) and with time after irradiation (data not shown). The level of chromatin-bound RPA also rose in cells exposed to UV, camptothecin, or hydroxyurea (Figure II-3B, lanes 2, 4, 6), consistent with a large body of evidence that these agents generate lesions that cause DNA unwinding at replication forks to be uncoupled from the replicative DNA polymerases (Ball et al., 2005). Also consistent with fork uncoupling or collapse, the amount of PCNA associated with chromatin decreased after camptothecin treatment (Figure II-3B, lane 4). These results demonstrate that additional HDHB was recruited to chromatin in cells exposed to a variety of DNA damaging agents.

Since agents known to uncouple DNA unwinding from replication increased the amount of HDHB on chromatin (Figure II-3), we asked whether damage-induced HDHB

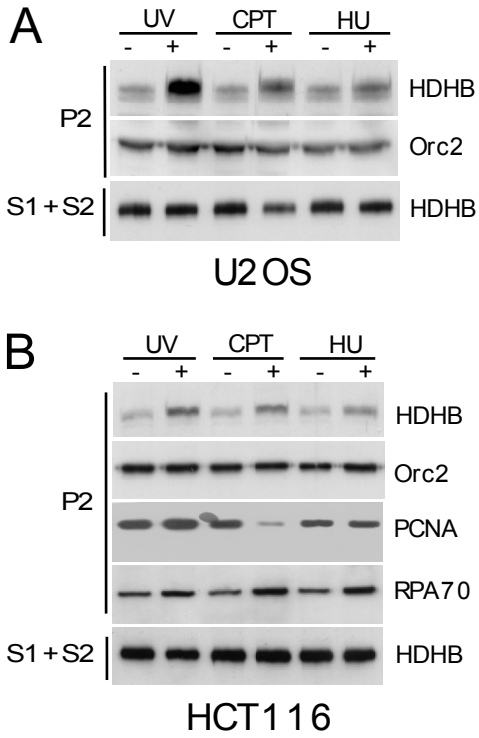

Figure II-3 **UV, camptothecin and hydroxyurea stimulate HDHB chromatin association.** (A) U2OS, or (B) HCT116 cells were treated with 100 J/m^2 UV, 10 μM camptothecin (CPT) or 5 mM hydroxurea (HU) as indicated. Two h later, cells were fractionated and extracts were analyzed by western blotting.

recruitment to chromatin might depend on the cell cycle. To examine this possibility, U2OS cells were enriched in G1, S, or G2/M phase and exposed to UV, camptothecin, hydroxyurea, or IR. UV, camptothecin, or hydroxyurea-induced accumulation of HDHB on chromatin was strongly increased in S phase cells, but little increase was detected in G1 or G2/M cells (Figure II-4). In contrast, IR-induced HDHB recruitment to chromatin was identical in G1, S, and G2/M cells (Figure II-4D). Little or no change in the level of soluble HDHB was noted in the cell cycle, with or without genotoxin treatment (Figure II-4).

Soluble Nuclear HDHB Redistributes to Chromatin in Response to DNA Damage.

The damage-induced increase in chromatin-bound HDHB could arise through a variety of different mechanisms, e.g. increased gene expression, reduced protein turnover, or redistribution from the soluble fraction. Since S phase cells displayed the greatest increase in chromatin-bound HDHB (Figure II-3) and contain most of the soluble HDHB in the cytoplasm (Gu et al., 2004), we used S phase cells to investigate whether HDHB redistributes from the soluble fraction to chromatin after exposure to camptothecin or UV. The plasma membrane was permeabilized with digitonin in isotonic buffer to preferentially extract cytoplasmic proteins. The residual nuclei were then extracted to separate soluble nuclear proteins from chromatin-bound proteins. The levels of HDHB and several known damage response proteins were visualized by western blots of each fraction (Figure II-5). HDHB levels in the cytoplasmic fraction were not significantly altered after DNA damage (Figure II-5, lanes 1-3). However, the amount of HDHB in the soluble nuclear fraction was reduced after DNA damage (compare lane 4 with 5, 6),

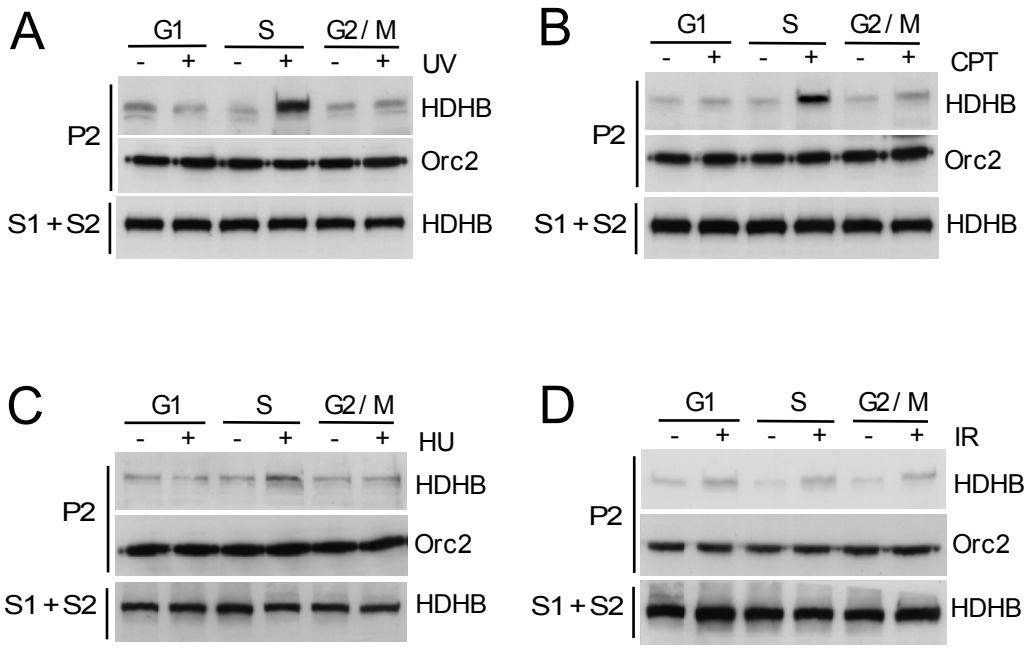

Figure II-4. **Damage-induced accumulation of HDHB on chromatin varies in the cell cycle**. U2OS cells were released from a double thymidine block for 3 h into S phase or for 9 h into G2/M phase. Cells were released from a nocodazole block into G1 phase for 4 h. Cells in each phase were treated with (A) 100 J/m^2 UV, (B) 10 μM camptothecin (CPT), (C) 5 mM hydroxyurea (HU), or (D) 20 Gy IR. Two h later, chromatin was isolated and subjected to western blotting.

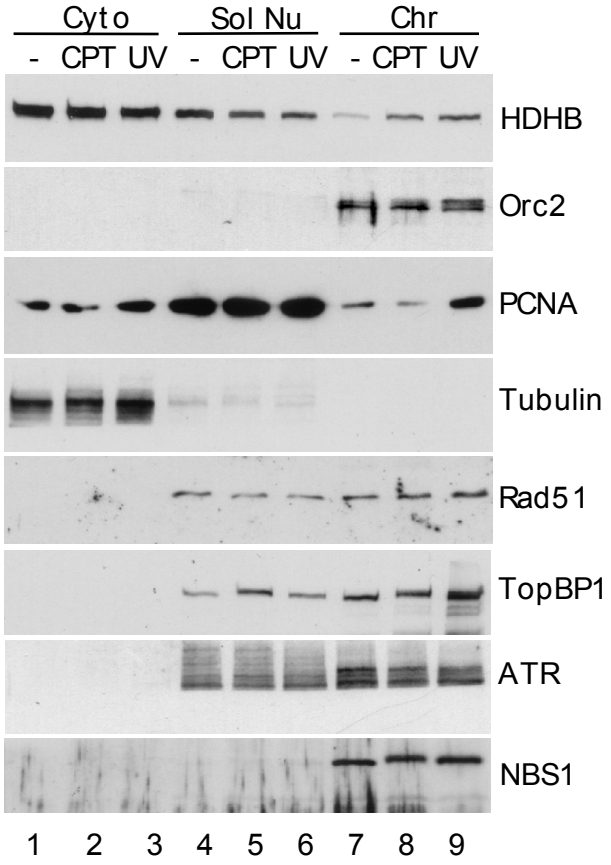

Figure II-5. **Soluble nuclear HDHB migrates to chromatin in response to UV irradiation and CPT treatment.** U2OS cells progressing synchronously through S phase were treated with 10 μM camptothecin (CPT) or 100 J/m^2 UV. Two h later, cells were extracted with digitonin to separate cytosol (Cyto) from nuclei as described (Gu et al., 2004). Then the nuclei were extracted with solution B to separate soluble nuclear (Sol Nu) and chromatin fractions (Chr), as described in materials and methods. Proteins in each fraction were visualized by western blotting.

approximately in proportion to the increase in chromatin-bound HDHB (compare lane 7 to lanes 8, 9). Bands of NBS1 and TopBP1 migrated more slowly after damage (compare lane 7 to lanes 8, 9), consistent with their reported phosphorylation by checkpoint kinases (Abraham, 2001; Garcia et al., 2005; Hashimoto et al., 2006; Kumagai et al., 2006). The levels of chromatin-bound Rad51, TopBP1, and PCNA (compare lanes 7 and 9) also increased slightly after UV. Taken together, these data argue that most of the genotoxin-induced increase in chromatin-bound HDHB is derived from redistribution of soluble nuclear HDHB to chromatin.

Damage-induced Recruitment of HDHB to Chromatin does not Require Checkpoint Kinase Activity.

DNA damage activates protein kinases of the PIKK family ATM, ATR, DNA-PK, which in turn activate downstream effector kinases CHK1 and CHK2 whose activities promote cell cycle arrest and DNA repair (Abraham, 2001; Bartek et al., 2004; Collis et al., 2005; Uziel et al., 2003). To assess whether checkpoint kinase activity is necessary for damage-induced recruitment of HDHB to chromatin, U2OS cells were treated with wortmannin, a broad spectrum inhibitor of ATM, ATR, DNA-PK, and related lipid kinases at a dose sufficient to inhibit this family of kinases (Sarkaria et al., 1998). The effectiveness of inhibition was verified by examining the phosphorylation of CHK1 and CHK2, which are substrates of ATR and ATM after DNA damage (Goldberg et al., 2003). Phosphorylation of CHK2 threonine 68 was triggered by IR, UV, and camptothecin, and was strongly inhibited by wortmannin (Figure II-6A). Phosphorylation of CHK1 on serine 345 was also inhibited in the presence of the drug (Figure II-6B), indicating that

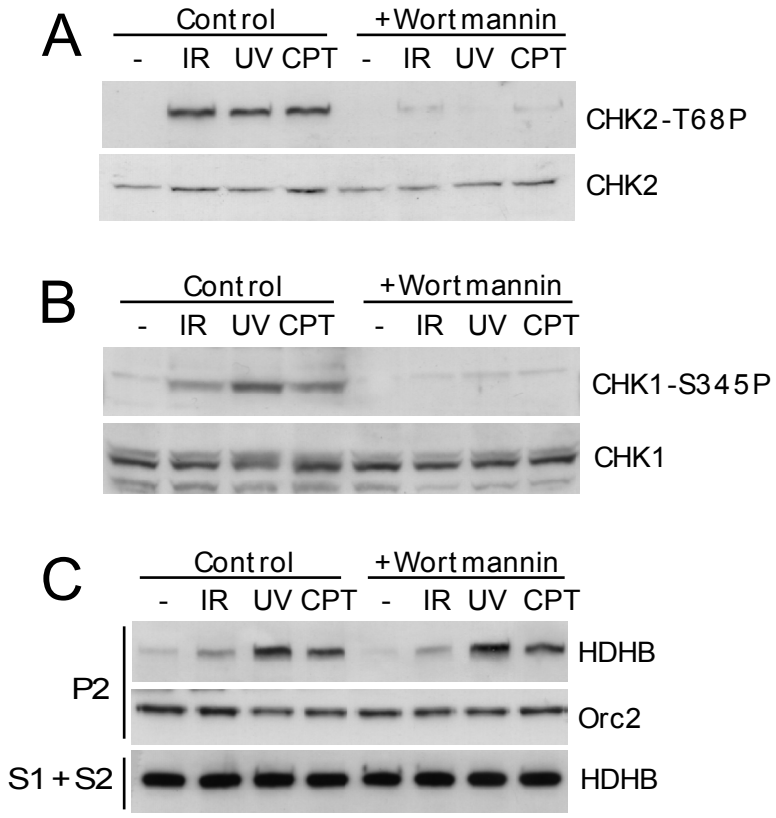

Figure II-6. **Genotoxin-induced accumulation of HDHB on chromatin does not require checkpoint signaling.** U2OS cells were treated with DMSO (control) or 200 μM wortmannin for 30 min prior to 20 Gy IR, 100 J/m^2 UV or 10 μM camptothecin (CPT) treatment. Two h later, whole cell extracts were prepared and subjected to western blotting with (A) anti-Chk2 and anti-phospho-Chk2 (Thr68), or (B) anti-Chk1 and anti-phospho-Chk1 (Ser345) antibodies. C, U2OS cells were treated with wortmannin and genotoxins as in A and B, then fractionated and analyzed by western blotting as indicated.

wortmannin effectively inhibited ATM, ATR, and DNA-PK activities in vivo. However, in the presence of wortmannin, IR, UV, and camptothecin still induced HDHB recruitment to chromatin (Figure II-6C). Furthermore, siRNA against ATM or ATR did not inhibit damage-induced accumulation of HDHB on chromatin (data not shown). These results provide evidence that genotoxin-induced recruitment of HDHB to chromatin does not depend on PIKK signaling in vivo.

The Chromatin-associated Fraction of HDHB Functions Together with RPA, Rad9, and TopBP1 in the Early Steps of the Intra-S phase DNA Damage Response.

The observation that PIKK signaling was not required for damage-induced chromatin-binding of HDHB (Figure II-6C) suggested that HDHB might bind directly to DNA lesions or to other damage response proteins that are recruited to lesions independently of PIKK signaling, such as RPA, the Rad9-Hus1-Rad1 checkpoint clamp, and TopBP1 (Byun et al., 2005; Ellison and Stillman, 2003; Greer et al., 2003; Hashimoto et al., 2006; Kumagai et al., 2006; Makiniemi et al., 2001; Parrilla-Castellar and Karnitz, 2003; Yan et al., 2006; You et al., 2002). As a first step to assess this idea, we compared the kinetics of HDHB chromatin recruitment with those of damage response proteins recruited early in the intra-S phase damage response. We exposed S phase U2OS cells to UV, fractionated the cells at different time points, and detected chromatin-bound proteins by western blot. Although the relative levels of chromatin-bound proteins cannot be evaluated from western blots, it is possible to track the time-dependent recruitment of each protein to chromatin. The levels of chromatin-bound HDHB, RPA, and Rad9 increased in parallel in the first hour after UV irradiation (Figure

II-7A). RPA and Rad9 levels then reached a plateau, while HDHB levels appeared to increase further (Figure II-7A, B). However, no change in the level of chromatin-bound TopBP1 or Orc2 was detected.

The parallel recruitment of HDHB, RPA, and Rad9 to chromatin after UV exposure raised the question of whether HDHB co-localizes with these proteins on chromatin. Since our antibodies against HDHB cannot detect the endogenous protein by immunofluorescence microscopy of human cells (data not shown), we transiently expressed GFP-tagged HDHB in U2OS cells and stained endogenous TopBP1 or Rad9 to test for co-localization in foci with HDHB. Two different focal staining patterns were observed (Figure II-8A, B). In pattern 1, GFP-HDHB nuclear foci partially co-localized with TopBP1 or Rad9 foci, whereas little co-localization was observed in pattern 2. About half of the transfected cells showed HDHB foci that co-localized with TopBP1 and about 60% of the transfected cells showed HDHB foci that co-localized with Rad9 (Figure II-8C).

Partial co-localization of HDHB with TopBP1 or Rad9 would be consistent with HDHB interaction with these proteins. To test whether HDHB interacts directly with TopBP1, co-immunoprecipitation experiments were performed with purified recombinant proteins. Bacterially expressed human TopBP1 was incubated with HDHB or with buffer control, collected on beads coated with anti-HDHB antibody, and detected by western blot (Figure II-8D). A small fraction of the TopBP1 was co-precipitated in the presence of HDHB (lane 2), but not in the control lacking HDHB (lane 1), demonstrating that the two proteins are capable of direct interactions with each other in vitro.

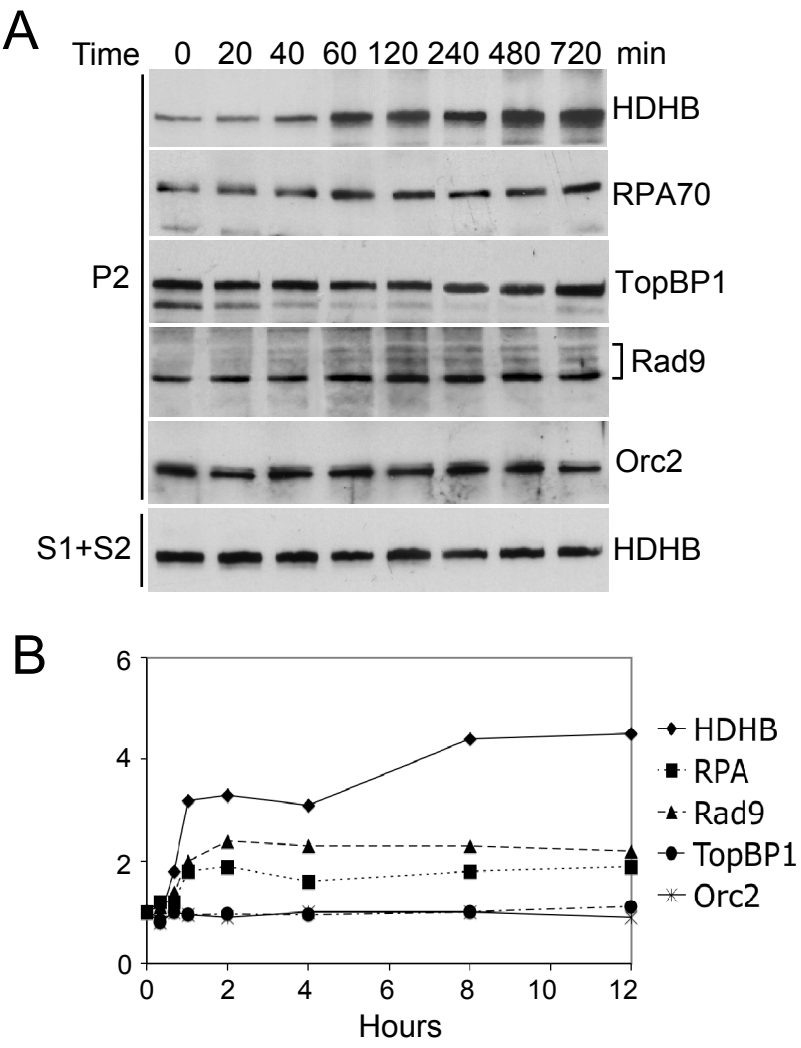

Figure II-7. **Time course of HDHB, RPA, TopBP1, and Rad9 chromatin association in UV-treated S phase cells.** U2OS cells were released from a double thymidine block for 3 h into S phase and then treated with 100 J/m^2 UV. At the indicated time points after UV, cells were fractionated and extracts were analyzed by western blotting.

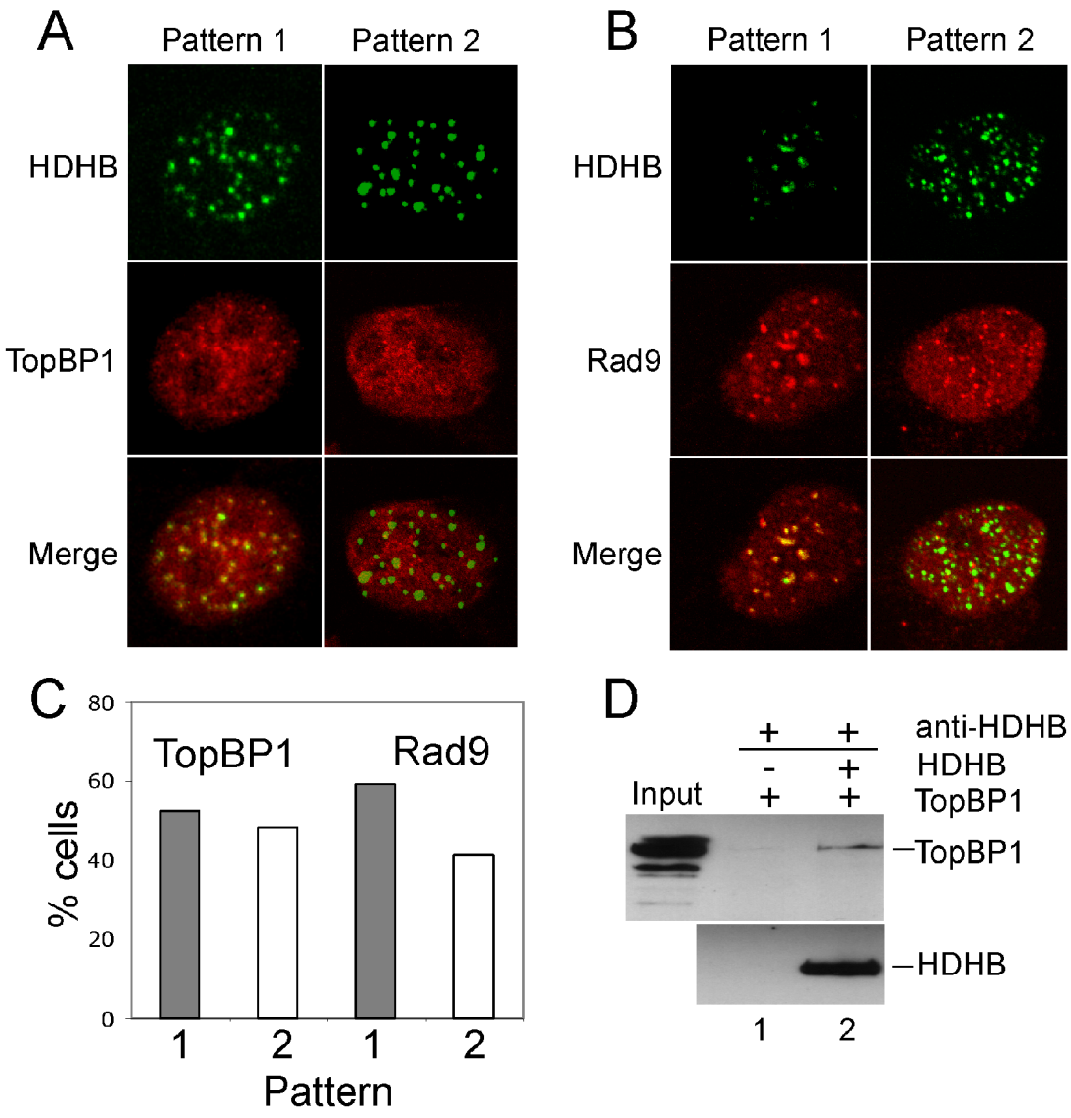

Figure II-8. **HDHB partially co-localizes with TopBP1 and Rad9 foci and interacts directly with TopBP1.** Asynchronous U2OS cells transiently expressing GFP-HDHB were extracted, fixed, and stained for endogenous TopBP1 (A) and Rad9 (B). Chromatin-bound proteins were visualized by confocal fluorescence microscopy. C, Percentage of GFP-positive cells with co-localizing GFP-HDHB and TopBP1 or Rad9 foci (pattern 1) or with separated foci (pattern 2). D, Purified bacterially expressed GST-TopBP1 was incubated in the presence (+) or absence (-) of purified HDHB. Proteins complexes were immunoprecipitated with polyclonal anti-HDHB antibody and analyzed by western blotting. Input lane, 10% of the GST-TopBP1 added to the reactions in lanes 1, 2.

The co-recruitment and co-localization of HDHB with proteins known to function early in the intra-S phase DNA damage response and its interaction with TopBP1 (Figure II-7, 8) suggested that HDHB might affect recruitment of other damage response proteins to sites of damage. If so, silencing of HDHB in human cells would be predicted to slow or inhibit recruitment of downstream proteins to damaged chromatin. Conversely, silencing of HDHB should not affect recruitment of any upstream damage response proteins. To test this possibility, we depleted endogenous HDHB from human cells using three different small hairpin RNAs (shRNAs) directed against HDHB coding sequences or control sequences. All three shRNAs were effective and no depletion was observed with empty vector or control shRNA (Figure II-9A). Transient HDHB silencing by shRNA-2 was characterized in greater detail. Transient HDHB depletion was also ~80% effective, and importantly, it did not detectably affect the levels of several other DNA damage response proteins (Figure II-9B) or the cell cycle distribution of shRNA-expressing cultures (Figure II-9C).

The time course of UV-induced recruitment of RPA and TopBP1 into chromatin-bound foci was then visualized by confocal immunofluorescence microscopy in U2OS cells in which HDHB had been transiently silenced with pSuper expressing shRNA-2 against HDHB or vector alone. Few unirradiated cells displayed chromatin-bound RPA, but it was clearly detected within 30 min after UV (Figure II-10A, B). Most of the chromatin-bound RPA was distributed throughout the nucleus, but more than half of the cells also contained distinct foci of RPA. The fraction of cells containing 3 or more distinct RPA foci was determined in a double-blind counting protocol in three independent experiments, each with 250 cells. The fraction of cells with RPA foci was

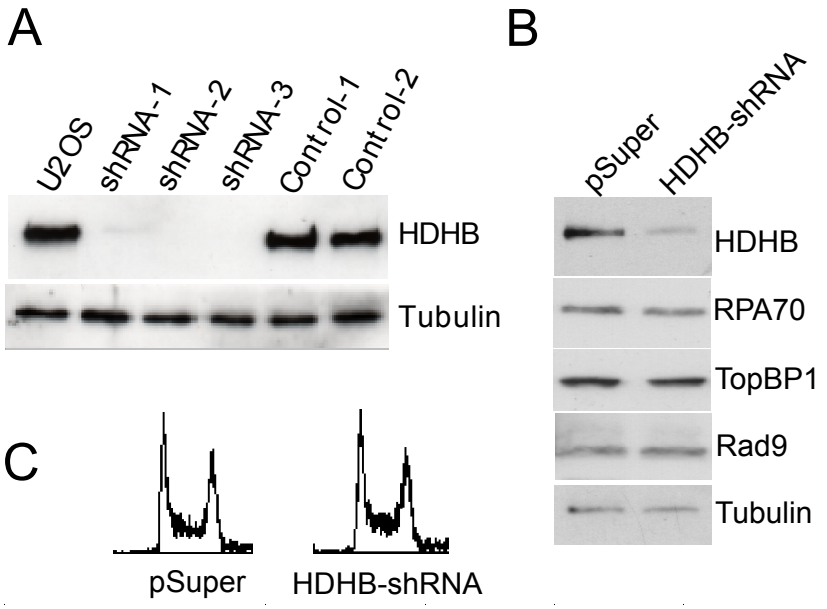

	G1	S	G2/M
pSuper	41.3%	23.3%	29.9%
HDHB-shRNA	41.0%	23.9%	28.3%

Figure II-9. **Silencing of endogenous HDHB in human cells does not significantly perturb cell cycle distribution**. A, RIPA extracts of stable control-knockdown (control-1 and -2) and HDHB-knockdown cultures of U2OS cells (sh-1, -2, and -3) were separated by 7.5% SDS-PAGE and immunoblotted with HDHB and tubulin antibodies. B, U2OS cells were transiently transfected with pSuper or pSuper vector expressing HDHB sh-2. Western blotting of whole cell extracts was performed 3 days later. C, Cell cycle profiles of asynchronously growing U2OS cells transiently transfected with sh-2 or pSuper.

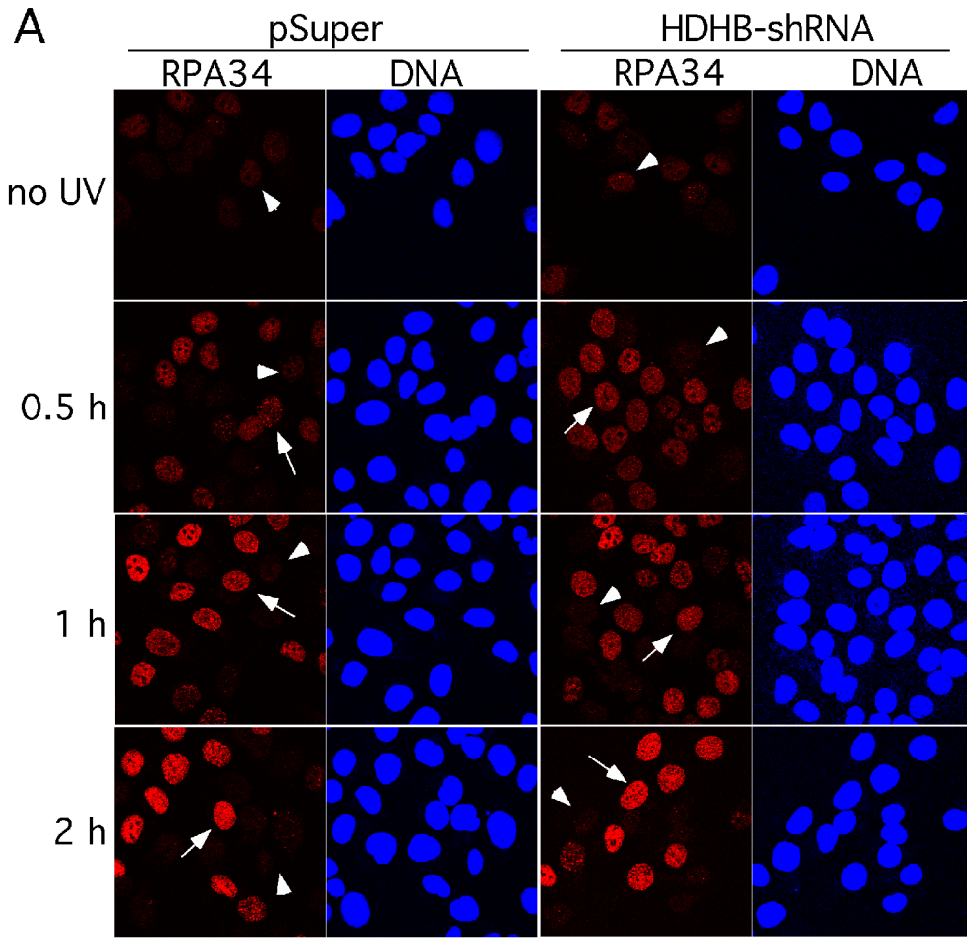

Figure II-10--cont.

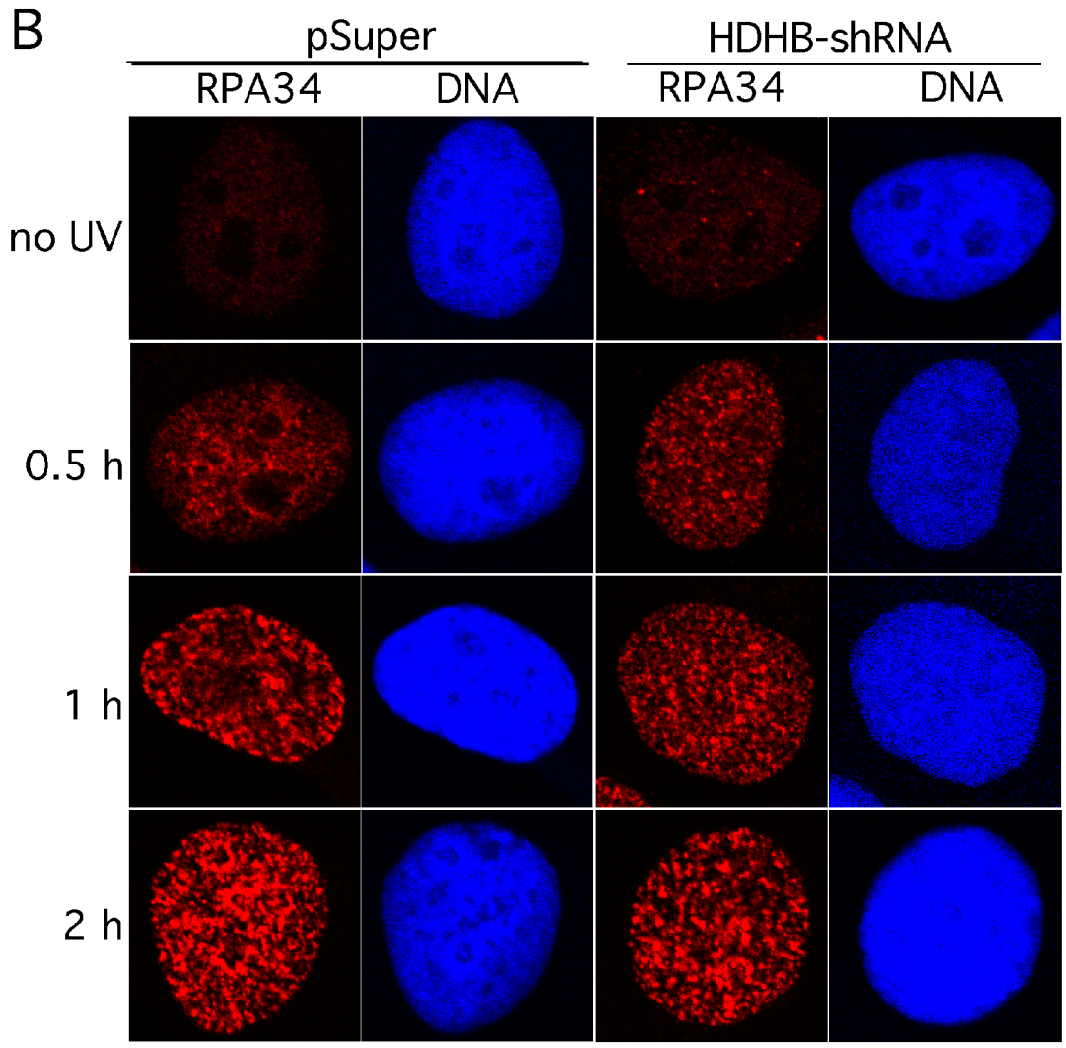

Figure II-10--cont.

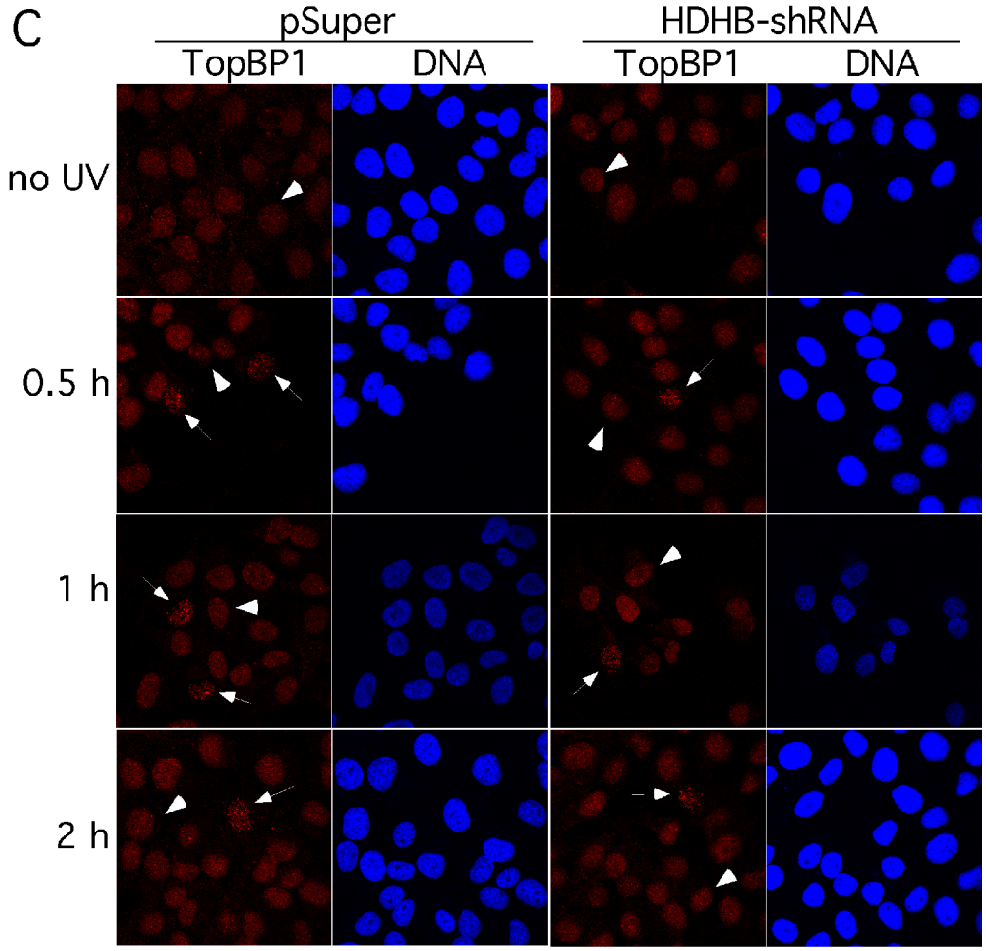

Figure II-10--cont.

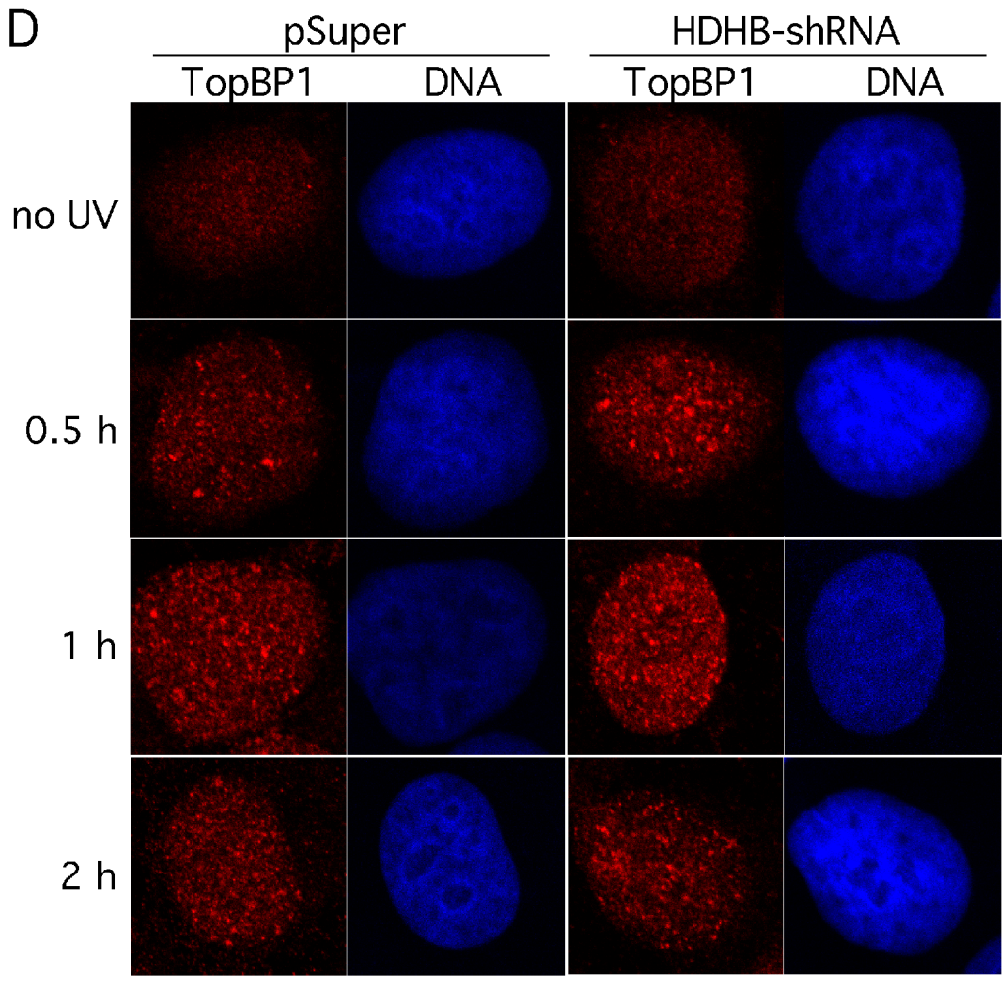

Figure II-10--cont.

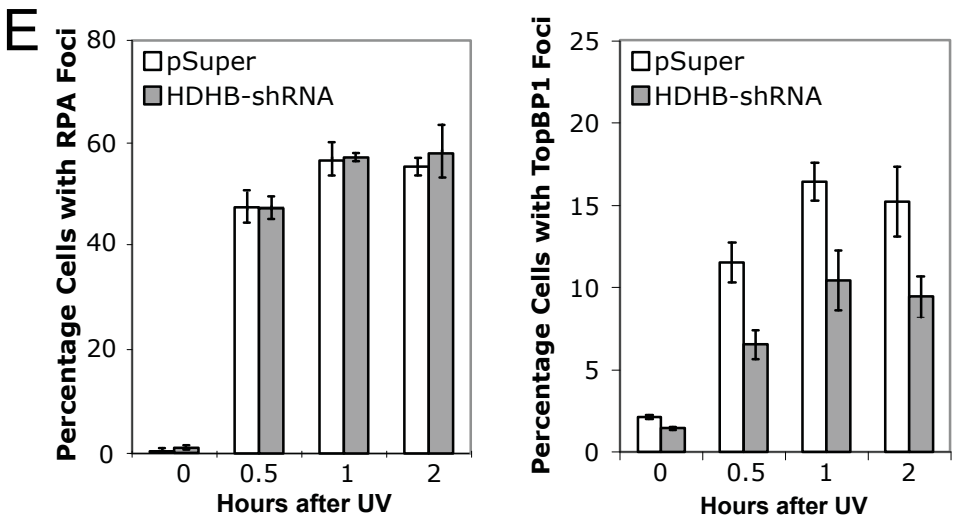

Figure II-10. **HDHB silencing diminishes UV-induced TopBP1 focus formation.** A, C, Fields of U2OS cells transiently transfected with pSuper or HDHB-sh2 were UV-irradiated (30 J/m^2), stained for DNA and chromatin-bound RPA (A) or TopBP1 (C) after the indicated times, and examined by confocal immunofluorescence microscopy. B, D, Single nuclei with UV-induced RPA (B) or TopBP1 (D) foci in pSuper- or HDHB-shRNA-transfected cells. E, Percentage of cells with 3 or more distinct RPA34 or TopBP1 foci after UV damage (evaluated in 3 independent experiments by double-blind counting of 250 cells at each time point). To distinguish bright foci from chromatin-bound RPA or TopBP1, view panel A and C as high resolution images with zoom-in setting. Arrows in panels A and C indicate cells with UV-induced foci (3 or more per nucleus); arrowheads indicate cells without foci or fewer than 3 per nucleus.

essentially identical in cultures depleted of HDHB or mock-depleted (Figure II-10E). Although TopBP1 resided on chromatin even in unirradiated cells (Figure II-7), few TopBP1 foci were visualized in unirradiated cells (Figure II-10C, D). However, within 30 min after UV exposure, TopBP1 was clearly detected in nuclear foci in some of the cells (Figure II-10C, D). Notably, UV-induced TopBP1 focus formation was significantly impaired in HDHB-depleted cultures relative to mock-depleted cultures (Figure II-10E). We conclude that HDHB silencing had no effect on UV-induced RPA chromatin-binding or focus formation, but significantly diminished TopBP1 focus formation.

DNA-damage Induced CHK1 Phosphorylation is Impaired in HDHB-depleted Cells

Since HDHB responses to stalled replication forks and is required for TopBP1 focus formation after UV, we reasoned that HDHB might be important for ATR-dependent phosphorylation events. Thus we tested the level of CHK1 phosphorylation after IR, which is reported to be consequence of ATR and ATM kinase activities, especially ATR (Brown and Baltimore, 2003), in stable control- and HDHB-depleted HCT116 cells. HDHB-shRNA-3 specifically reduced HDHB levels in HCT116 cells. CHK1 ser345 showed reduced phosphorylation induction in HDHB-knock down cells, although ATM ser1981 autophosphorylation and CHK2 phosphorylation showed no difference in HDHB-knock down cells and control cells (Figure II-11A).

We also used aphidicolin to treat HCT116 cells. As shown in Figure II-11B, there was less CHK1 phosphorylation in stable HDHB-knock down cells after 2 μM aphidicolin treatment. To exclude the possible influence of cell cycle distribution on CHK1 phosphorylation, we synchronized cells in S phase by double thymidine block and

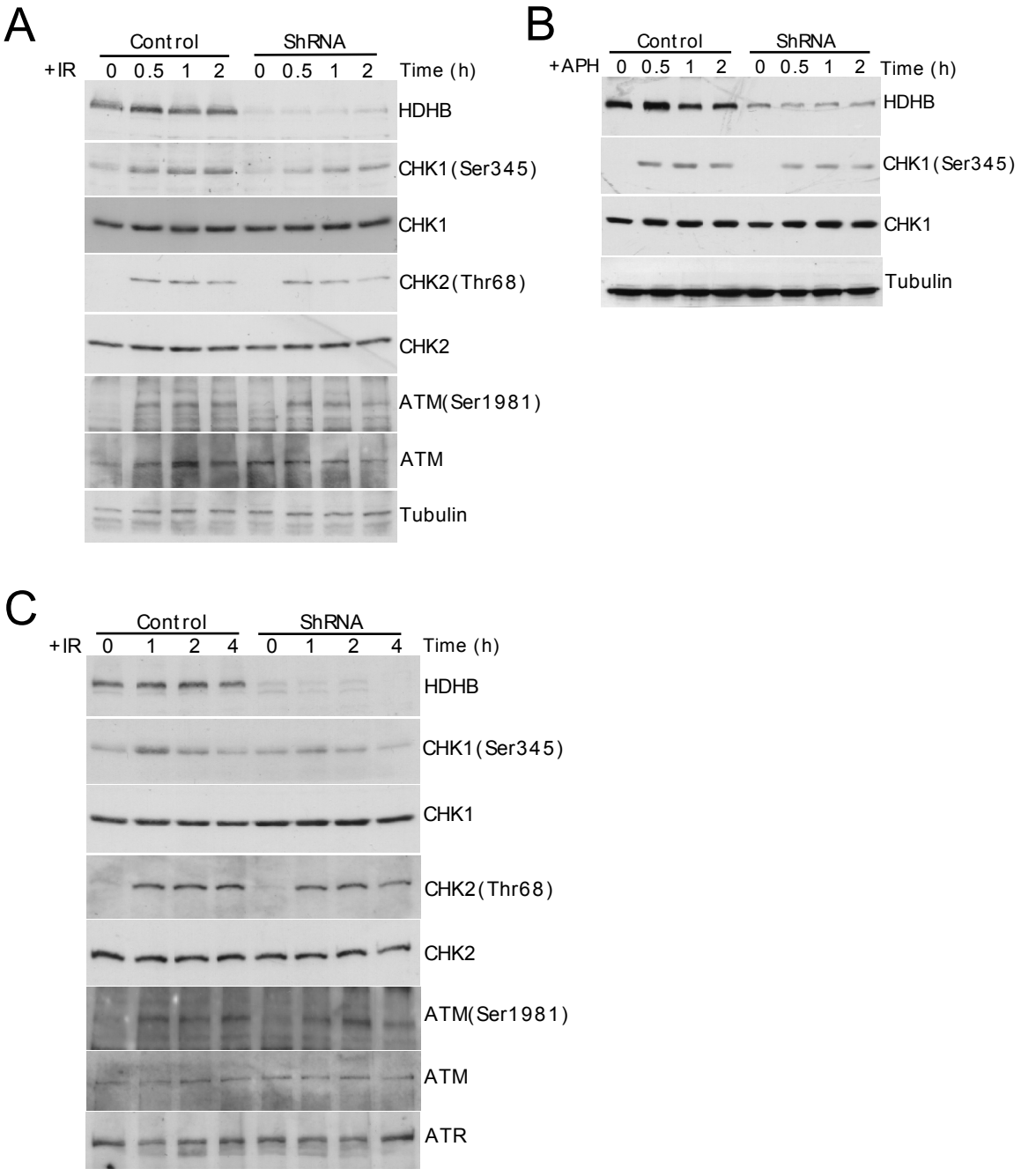

Figure II-11. **HDHB-depleted Cells show less CHK1 phosphorylation after DNA damage.** A, HDHB-depleted HCT116 cells or control cells were treated with 5 Gy IR. Whole cells extracts were prepared at indicated time points and analyzed by western blotting. B, Cells were treated with 2 μM Aphidicolin (APH) and analyzed as in panel A. C, HCT116 cells were synchronized in S phase cells by double thymidine block, treated with 5 Gy IR and analyzed as in panel A.

treated cells with 5 Gy IR. 1 h after IR, phosphorylated CHK1 reached maximal level (Figure II-11C). There was less induction of phosphorylated CHK1 in HDHB-depleted cells than control-depleted cells (Figure II-11C). These results support our hypothesis that HDHB couples with TopBP1 to enhance DNA damage signaling.

Discussion

We have shown here that in response to a variety of DNA damaging agents, soluble nuclear HDHB is recruited to chromatin. HDHB recruitment to chromatin is most effective in response to agents that result in uncoupling of replication forks in S phase cells. Damage-induced recruitment of HDHB occurs in parallel with recruitment of RPA and Rad9 to chromatin and does not depend on checkpoint kinase signaling. Chromatin-bound HDHB partially co-localizes in foci with Rad9 and TopBP1. In vitro, HDHB interacts physically with TopBP1 and in vivo, silencing of HDHB correlates with reduced formation of TopBP1 foci on damaged chromatin. In contrast, although HDHB also interacts with RPA ((Taneja et al., 2002) and Guler and Fanning, unpublished), HDHB depletion in human cells does not diminish damage-induced RPA recruitment to chromatin or focus formation. These results suggest that HDHB functions in an early step of the intra-S phase damage response that is needed for optimal TopBP1 focus formation.

How might HDHB function in the S phase DNA damage response to stimulate TopBP1 focus formation? The current model for activation of the S phase damage response involves two independent pathways that converge to activate ATR kinase activity (Kumagai et al., 2006). Both pathways begin with extended stretches of RPA-ssDNA, a common intermediate that results from damage processing or helicase-polymerase uncoupling of replication forks (Ball et al., 2005). In one pathway, ATR

binds to RPA-ssDNA in an ATRIP-dependent manner. This interaction recruits the kinase to sites of damage, but is not sufficient to activate ATR to phosphorylate the effector kinase CHK1 (Ball et al., 2005; Kim et al., 2005; Zou and Elledge, 2003). In the second pathway, Rad17-RFC loads the Rad9-Hus1-Rad1 clamp at recessed 5' primer ends on the RPA-ssDNA (Bermudez et al., 2003; Ellison and Stillman, 2003; Parrilla-Castellar et al., 2004; Zou and Elledge, 2003). Loading of the Rad9-Hus1-Rad1 clamp requires that pol-prim first generate these primers on the RPA-ssDNA template (Byun et al., 2005; Parrilla-Castellar and Karnitz, 2003; Yan et al., 2006; You et al., 2002).

Given the abundance of intracellular RPA, the ability of pol-prim to generate primers on RPA-saturated ssDNA is restricted and likely requires a mediator protein to remodel ssDNA-bound RPA into a state that dissociates more readily and, in concert, load pol-prim for primer synthesis (Fanning et al., 2006). HDHB displays such mediator activity in reactions reconstituted with purified recombinant proteins (Taneja et al., 2002), suggesting its potential function in this second branch of the S phase damage response. Consistent with this speculation, HDHB is recruited to damaged chromatin in parallel with RPA and Rad9 (Figure II-7) and partially co-localizes with Rad9 foci (Figure II-8B, C).

The fact that HDHB has robust DNA helicase activity (Taneja et al., 2002) might suggest its involvement in generating the extended stretches of RPA-ssDNA that initiate the S phase damage response. However, we doubt that this is a physiological function of HDHB. There is abundant evidence that the Cdc45-MCM2-7-GINS complex unwinds duplex DNA at the fork and that its activity is needed to generate the extended RPA-ssDNA (Byun et al., 2005). Moreover, the level of endogenous HDHB is low and most of

it is in the cytoplasm during S phase (Gu et al., 2004) (Figure II-5). Lastly, depletion of HDHB has no detectable effect on the recruitment of RPA to chromatin in response to damage in S phase cells (Figure II-10A, B, E).

The two branches of the S phase damage response are thought to converge in a process that requires TopBP1 (Ball et al., 2007; Hashimoto et al., 2006; Kumagai et al., 2006; Yan et al., 2006). TopBP1 binding to ATRIP (Ball et al., 2007; Hashimoto et al., 2006; Kumagai et al., 2006) and to the Rad9 clamp (Garcia et al., 2005; Greer et al., 2003) is required for CHK1 phosphorylation by ATR. Moreover, TopBP1 is required for pol-prim recruitment to damaged DNA (Parrilla-Castellar and Karnitz, 2003), suggesting a potential function for the observed HDHB interaction with TopBP1 (Figure II-8D) and a possible mechanism for the impaired TopBP1 focus formation in HDHB-depleted human cells (Figure II-10C-E).

The speculative model above is plausible and consistent with the available evidence. If HDHB functions in the S phase damage response as speculated above, we would expect it to be required for ATR-dependent phosphorylation of CHK1. In fact, we observed a reduced CHK1 phosphorylation after DNA damage in HDHB-depleted cells (Figure II-11). The model further predicts that the level of HDHB should have influence on Rad9 recruitment to chromatin or focus formation in damaged S phase cells, but not on ATRIP or ATR recruitment. This model is testable and much work remains for the future.

CHAPTER III

HUMAN DNA HELICASE B PROMOTES HOMOLOGOUS RECOMBINATION BY STIMULATING 5'-3' HETERODUPLEX EXTENSTION

Introduction

DNA helicase B, a mammalian member of superfamily I (SF1) DNA helicases, has been identified in mouse (Tada et al., 2001) and human (Taneja et al., 2002). Both mouse and human DNA helicase B (HDHB) can interact with DNA polymerase α-primase and stimulate the activity of DNA primase in vitro (Saitoh et al., 1995; Taneja et al., 2002). Microinjection of Walker B mutant HDHB into the nucleus of G1 phase cells inhibited DNA synthesis (Taneja et al., 2002), suggesting that HDHB may regulate DNA synthesis in vivo, possibly by participating in DNA replication initiation.

Endogenous HDHB localizes in both cytoplasm and nucleus in asynchronously growing cells, a process partially regulated by CDK-depdendent phosphorylation (Gu et al., 2004). Ectopically expressed GFP-HDHB forms nuclear foci, which are stimulated by different DNA damaging agents such as topoisomerase II inhibitor etoposide, or topoisomerase I inhibitor camptothecin (Gu et al., 2004). This suggests that HDHB nuclear foci are associated with DNA damage response.

HDHB shares sequence motifs with *E. coli* RecD and T4 dda helicases (Taneja et al., 2002). Both of these prokaryotic proteins are involved in homologous recombination (Dudas and Chovanec, 2004; Paques and Haber, 1999), raising the question of whether HDHB might function in homologous recombination. We recently found that HDHB accumulates on chromatin in cells exposed to camptothecin, HU, or UV (Chapter II).

This damage-induced recruitment of HDHB to chromatin was specific for S phase cells, implicating stalled or collapsed replication forks in HDHB recruitment. Furthermore, UV- or camptothecin-induced chromatin binding of HDHB did not require DNA damage signaling. HDHB interacted directly with purified TopBP1 and was required for TopBP1 focus formation after UV (Chapter II). We speculated that HDHB functions with TopBP1 to initiate DNA damage signaling during replication fork arrest.

Here we have further characterized the role of HDHB in DNA damage response. We show that HDHB-depleted cells are more sensitive than control-depleted cells to damage induced by mitomycin C, camptothecin, and IR. Repair of these lesions is known to depend on homologous recombination (Adachi et al., 2004; McHugh et al., 2001), suggesting that HDHB may function in homologous recombination. Consistent with this notion, HDHB-depleted cells exhibit more chromosome breaks and gaps after aphidicolin treatment and undergo fewer sister chromatid exchange events than control-depleted cells. Moreover, homologous recombination induced by I-SceI cleavage in a chromosomal recombination reporter cassette was reduced in HDHB-depleted cells. In an *in vitro* assay conducted with purified proteins, HDHB stimulated Rad51-mediated 5'-3' heteroduplex extension. The results provide evidence that HDHB functions in homologous recombination repair, likely in post-synaptic processes.

Materials and Methods

Cell Culture and Plasmids

Human osteosarcoma U2OS cells and colon carcinoma HCT116 cells were grown as monolayers in Dulbecco-modified Eagle medium (DMEM) (Gibco BRL Lifetechnologies, Carlsbad, CA) supplemented with 10% fetal bovine serum (FBS) (Atlanta Biologicals, Norcross, GA) in a humidified incubator at 37°C and 10% carbon dioxide. SW480/SN.3 cells (Mohindra et al., 2002) which carry an SCneo substrate (Johnson et al., 1999), a kind gift from Dr. Mark Meuth, were grown in DMEM with 10% FBS and 100 μg/ml hygromycin B in a humidified 5% carbondioxide incubator, at 37°C. pCMV5-I-SceI was a kind gift from Dr. Mark Meuth. pEGFP-C1 was purchased from Clontech (Mountain View, CA). Preparation of pSuper-HDHB-shRNAs and stable knock-down of HDHB in HCT116 cells were performed as described in Chapter II. pSuper-Rad51-shRNA was prepared by inserting target sequence 5'-GAGCTTGACAAACTACTTC-3' into the pSuper vector.

Clonogenic Survival Assay

HCT116 cells were seeded in 60-mm dishes (~800 per dish). Cells were allowed to attach to the dish for 12 h and then treated in triplicate with different concentrations of camptothecin for 12 h, or mitomycin C for 4 h, or exposed to ionizing radiation (IR). Then cells were washed twice with PBS, and incubated in fresh DMEM for 10 days. Cell colonies were fixed and stained with 0.5% crystal violet in 70% ethanol. Visible colonies were counted. Experiments were repeated at least 3 times for each DNA damaging treatment.

Aphidicolin-induced Chromosome Breaks and Sister Chromatid Exchange Assay

Asynchronous HCT116 cells were grown in 100 mm dish to about 30% confluence. At that point aphidicolin (Sigma, St. Louis, MO) was added to a final concentration of 0.2 or 0.4 μM and the cells were cultured for 24 hours. 100 ng/ml colcemid (Roche Diagnostics, Indianapolis, IN) was added to the cells 2 h before harvesting. Cells were trypsinized and washed once with PBS. Cells were resuspended in 10 ml pre-warmed 75 mM KCl and incubated for 10 min at 37°C. After that, cells were collected by centrifuging for 5 min at 800 rpm and resuspended in 200 μl 75 mM KCl. While gently vortexing, 5 ml pre-chilled acetic acid/methanol (1:3) was dropped into the cell suspension and mixed immediately. Fixation was performed for at least 30 min on ice. For staining, cells were collected by centrifugation at 800 rpm for 5 min, washed once with cold flesh fixative, resuspended in fresh fixative (500 μl for ~10^7 cells), and dropped onto wet cold slides (slides were stored in 70% ethanol at -20°C) on ice from ~10 cm height. Slides were air-dried, baked at 65°C for 2 h, and stained with 4% Giemsa in 10 mM phosphate buffer for 15 min. Slides were rinsed with water, dried, and mounted on cover slips with Cytoseal 60 (Richard-Allan Scientific, Kalamazoo, MI). Slides were observed under bright field microscope. Only cells with 45-46 chromosomes were counted.

To measure sister chromatid exchange, HCT116 cells were grown in the presence of 15 μM BrdU in 100 mm dishes for two cell cycles (about 36 h) in the dark. Then cells were collected and fixed exactly as described above, except that slides were air-dried for 3-5 min at 50°C and stained with 10 μg/ml Hoechst 33258 (Invitrogen, Carlsbad, CA) in 10 mM phosphate buffer pH 6.8 for 20 min. Then slides were rinsed with dH_2O, mounted with buffer (164 mM Na_2HPO_4 pH 7.0, 16 mM citric acid) under large-size cover slips,

and exposed to long-wave UV for 1 h at 56°C. Slides were rinsed with water and immersed in 2×SSC (30 mM sodium citrate pH 7.0, 300 mM NaCl) at 60°C for 1 h. Slides were briefly dried in air, stained with 3% Giemsa in 10 mM phosphate buffer for 12 min, mounted and observed as described above.

In vivo Recombination Assay

About 1.2×10^6 SW480/SN.3 cells were replated onto a 60 mm dish. 24 h later, cells were transiently transfected with 6 μg pSuper or pSuper-HDHB-shRNA together with 2 μg pCMV5-I-SceI in Lipofectamine 2000 (Invitrogen, Calsbad, CA) according to the manufacturer's manual. Cells were grown in DMEM for 48 h, with one change of fresh DMEM medium at 24 h after transfection. Then cells were trypsinized and replated in triplicate into 100 mm dishes with fresh DMEM. To measure the plating efficiency, about 800 cells were plated in dishes without G418. To select neo-resistant cells, 1×10^6 cells were replated into a dish supplemented with 1 mg/ml G418 in the medium. Colonies formed after growth for 11-12 days were stained with 0.5% crystal violet in 70% ethanol.

To verify the recombination products in cells, single colonies were picked and expanded. Genomic DNA was extracted with DNAeasy kit (QIAGEN, Valencia, CA). PCR amplification was performed by using two primers: 5'-CGAGCAGTGTGGTTTTGCAAGAGG-3' and 5'-GTCAAGAAGGCGATAGAAGGC-GATG-3' against the recombination substrate on the genomic DNA. PCR products were purified by QIAquick PCR purification kit (QIAGEN) and cut with NcoI. The digestion products were electrophoresed through 2% agarose gel in 0.5×TBE buffer and visualized by ethidium bromide staining.

Flow Cytometry and Cell Sorting

Cell cycle analysis by flow cytometry was performed as described in Chapter II. To sort GFP-positive cells, cells were co-transfected with pEGFP-C1 (Clontech, Mountain View, CA) and HDHB-shRNA, and sorted on a FACSAria (BD Biosciences, San Diego, CA) at Vanderbilt Flow Cytometry Services Facility.

Fluorescence Microscopy

DNA damage treatment, cell fixation and staining were performed as described in Chapter II. Fluorescence pictures were taken on an Axioplan 2 imaging system as described (Gu et al., 2004). Monoclonal anti-Rad51 primary antibody was purchased from Novus (Littleton, CO) and diluted 1:300 in PBS with 10% FBS. Rabbit anti-H2AX phospho-Ser139 antibody was from Upstate (Charlottesville, VA) and diluted 1:500 in PBS with 10% FBS. BrdU monoclonal antibody was from Becton Dickinson (Franklin Lakes, NJ).

DNA Substrates

ϕX174 circular ssDNA and RFI dsDNA were purchased from NEB (Ipswich, MA). Linear ϕX174 dsDNAs with different types of termini were prepared by cleaving ϕX174 RFI dsDNA with restriction endonucleases. Linear dsDNA with two blunt ends was made by digestion with *Ssp*I endonuclease. Linear dsDNA with 3'-overhangs was made with *Pst*I digestion. Linear dsDNA with 5'-overhangs was made with *Xho*I digestion. The digested DNA was purified with a QIAquick PCR purification kit

(QIAGEN). Linear dsDNA with a blunt end and a 3'-overhanging terminus was created with a double digestion of *Pst*I and *Stu*I. Linear dsDNA with a blunt end and a 5'-overhanging terminus was created with a double digestion of *Xho*I and *Ssp*I. Linear dsDNA with a blunt end and a 3'-recessive terminus was made by double digestion with *Xho*I and *Stu*I. Linear dsDNA with a blunt end and a 5'-recessed terminus was made by double digestion with *Pst*I and *Ssp*I. After the double digestions, the products were separated by 1% agarose gel electrophoresis and the large DNA fragment was purified with the QIAquick gel extraction kit (QIAGEN). To label the linear dsDNA with 3'-overhanging termini, *Pst*I-digested ϕX174 dsDNA was first dephosphorylated with Antarctic phosphatase (NEB). To get more efficient labeling of the 5'-recessed end, DNA was heated at 70°C for 10 min, chilled on ice, and then labeled with T4 polynucleotide kinase (NEB) and [γ^{32}-P]-ATP (Amersham Biosciences, UK). The labeled dsDNA was purified with a Sephadex G-50 column (Roche). To prepare the nicked-circular DNA marker, 0.5 μg linear dsDNA and 1.5 μg circular ssDNA was denatured and annealed in 20 μl annealing buffer (20 mM Tris-HCl pH 8.0, 50 mM NaCl, 10 mM $MgCl_2$).

The DNA helicase substrate was created by annealing ^{32}P-5'-labeled 17-nt oligonucleotide 5'-GTAAAACGACGGCCAGT-3' with M13 mp18 ssDNA (USB, Cleveland, OH) as described (Taneja et al., 2002).

Proteins

E. coli vector pET15b-Rad51-Δ2 expressing wild-type full-length 6×His-Rad51 was a kind gift from Dr. Walter Chazin. The purification of Rad51 was performed as described (Stauffer and Chazin, 2004). Briefly, pET15b-Rad51-Δ2 was transformed into

Rosetta (DE3) pLys cells and grown in a 40 ml LB culture supplemented with 100 ug/ml ampicillin and 30 ug/ml chloramphenicol overnight. On the next day, 4 L LB medium with 100 ug/ml ampicillin and 30 ug/ml chloramphenicol was inoculated with 40 ml overnight culture and grown at 37°C, 250 rpm, until the O.D.600 reached 0.6. IPTG was added to a final concentration of 1 mM and the induction was continued for 3 h. Cells were collected, frozen at -80°C, and resuspended in 40 ml lysis buffer (50 mM Tris-Cl pH 8.0, 500 mM NaCl, 5 mM β-mercaptoethanol, 10% glycerol, 10 mM imidazole, 0.5 mg/ml lysozyme, 1 mM PMSF, 10 μg/ml aprotinin, 1 μM leupeptin) and incubated on ice for 20 min. Cell extract was split into 50-ml centrifuge tubes with 15 ml in each tube and sonicated 6×30 sec. Cell extract was then centrifuged at 20,000×g for 30 min at 4°C. The supernatant was mixed with 2 ml (packed volume) Nickel-NTA (QIAGEN) beads pre-washed with buffer A (50 mM Tris-Cl pH 8.0, 500 mM NaCl, 5 mM β-mercaptoethanol, 10% glycerol, 10 mM imidazole, 1 mM PMSF, 10 μg/ml aprotinin, 1 μM leupeptin) at 4°C for 1 h. The beads were collected by centrifuging at 2000 rpm for 5 min, packed into a column, and washed with 6 ml buffer A. Beads were then sequentially washed with 10 ml of 30 mM imidazole in buffer A, 10 ml of 50 mM imidazole in buffer A, and 10 ml of 60 mM imidazole in buffer A. Proteins were eluted with 12 ml of 350 mM imidazole in buffer A. After this step, Rad51 protein purity is at least 95% based on Coomassie staining. The yield is 15 mg. To remove His-tag, about 6 mg His-Rad51 was diluted in 20 ml HAP buffer A (100 mM KPi pH 6.8, 100 mM KCl, 2 mM β-mercaptoethanol, 5% glycerol) and dialyzed in 2 × 1 L HAP buffer A overnight. About half of the Rad51 precipitated during dialysis and was removed by centrifuging at 12,000 rpm for 20 min. 20 U thrombin (Novagen, Madison, WI) were added and the protein was incubated at

4°C for 6 h. The digestion was monitored by SDS-PAGE. After the completion of thrombin digestion, the sample was loaded onto a 2 ml hydroxyapatite column (Bio-Rad, Hercules, CA) equilibrated with HAP buffer A. The column was washed with 6 ml HAP buffer A and protein was eluted with 8 ml HAP buffer B (800 mM KPi pH 6.8, 100 mM KCl, 2 mM β-mercaptoethanol, 5% glycerol). Peaks containing Rad51 were diluted in 15 ml HAP buffer A to decrease protein loss during dialysis and dialyzed against 2×1 L storage buffer (20 mM Tris-Cl pH 8.0, 100 mM KCl, 10% glycerol, 1 mM DTT) overnight. Rad51 was concentrated with Amicon Ultra Filter (10k, 15 ml) (Millipore, Billerica, MA) and the protein concentration was determined by densitometric scanning, using IPLabgel 1.5 (Signal Analytics Corp., Vienna, VA), of Coomassie-stained protein bands in SDS-polyacrylamide gels with 1 mg/ml BSA as standard. The final Rad51 protein concentration was 1 mg/ml.

Wild-type HDHB was prepared as described in Chapter II. To remove a trace contamination of DNA ligase, wild-type HDHB sample in 1 ml was loaded on a Sephacryl S-300 gel filtration column (Amersham Biosciences, UK) and eluted with 120 ml buffer (20 mM Tris-HCl pH 8.0, 50 mM NaCl, 10% glycerol, 1 mM DTT). HDHB protein peaks were pooled and the concentration was determined by densitometric scanning of Coomassie-stained protein bands in SDS-polyacrylamide gels. Walker B mutant HDHB was prepared as described (Taneja et al., 2002).

Recombinant human RPA heterotrimer was expressed and prepared as described (Henricksen et al., 1994). RPA was diluted in dialysis buffer (20 mM Tris-HCl pH 7.8, 50 mM NaCl, 10 μM $ZnCl_2$, 5% glycerol, 1 mM DTT) to about 1 mg/ml to reduce

protein loss during dialysis and dialyzed overnight. RPA concentration was determined with the Bradford assay (Bio-Rad).

Strand Exchange Assay and Helicase Assay

Rad51-mediated strand exchange reactions (20 μl) were performed in reaction buffer (40 mM Tris-HCl pH7.5, 1 mM $MgCl_2$, 1 mM DTT, 2.5 mM ATP, 8 mM creatine phosphate, 28 μg/ml creatine kinase) supplemented with different salts as indicated in the figure legends. Rad51 (7.5 μM) was mixed with ϕX174 circular ssDNA (30 μM as nucleotides) at 37°C for 5 min, followed by the addition of RPA (1.5 μM) and the incubation was continued for another 5 min. Then different amounts of HDHB were added into the reaction. Strand exchange was initiated by adding linearized ϕX174 dsDNA (30 μM as nucleotides) to the reaction. For reactions performed with $(NH_4)_2SO_4$ as the salt, $(NH_4)_2SO_4$ was added between the additions of RPA and HDHB. Aliquots were withdrawn from the reaction at indicated times, and deproteinized by adding SDS to 0.5% and proteinase K to 1 mg/ml, followed by incubation at 37°C for 20 min. Reaction products were mixed with 6×loading dye (30% glycerol, 0.25% bromophenol blue, 0.25% xylene cyanol) and separated by electrophoresis in a 0.9% agarose gel in 1 × TAE buffer. Both the gel and the running buffer were supplemented with 1 μg/ml ethidium bromide. The electrophoresis was performed at 2 V/cm for about 3 h. The gel was destained in ample dH_2O for 4 h and visualized under short-wave UV. Helicase assays were performed as described (Taneja et al., 2002). Quantification of reaction products was conducted by densitometric scanning, using IPLabgel 1.5 (Signal Analytics Corp.), of the autoradiograph film.

Co-immunoprecipitation

T7-HDHB was expressed in High Five insect cells as described (Taneja et al., 2002). 2×10^7 cells containing about 5 μg HDHB were lysed in 1.5 ml buffer (20 mM Tris-HCl pH 8.0, 100 mM NaCl, 0.2% NP-40, 1 mM DTT, 1 mM PMSF, 10 μg/ml aprotinin, 1 μM leupeptin) on ice for 20 min. Cell debris was removed by centrifuging at 12,500 rpm for 15 min. The supernatant was mixed with 20 μl T7-tag antibody agarose (Novagen, Madison, WI) for 1 h at 4°C. Then the beads were washed 3 times with binding buffer (30 mM Hepes pH 7.8, 10 mM KCl, 7 mM $MgCl_2$). 0.75 μg purified Rad51 was incubated with the T7-HDHB-coated beads in 400 μl binding buffer supplemented with 1% non-fat milk for 3 h at 4°C. Then the beads were washed three times with 800 μl wash buffer (30 mM Hepes pH 7.8, 75 mM KCl, 7 mM $MgCl_2$, 0.25% inositol, 0.01% NP-40). The beads were incubated in wash buffer at 4°C for 5 min for each wash. After wash, beads were boiled in 40 μl 2×SDS sample buffer for 5 min. The sample was separated with 8.5% SDS-PAGE electrophoresis and proteins were detected by western blotting.

Results

HDHB-depleted Cells are Sensitive to DNA Damaging Agents and Replication Fork Uncoupling

To assess the importance of HDHB in DNA damage response, endogenous HDHB was stably depleted from HCT116 cells with small hairpin RNA (shRNA) (Figure

III-1A). Depletion of HDHB did not alter cell cycle distribution, compared to that observed in control-shRNA-depleted cells (Figure III-1B). Equal numbers of HDHB-depleted cells and control cells were treated with increasing doses of camptothecin, mitomycin C, or IR. Colonies formed by surviving cells were stained after 10 days and counted. The ability of HDHB-depleted HCT116 cells to survive and form colonies after camptothecin or IR exposure was reproducibly reduced to about half that of control-depleted cells (Figure III-1C). Moreover, HDHB-depleted cells were significantly more sensitive to mitomycin C than control-depleted cells (Figure III-1C). Since homologous recombination plays an important role in the repair of mitomycin C- and camptothecin-induced DNA damage (Adachi et al., 2004; McHugh et al., 2001), these results would be consistent with a function of HDHB in damage repair, possibly by homologous recombination

Aphidicolin is a DNA polymerase inhibitor that uncouples DNA unwinding from polymerases at replication forks and induces chromosome breaks at common fragile sites (Arlt et al., 2003; Byun et al., 2005). To further explore the possible function of HDHB in repairing chromosome breaks, we treated control- and HDHB-depleted HCT116 cells (Chapter II) with 0.2 or 0.4 μM aphidicolin for 24 h and then prepared chromosome spreads. As shown in Figure III-2A, aphidicolin treatment significantly increased the frequency of chromosome breaks *in vivo*. Furthermore, HDHB-depleted cells show more chromosome aberrations than control-depleted cells (Figure III-2B). Thus, depletion of HDHB did not appear to induce breakage by itself, but did exacerbate the effect of aphidicolin on chromosome stability. These observations indicate a role for HDHB in

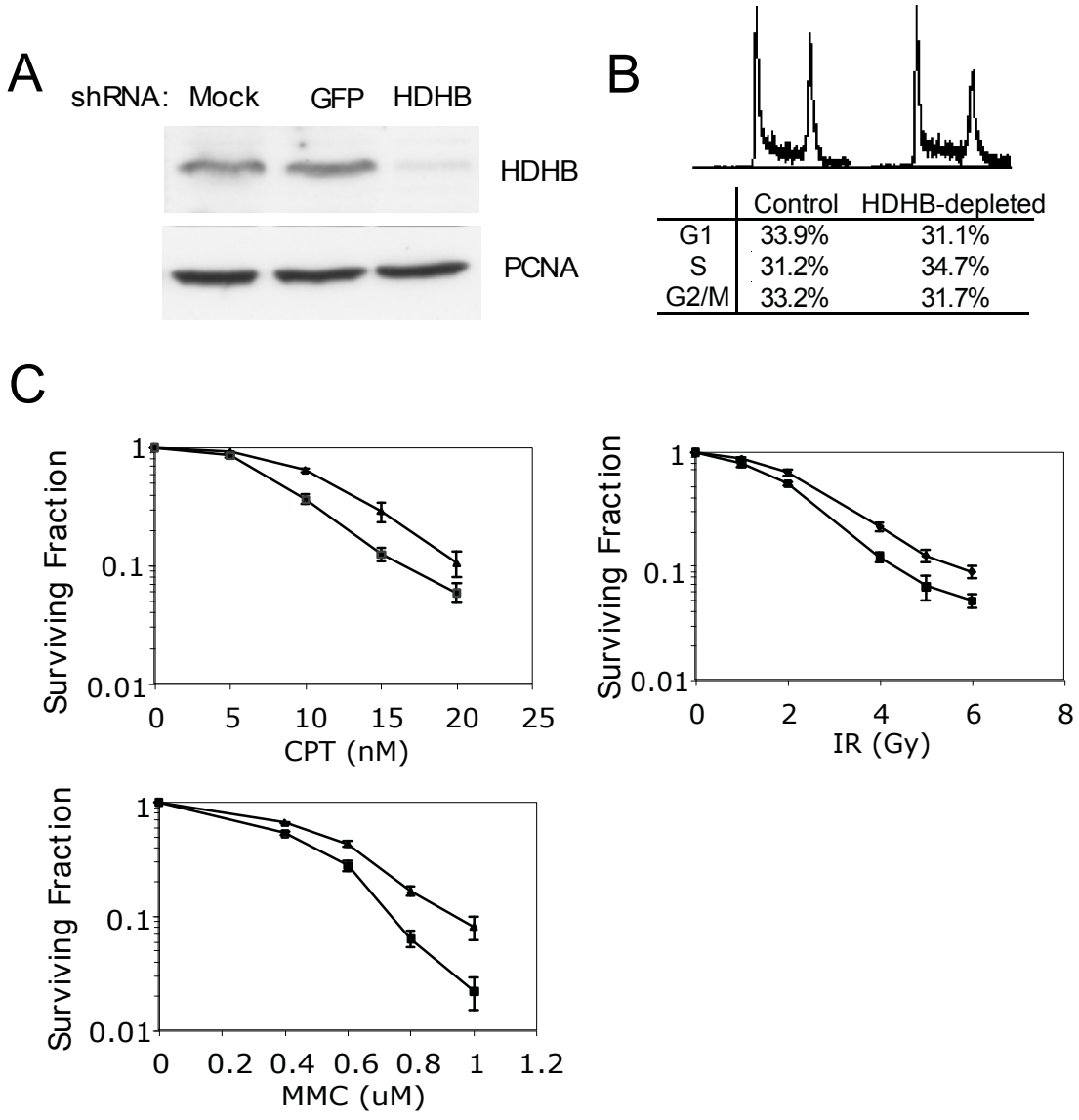

Figure III-1. **Clonogenic survival assay with HDHB-depleted cells**. A, Western blotting of HCT116 cells stably expressing short hairpin RNA (shRNA) against GFP or HDHB. B, Cell cyle analysis of control and HDHB-depleted cells. C, Colonies formed by surviving HCT116 cells treated with camptothecin (CPT), mitomycin C (MMC), or ionizing radiation (IR). Untreated cells were counted as 100% survival. Triangle, HCT116 cells expressing shRNA against GFP. Square, HCT116 cells expressing shRNA against HDHB.

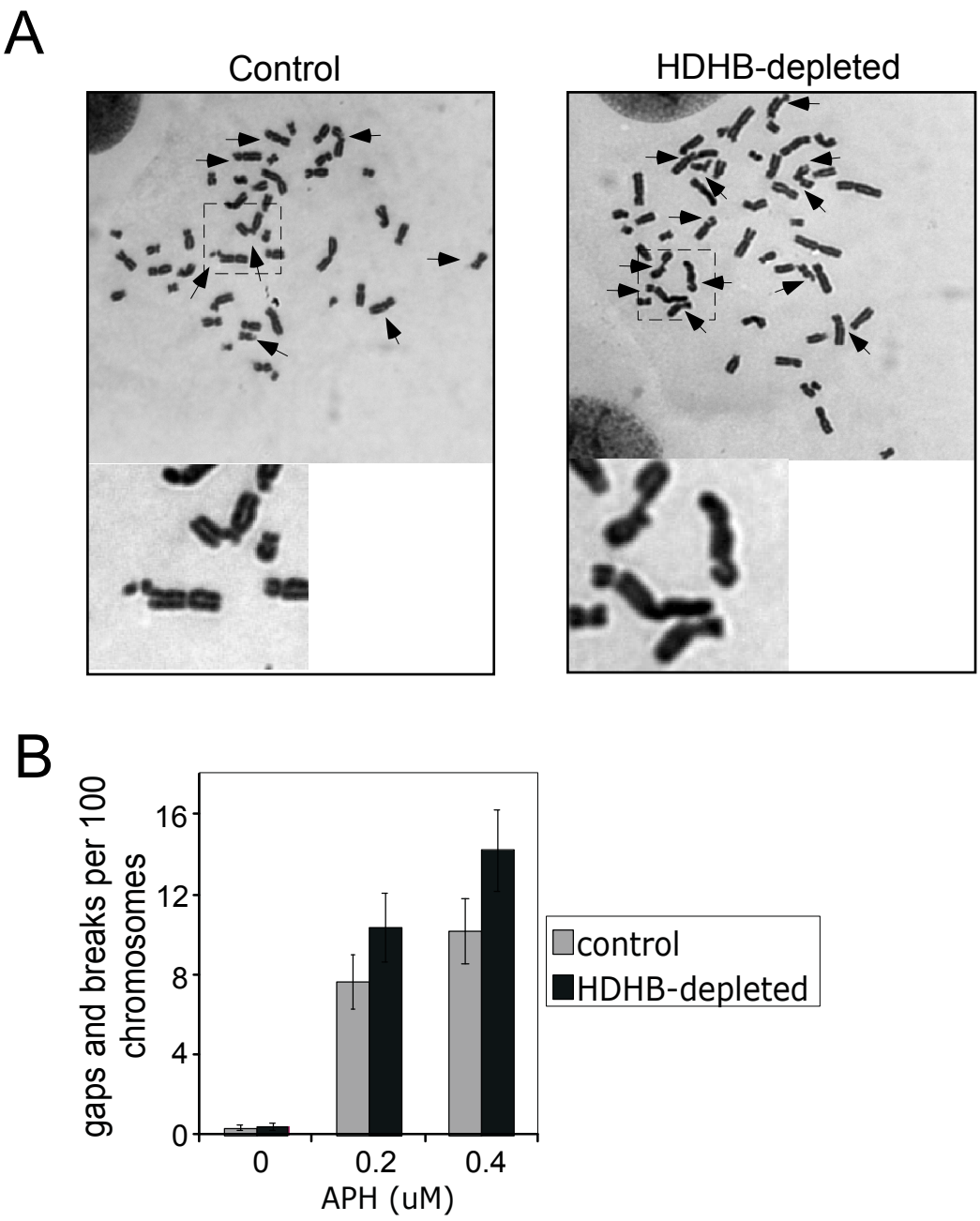

Figure III-2. **Frequency of aphidicolin-induced chromosome damage is greater in HDHB-depleted cells**. A, Representative pictures of chromosome breaks induced by 0.4 μM aphidicolin (APH) in control (control-shRNA) cells and HDHB-depleted (HDHB-shRNA) cells. Arrows indicate chromosome gaps and breaks. Bottom, enlarged regions of the top pictures showing chromosome breaks. B, APH-induced chromosome breaks in control cells and HDHB-depleted cells. 50-100 cells were counted for each treatment and the experiments were repeated 3 times.

stabilizing or re-activating stalled replication forks, or repairing double-strand breaks arising from collapsed replication forks.

HDHB Facilitates Homologous Recombination

Since homologous recombination has been shown to mediate sister chromatid exchange (Sonoda et al., 1999), we reasoned that if HDHB functions in homologous recombination to stabilize or repair damaged DNA, sister chormatid exchange should be reduced by HDHB silencing. To test this prediction, we treated HDHB-depleted HCT116 cells and control-depleted cells with mitomycin C and differentially stained the two sister chromatids in metaphase-arrested cells (Figure III-3A). The frequency of spontaneous sister chromatid exchange events was lower in HDHB-depleted cells than in control GFP-shRNA expressing cells in the absence of DNA damage treatment (Figure III-3B). Student t-test showed the difference between the two cells was statistically significant at the 5% level. Treatment with 100 μg/ml mitomycin C increased sister chromatid exchange rate in both cells. However, HDHB-depleted cells again showed fewer sister chromatid exchanges per cell than did control-depleted cells after exposure to mitomycin C (Figure III-3C). These findings provide initial evidence that HDHB functions in homologous recombination in the absence of exogenous damage, as well as after exposure to damaging agents.

To further test the potential role of HDHB in homologous recombination, we used an *in vivo* recombination assay developed by Jasin and colleagues (Johnson et al., 1999). SW480/SN.3 cells bearing an integrated SCneo recombination reporter casette were obtained from Dr. Mark Meuth (Mohindra et al., 2002). This SCneo reporter cassette

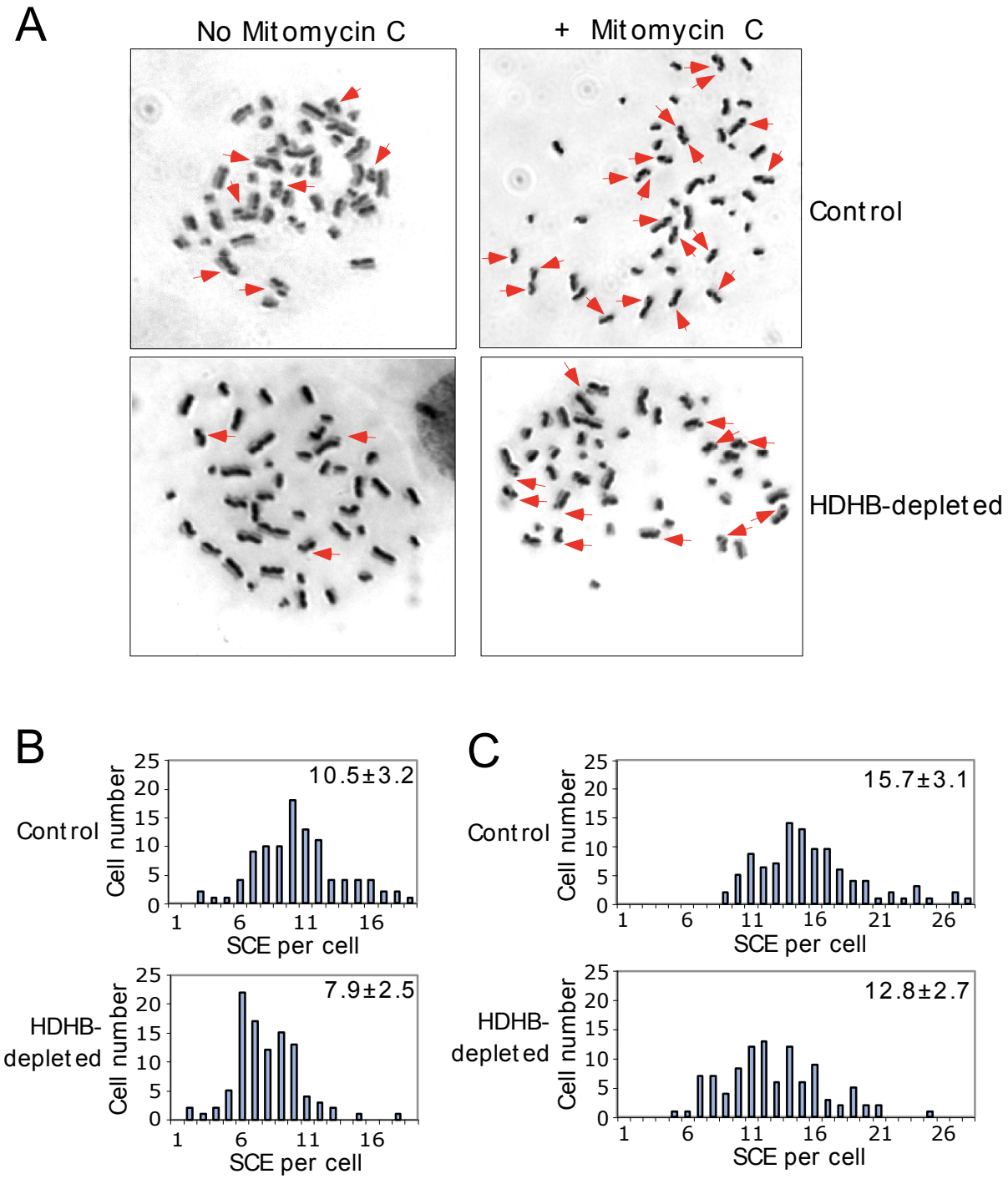

Figure III-3. **Sister chromatid exchange (SCE) in HCT116 cells.** A, Sister chromatid exchange of control and HDHB-depleted HCT116 cells without mitomycin C (left) or with 100 ng/ml mitomycin C treatment (right). Arrows indicate the exchange events. B and C, Analysis of sister chromatid exchange events in 100 control or HDHB-depleted cells without (B) or with (C) 100 ng/ml mitomycin C treatment. The value at the top right of each panel is the mean SCE per cell.

contains a neomycin-resistant gene disrupted by an I-SceI restriction site. An intact copy of the disrupted portion of the neomycin gene is present at the other end of the casette. A single double-strand break in the cassette can be created by transient expression of I-SceI endonuclease in the cells (Figure III-4A). If the double-strand break is repaired by homologous recombination, an intact neomycin-resistant gene will be generated and the cells that have undergone successful homologous recombination can be identified and evaluated by selecting for growth in G418.

We co-transfected SW480/SN.3 cells with I-SceI expression vector and vectors encoding two different shRNAs against HDHB or a control shRNA (Chapter II). After 48 h, cells were replated in G418 selection medium and allowed to grow for 11 days. Drug-resistant colonies were stained with crystal violet and counted. To check the transfection efficiency, we co-transfected pEGFP vector together with HDHB-shRNA vector in a parallel experiment. Co-transfection with HDHB-shRNA showed no significant effect on GFP expression (Figure III-4B). To evaluate the depletion of HDHB in cells, we sorted GFP-positive cells co-transfected with pEGFP and HDHB-shRNA vector. Western blotting showed about 70% HDHB knock-down efficiency (Figure III-4C). Transfection of HDHB-shRNA into the cells appeared to have no significant influence on cell viability or growth, as similar numbers of colonies from cells transfected with HDHB-shRNA or with pSuper empty vector were obtained after growth in medium without G418. Transfection of HDHB-shRNA also had no significant effect on cell cycle distribution (Figure III-4D). Transfection of I-SceI into the cells promoted the formation of G418-resistant colonies, while transfection with pFLAG vector did not increase the number of G418-resistant colonies (Figure III-4E). After G418 selection, HDHB-shRNA transfected

Figure III-4. ***In vivo* recombination assay.** A, SCneo substrate contains a neo-resistance gene (S2-neo) disrupted by an I-SceI site. 3'-neo is an intact copy of the 3' region of a neo-resistance gene. Expression of I-SceI endonuclease in cells will generate a double-strand break, which can be repaired by homologous recombination and result in short tract gene conversion (STGC) or long tract gene conversion (LTGC)/sister chromatid exchange (SCE). An intact neo-resistance gene will be generated and cells can be selected with G418. Arrows indicate the target positions of PCR primers used in panel F. B, Transfection efficiency of pSuper and HDHB-shRNAs into SW480 cells evaluated by GFP co-transfection and expression. C, Western blotting of whole cell extracts from FACS-sorted GFP-positive cells co-transfected with pEGFP and HDHB-shRNAs. D, Cell cycle analysis of SW480 cells transfected with pSuper or HDHB-shRNAs. E, G418-resistant colonies formed after co-transfection of I-SceI with pSuper or HDHB-shRNAs. pFLAG is a negative control vector for I-SceI expression. F, PCR products amplified from the genomic DNA of surviving colonies were cut with NcoI and analyzed by agarose-gel electrophoresis. (E, together with Nilesh Kashikar and Amanda Hafer)

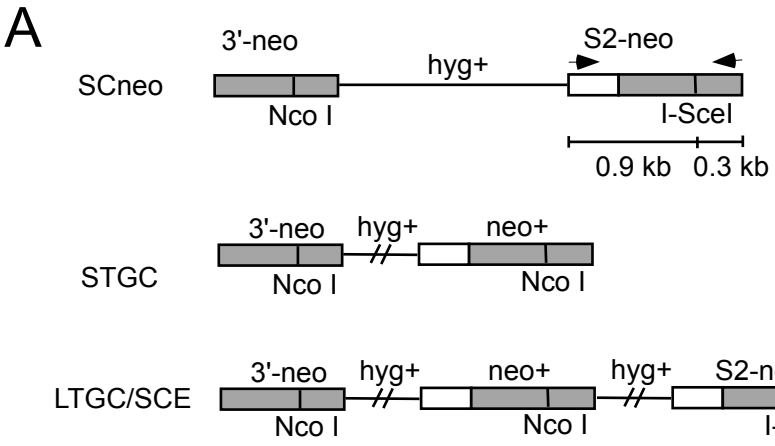

(Adapted from Johnson et al., *Nature*, 1999)

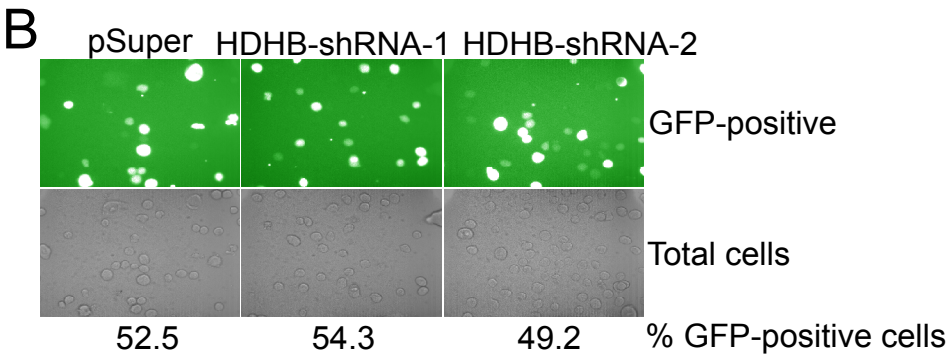

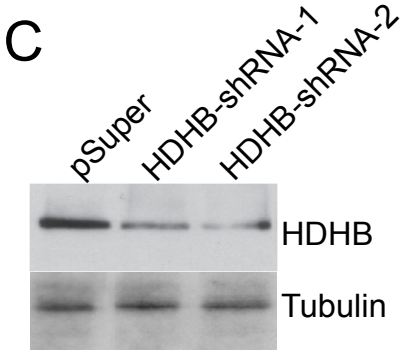

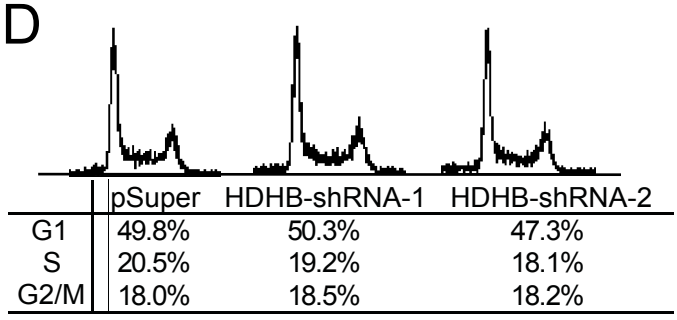

	pSuper	HDHB-shRNA-1	HDHB-shRNA-2
G1	49.8%	50.3%	47.3%
S	20.5%	19.2%	18.1%
G2/M	18.0%	18.5%	18.2%

Figure III-4--cont.

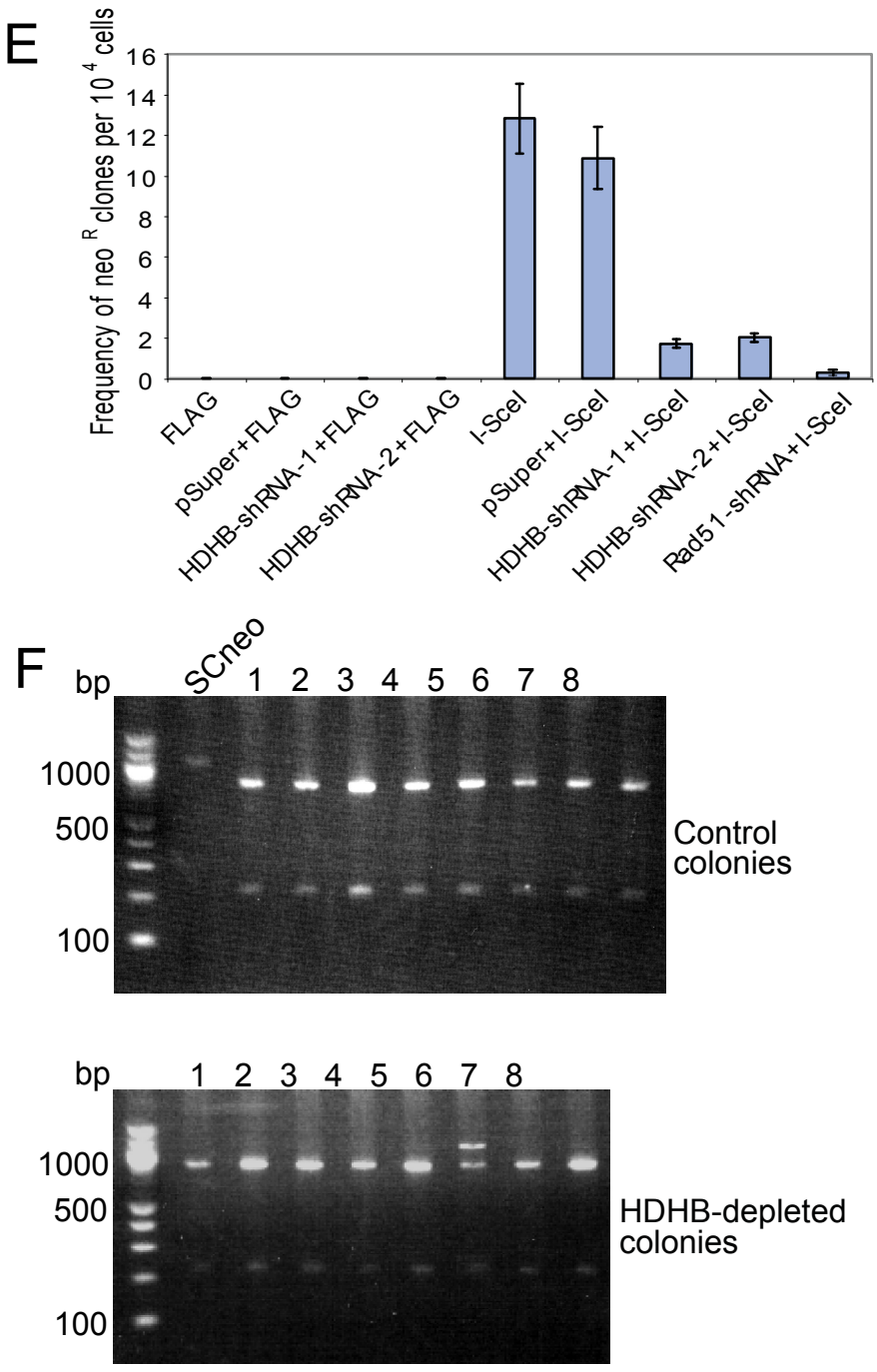
E
Frequency of neo R clones per 10 4 cells
16
14
12
10
8
6
4
2
0
FLAG
pSuper+FLAG
HDHB-shRNA-1+FLAG
HDHB-shRNA-2+FLAG
I-SceI
pSuper+I-SceI
HDHB-shRNA-1+I-SceI
HDHB-shRNA-2+I-SceI
Rad51-shRNA+I-SceI
F
bp
SCneo
1 2 3 4 5 6 7 8
1000
500
100
Control colonies
bp
1 2 3 4 5 6 7 8
1000
500
100
HDHB-depleted colonies

Figure III-4

cells showed a significant reduction in colony formation compared to control-transfected cells (Figure III-4E). In a positive control for the assay, Rad51-shRNA co-transfected with I-SceI showed the expected reduction in drug-resistant colonies (Figure III-4E). To confirm that viable colonies obtained by G418 selection had undergone recombination of the neomycin-resistance gene at the I-SceI site, we picked up individual colonies, extracted genomic DNA, and amplified a region of the recombination substrate cassette using PCR. If the I-SceI-induced double-strand break was repaired by homologous recombination, the I-SceI site should be converted to an NcoI site. As shown in Figure III-4F, NcoI cleaved the PCR products amplified from the genomic DNA of all of the viable colonies. In one of the colonies, we observed a long tract gene conversion or sister chromatid exchange (LTGC/SCE) (Figure III-4F bottom, lane 7). These results indicate that the depletion of HDHB impairs homologous recombination in cells.

Delayed Formation of RPA Damage Foci after Ionizing Radiation of HDHB-depleted Cells

In Chapter II, we showed that UV-induced RPA focus formation is not affected by the depletion of HDHB. While UV treatment induces replication fork stalling that can lead to double-strand breaks (Heller and Marians, 2006), ionizing radiation (IR) directly generates double-strand breaks (Olive, 1998). RPA is thought to have two roles in homologous recombination-mediated repair of double-strand breaks, first in facilitating formation of the recombinogenic Rad51-ssDNA filament, and later in stabilizing the displaced ssDNA after Rad51-mediated strand invasion of a homologous duplex DNA (Sugiyama et al., 1997; Sung, 1994; Wang and Haber, 2004). To better understand how

HDHB participates in homologous recombination, we tested IR-induced RPA focus formation in HCT116 cells that had been stably HDHB- or control-depleted. After irradiation, small bright foci of Rad51 and H2AX formed within 0.5-1 h (Figure III-5A, B, C). There was no significant difference between HDHB- and control-depleted cells in the percentage of cells displaying Rad51 or H2AX foci (Figure III-5B, C). Moreover, the number of Rad51 foci per cell was similar in HDHB- and control-depleted cells. However, bright foci of RPA34 appeared more gradually during the first 2 h after IR and the fraction of cells displaying IR-induced RPA foci was greater for control-depleted cells than for cells depleted of HDHB (Figure III-5D). This result indicates that depletion of HDHB delays RPA focus formation during DNA double-strand break processing without affecting H2AX or Rad51 focus formation on chromatin.

To corroborate these results, we also depleted HDHB from U2OS cells by transient transfection with pSuper-HDHB-shRNA or empty vector as a control, exposed the cells to IR, and stained them to detect RPA foci on chromatin (Figure III-6). Again, IR-induced RPA34 foci formed more slowly in HDHB-depleted than in vector-depleted cells (Figure III-6B). Taken together, these results suggested that HDHB depletion impairs RPA-ssDNA formation during double-strand break processing, likely in a late step after Rad51 assembly on chromatin.

Physical Interaction of HDHB with Rad51

Ectopically expressed GFP-HDHB localizes in DNA damage foci (Gu et al., 2004). We found that GFP-HDHB transiently expressed in U2OS cells colocalized with endogenous Rad52, Rad51, RPA, or BrdU-prelabeled ssDNA (Figure III-7A).

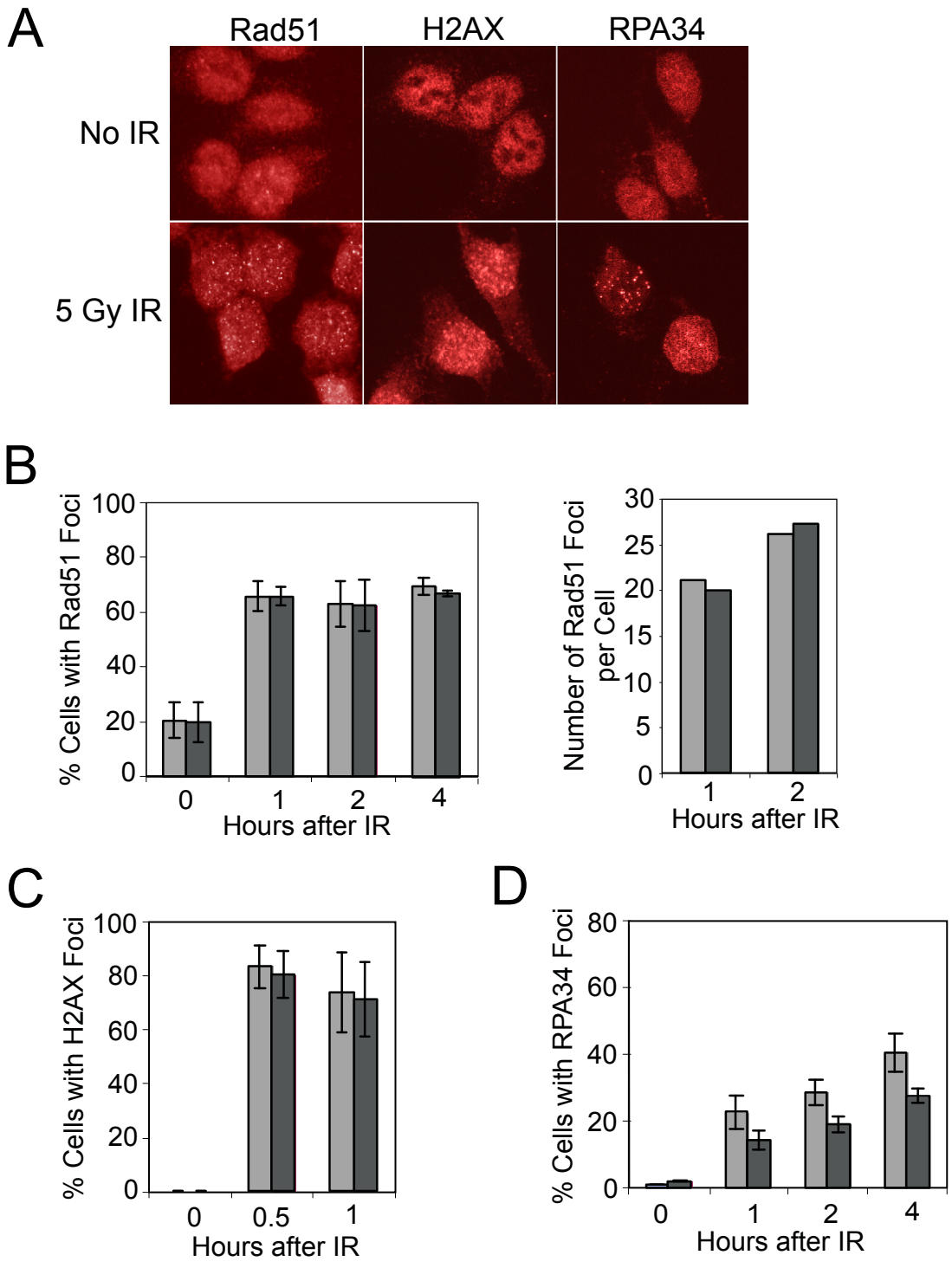

Figure III-5. **Ionizing radiation-induced Rad51, H2AX or RPA34 foci in HCT116 cells.** A, 5 Gy ionizing radiation (IR)-induced Rad51, H2AX or RPA34 foci in HCT116 cells 1 h after treatment. B, C and D, Percentage of cells with Rad51 (B, left), H2AX (C), or RPA34 (D) foci after 5 Gy IR. B, right, mean number of Rad51 foci per cell after IR. Light gray, control HCT116 cells expressing GFP-shRNA; dark gray, stable HDHB-depleted HCT116 cells.

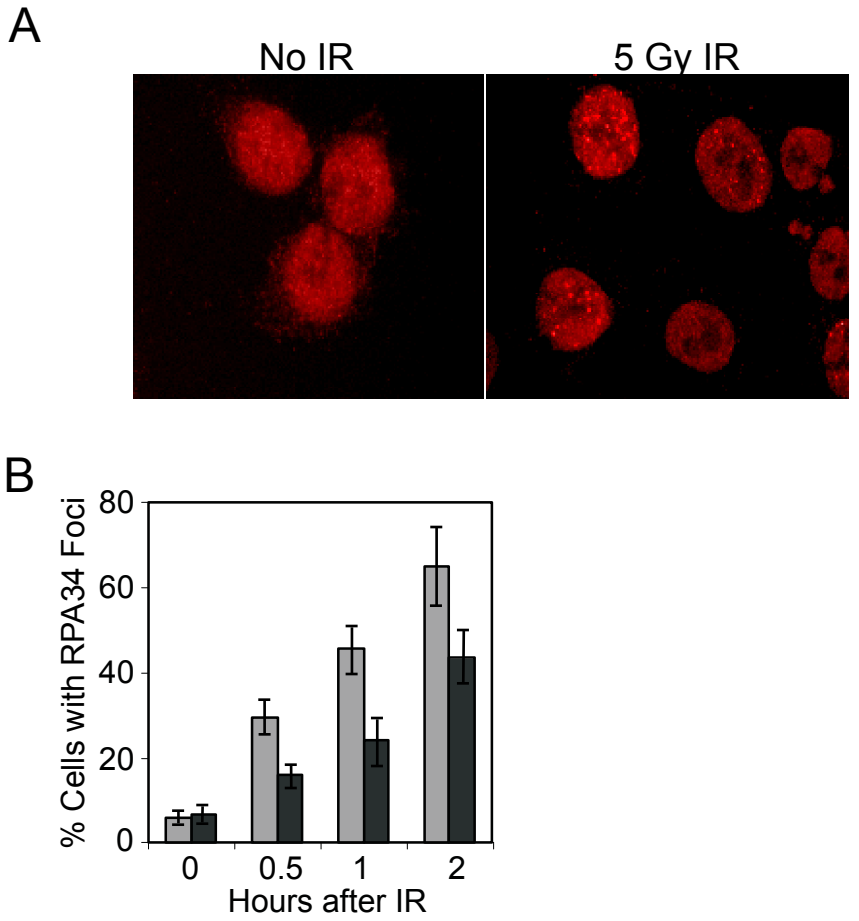

Figure III-6. **Ionizing radiation-induced RPA34 foci in U2OS cells.** A, U2OS cells were transiently transfected with pSuper or HDHB-shRNA-2 as described in Chapter II. Three days later, cells were exposed to 5 Gy IR and stained with anti-RPA34 antibody after 1 hr. B, Percentage of cells with RPA34 foci after 5 Gy IR at different time points. Light gray, control cells; dark gray, HDHB-depleted cells.

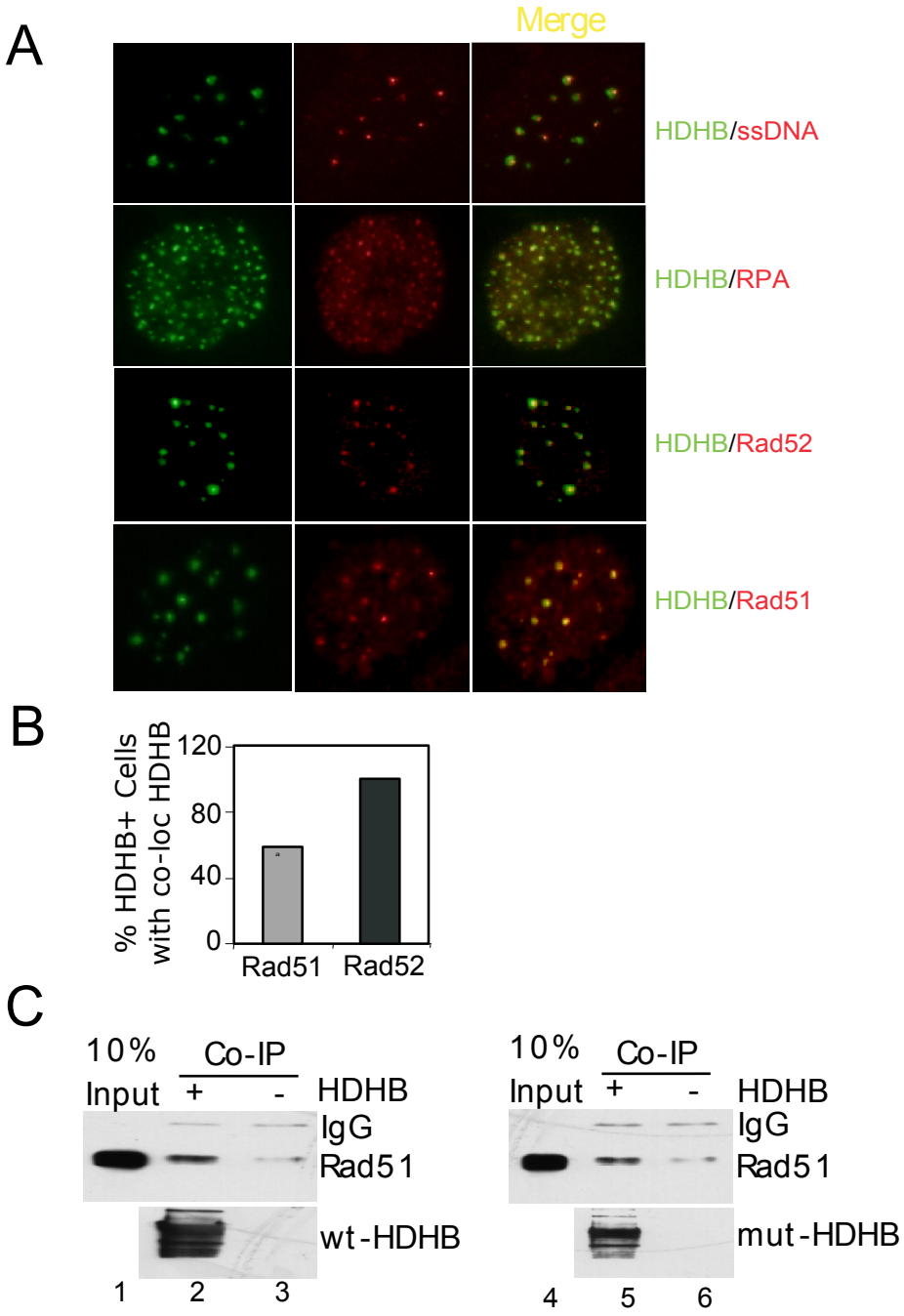

Figure III-7. **Colocalization and interaction of HDHB with Rad51.** A, GFP-HDHB was transiently expressed in U2OS cells. Cells were stained with antibodies against RPA, Rad52 or Rad51 and visualized by immunofluorescence. For ssDNA staining, cells were grown in 10 µg/ml BrdU for 30 h, fixed, and stained with anti-BrdU antibody. B, Percentage of HDHB-positive cells with colocalizing Rad51 or Rad52 foci with HDHB. C, Co-immunoprecipitation of purified Rad51 with HDHB bound to antibody beads. 0.75 µg purified Rad51 was incubated with T7 beads bound with T7-HDHB. After wash, beads were boiled in 2 SDS sample buffer. Proteins bound on beads were analyzed by western blotting. (A and B, by Peijun Yan and Shi Meng)

Furthermore, Rad52 co-localized completely with HDHB foci in HDHB-positive cells, while Rad51 co-localized with HDHB in about 60% of the HDHB-positive cells (Figure III-7B). These results suggested that over-expressed HDHB may interact with proteins involved in HR.

To test for a direct physical interaction of HDHB with Rad51, we purified recombinant Rad51 and performed pull-down assays with tagged recombinant HDHB bound to antibody beads. Western blotting of the proteins bound to the beads showed that a small fraction of the input Rad51 bound to both wild-type HDHB and Walker B mutant HDHB (Figure III-7C). Antibody beads with no HDHB were used as negative control and bound much less amount of Rad51 (Figure III-7C, lanes 3 and 6). The physical interaction between HDHB and Rad51 is consistent with the possibility that they could function together in homologous recombination *in vivo*.

HDHB Stimulates Rad51-mediated 5'-3' Heteroduplex Extension

Our *in vivo* recombination assays provided evidence of HDHB function in homologous recombination repair (Figure III-3 and 4). The observation that HDHB-depleted cells form Rad51 foci normally after IR, while induction of bright RPA foci is delayed or reduced (Figure III-5, 6), suggested that HDHB would likely function at a late stage in recombination, perhaps facilitating displacement of ssDNA after strand invasion to promote heteroduplex formation. A role for T4 dda protein in promoting uvsX-generated DNA heteroduplex extension has been proposed (Kodadek and Alberts, 1987). In this model, dda was thought to unwind the DNA duplex formed by strand invasion and drive UvsX-mediated strand exchange into the homologous DNA duplex. To investigate

whether HDHB has similar role in driving heteroduplex extension, we investigated Rad51-mediated strand exchange in the presence of HDHB.

Human Rad51 (hRad51) was purified to over 95% purity and the 6×His-tag on the original recombinant hRad51 was removed by thrombin digestion (Figure III-8A). An *in vitro* strand-exchange reaction between linear ϕX174 dsDNA and circular ssDNA catalyzed by hRad51 was performed (Figure III-8B). Because the optimal reaction for hRad51 requires either high salt or calcium (Bugreev and Mazin, 2004; Liu et al., 2004; Shim et al., 2006; Sigurdsson et al., 2001), all our reactions were performed in the presence of either $(NH_4)_2SO_4$ or $CaCl_2$. In a similar reaction promoted by RecA, the heteroduplex extension is unidirectional in the 5'-3' direction with respect to the ssDNA (Cox and Lehman, 1981; West et al., 1981). By contrast, yeast Rad51 can initiate the formation of joint molecules and promote heteroduplex extension in either direction, depending on whether there is a complementary overhanging ssDNA at the linear dsDNA termini (Namsaraev and Berg, 1997; Namsaraev and Berg, 1998; Namsaraev and Berg, 2000). To investigate the DNA-end requirement of hRad51, linear dsDNAs with different ends created by restriction digestions were used in the strand-exchange reaction (Figure III-8C). As expected, hRad51 did not promote strand exchange with blunt-ended dsDNA or dsDNAs with one blunt end and one recessive end on the complementary strand (Figure III-8C, Lanes 2, 12, 14). However, it promoted strand exchange in the reactions containing dsDNAs with at least one overhanging ssDNA tail on the complementary strand (Figure III-8C, Lanes 4, 6, 8, 10). Thus hRad51 has an enzymatic activity similar to that of the yeast homolog with respect to strand exchange polarity.

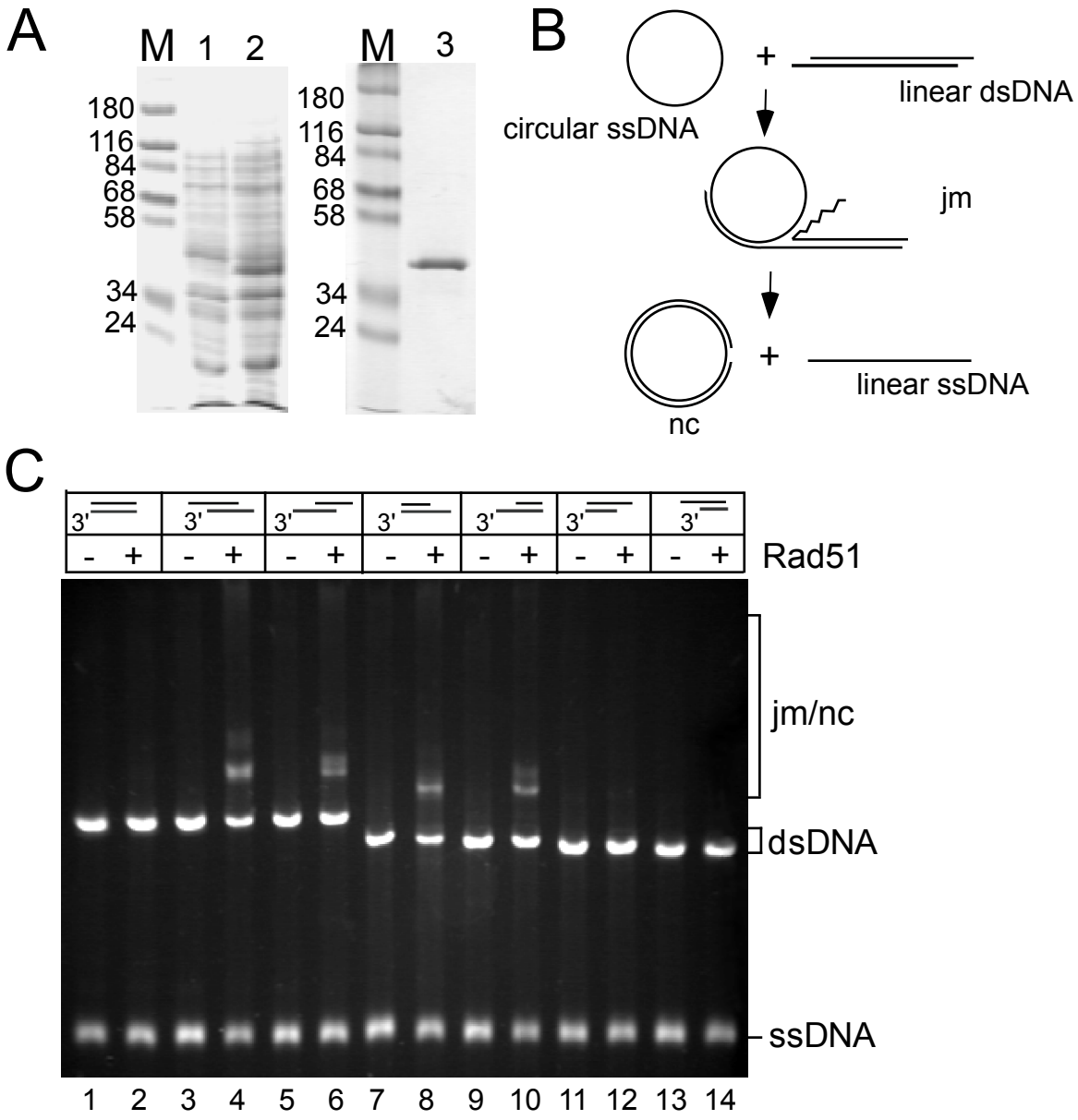

Figure III-8. **hRad51-mediated strand exchange reaction.** A, Expression and purification of hRad51. Lane 1, uninduced; lane 2, IPTG induced; lane 3, purified. B, Diagram of strand exchange reaction. Jm, joint molecule; nc, nicked-circular DNA. C, DNA-end requirements for hRad51-catalyzed strand exchange. Different linear dsDNA substrates as indicated were used in the strand exchange reaction supplied with 100 mM $(NH_4)_2SO_4$. The gray strand of each dsDNA substrate is the strand complementary to the circular ssDNA. The reactions were stopped 2 h after the reactions were initiated.

The hRad51-catalyzed strand-exchange reaction was then examined in the presence of HDHB. Reactions were performed in the presence of either 60 mM KCl and 2 mM $CaCl_2$ (Figure III-9A, B), or 50 mM $(NH_4)_2SO_4$ (Figure III-9C, D). In both conditions, HDHB stimulated the formation of nicked-circular DNA, a completely exchanged product, when the reaction was initiated from the 5'-end with respect to the displaced ssDNA. The DNA bands between the nicked-circular DNA and the linear dsDNA have also been observed previously in hRad51 strand exchange reactions (Bugreev et al., 2006; Liu et al., 2004). Because this band was dependent on the circular ssDNA and was not resistant to phenol-ethanol extraction (data not shown), we suspect that it represents an early form of joint molecules. The stimulation of heteroduplex extension was dependent on Rad51 and RPA, as HDHB alone could not stimulate nicked-circular DNA formation (Figure III-9A, C, lanes 6, 11). On the other hand, the formation of both nicked-circular DNA and joint molecules was inhibited by HDHB when the reaction started from the 3'-end of the displaced ssDNA (Figure III-9B, D). This could result from the disruption of nascent joint molecules by the 5'-3' translocation of HDHB on the circular ssDNA. HDHB did not promote the formation of pairing products with linear dsDNA with blunt or recessed ends (Figure III-9E).

A helicase-deficient Walker-B mutant HDHB (Taneja et al., 2002) was also tested in the strand exchange reaction. The mutant HDHB failed to stimulate the formation of nicked-circular DNA, indicating that HDHB helicase activity is required for the promotion (Figure III-10).

To better understand the mechanism of the stimulation, we labeled the 5'-end of the linear dsDNA with ^{32}P and quantified the products of the reaction. Rad51 promoted

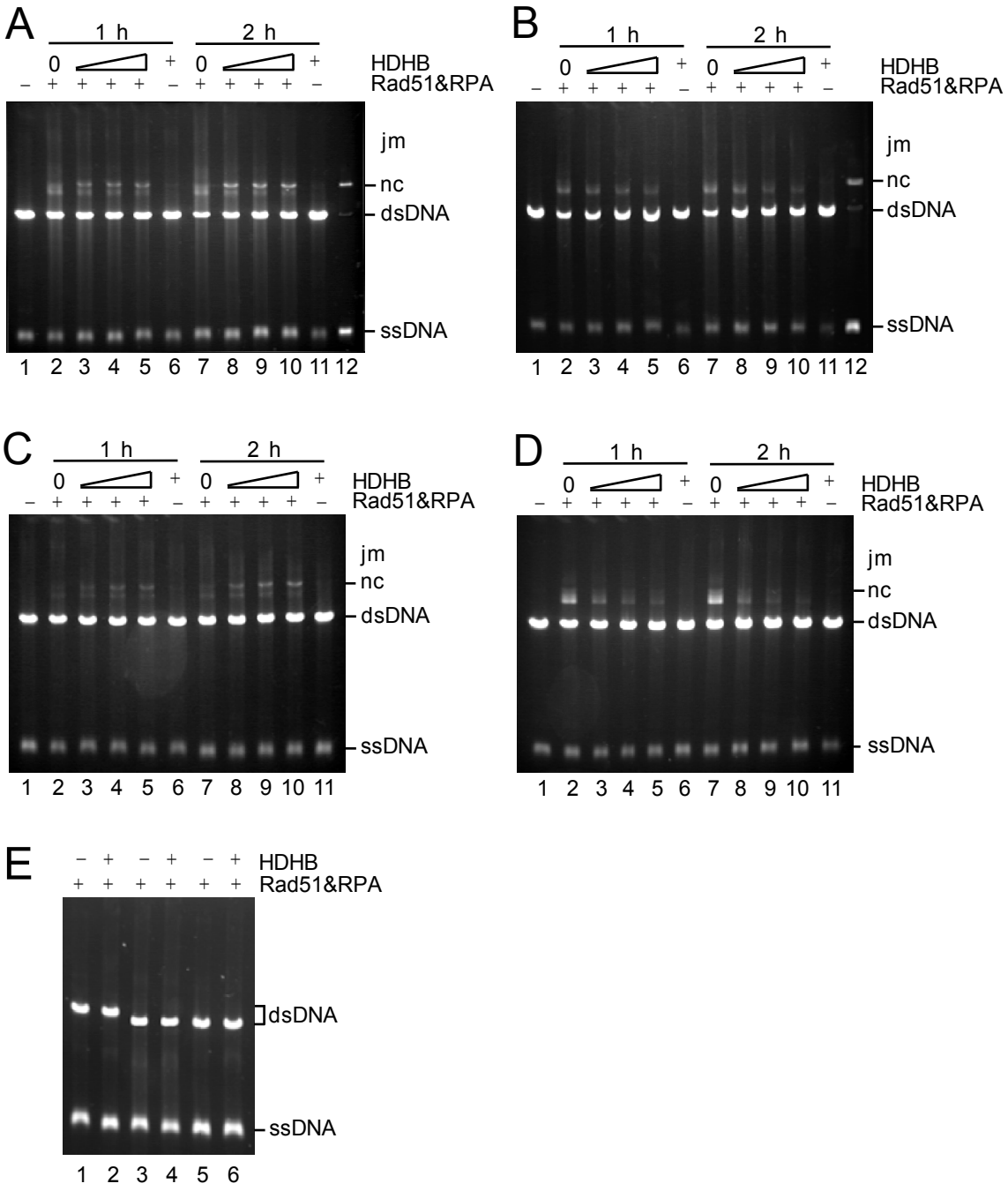

Figure III-9. **HDHB promotes the heteroduplex extension of hRad51-catalyzed strand exchange.** Reactions were performed in the presence of either 60 mM KCl and 2 mM $CaCl_2$ (A and B) or 50 mM $(NH_4)_2SO_4$ (C, D and E). Linear dsDNAs used in the reactions were: dsDNA with 3'-overhanging termini generated by *Pst*I cleavage (A and C); dsDNA with 5'-overhanging termini generated by *Xho*I cleavage (B and D); dsDNA with blunt-end termini generated by *Ssp*I cleavage (E, lanes 1 and 2); dsDNA with one blunt end and one 5'-recessed end (E, lanes 3 and 4); dsDNA with one blunt end and one 3'-recessed end (E, lanes 5 and 6). HDHB concentration in the reactions was: A, B, C and D, lanes 3 and 8, 50 nM; lanes 4 and 9, 100 nM; lanes 5 and 10, 150 nM. E, lanes 2, 4, 6, 100 nM. An annealed nicked-circular DNA marker is in lane 12 (A and B).

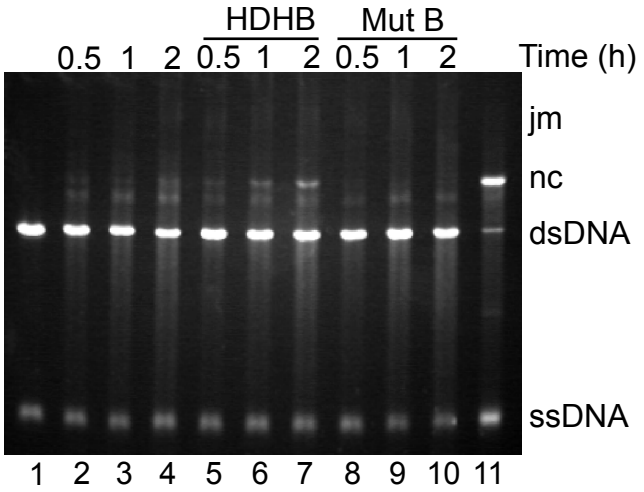

Figure III-10. **Walker B mutant HDHB did not promote the heteroduplex extension.** The strand exchange reaction was performed in the presence of 60 mM KCl and 2 mM $CaCl_2$. The concentration of wild-type (wt) HDHB and Walker B mutant HDHB (Mut B) was 100 nM. Lane 11, nicked-circular DNA marker. Aliquots from the reactions after 0.5, 1 and 2 h were taken and stopped.

the formation of joint molecules gradually in 3 h (Figure III-11A). However, little nicked-circular DNA was formed without HDHB. In the presence of HDHB, the formation of nicked circular DNA was significantly promoted (Figure III-11A). Furthermore, the formation of nicked-circular DNA was accompanied by the formation of linear ssDNA (Figure III-11A). The amount of joint molecules and nicked-circular DNA formed in the reactions was quantified in figure III-11B. Although more nicked-circular DNA was formed in the presence of HDHB than in its absence, the amount of joint molecules decreased in parallel (Figure III-11B). The total amount of reaction products (joint molecules and nicked circular DNA) were not promoted by HDHB, suggesting that HDHB stimulates nicked circular DNA formation by promoting the heteroduplex extension, but not the formation of joint molecules.

Another DNA helicase, SV40 large T-antigen, was also examined in the Rad51-catalyzed strand exchange reaction. SV40 large T-antigen is a viral replicative helicase with 3'-5' polarity (Goetz et al., 1988). We first performed a helicase assay to check the helicase activity of HDHB and T-antigen in our buffer systems. As shown in Figure III-12A, HDHB retained only about 30% activity in the presence of 50 mM $(NH_4)_2SO_4$, or 60 mM KCl and 2 mM $CaCl_2$, compared to a low salt condition (Taneja et al., 2002). In contrast, 300 nM T-antigen had twice the activity of 50 nM HDHB in the presence of 50 mM $(NH_4)_2SO_4$. However, even 600 nM T-antigen did not promote the formation of nicked-circular DNA in reactions from either direction, although the formation of joint molecules was slightly inhibited by T-antigen in both directions (Figure III-12B).

Discussion

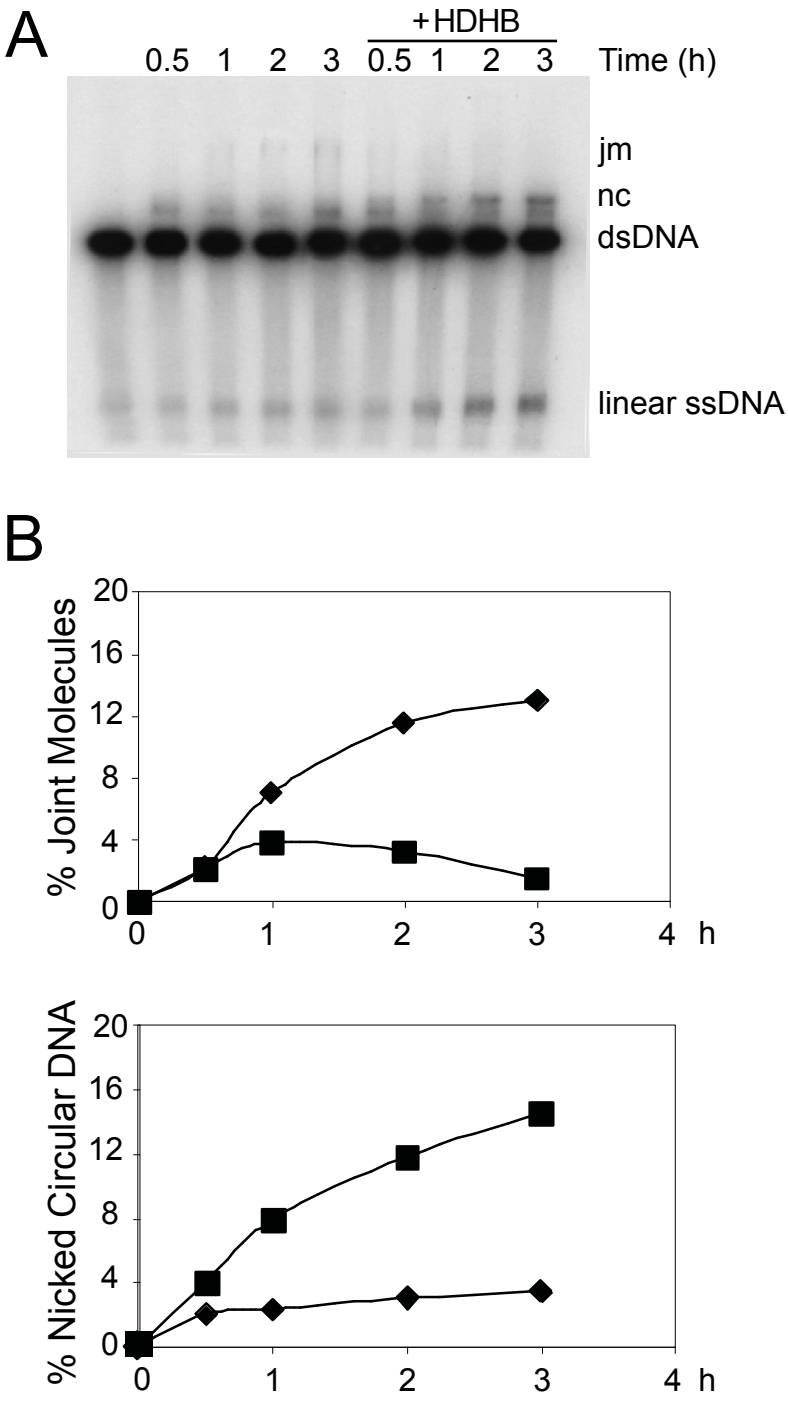

Figure III-11. **HDHB promotes heteroduplex extension but not joint molecule formation.** A, Strand exchange reaction was performed with ^{32}P-labeled linear dsDNA and in the presence of 50 mM $(NH_4)_2SO_4$. The concentration of HDHB was 100 nM. B and C, Quantitative analysis of joint molecules (B) and nicked-circular DNA (C) as the percentage of initial dsDNA. Square, with 100 nM HDHB; diamond, no HDHB.

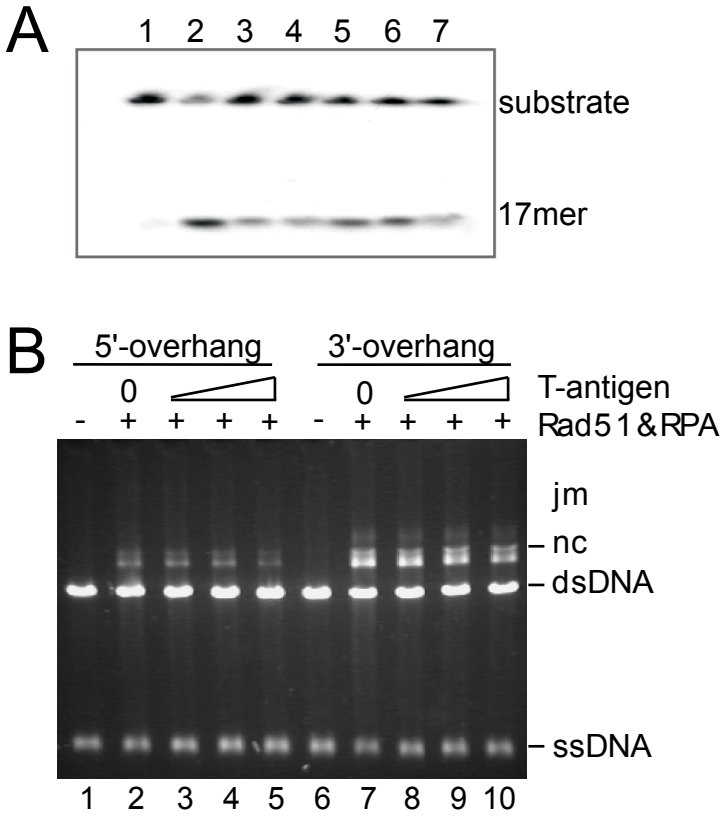

Figure III-12. **T-antigen does not promote heteroduplex extension.** A, Helicase assay performed with HDHB and T-antigen. Lane 1, initial substrate; lanes 2 and 5, helicase buffer (Taneja et al., 2002); lanes 3 and 6, strand exchange buffer with 50 mM $(NH_4)_2SO_4$; lanes 4 and 7, strand exchange buffer with 60 mM KCl and 2 mM $CaCl_2$. Protein concentration: lanes 2, 3 and 4, 50 nM HDHB; lanes 5, 6 and 7, 300 nM T-antigen. B, Strand exchange assay performed in the presence of 50 mM $(NH_4)_2SO_4$. Reaction was stopped 2 h later. T-antigen concentration used: lanes 3 and 8, 240 nM; lanes 4 and 9, 360 nM; lanes 5 and 10, 600 nM.

To assess the importance of HDHB in DNA damage response, we measured the survival rate of cells treated with different DNA damaging agents and found that HDHB-depleted cells were more sensitive than control-depleted cells to damage induced by mitomycin C, camptothecin, and IR (Figure 1). Repair of these lesions is known to depend on homologous recombination (Adachi et al., 2004; McHugh et al., 2001), suggesting that HDHB may function in homologous recombination. To evaluate the potential function of HDHB in homologous recombination, we monitored aphidicolin-induced chromosome breaks and sister chromatid exchange rate in HDHB-depleted cells. Aphidicolin induces replication-stress that results in expression of common fragile sites, manifested as chromosome breaks and gaps. Expression of common fragile sites also results when either BRCA1 or ATR checkpoint-mediated stabilization of stalled forks is compromised (Arlt et al., 2003). Homologous recombination and nonhomologous end-joining (NHEJ), two pathways for DNA double-strand break repair, are required to maintain the stability of fragile sites (Schwartz et al., 2005). The majority of sister chromatid exchanges occur at common fragile sites (Glover and Stein, 1987) and are known to be mediated by homologous recombination (Sonoda et al., 1999). We observed an increase of aphidicolin-induced chromosome breaks in HDHB-depleted cells and a decrease of sister chromatid exchange (SCE) (Figure III-2, 3). Both observations are consistent with the interpretation that depletion of HDHB reduces homologous recombination-dependent double-strand break repair, thereby reducing SCE and increasing unrepaired chromosome breaks under conditions of replication-stress. However, the results do not rule out a role for HDHB in NHEJ or fork stabilization.

Additional evidence for HDHB function in HR comes from an *in vivo* recombination assay, which directly measures the homologous recombination rate induced by a single chromosomal double-strand break in cells. These experiments showed that HDHB depletion by shRNA impaired homologous recombination (Figure III-4). We note that even in the absence of HDHB, Rad51 by itself can still complete the strand-exchange reaction to some extent, thus HDHB might not be absolutely required for homologous recombination. This could be reflected from the *in vivo* recombination experiment performed with both Rad51- and HDHB-shRNA. Depletion of Rad51 shows even larger inhibition of HR than depletion of HDHB (Figure III-4E).

To gain more insight into the function of HDHB in HR, we characterized the recruitment of damage response proteins in IR-induced nuclear foci in HDHB- and control-depleted cells. Rad51 and RPA form foci after ionizing radiation, which co-localize with H2AX foci, an indicator of double-strand breaks (Balajee and Geard, 2004; Paull et al., 2000; Rogakou et al., 1999). In HDHB-depleted cells, H2AX foci formed equally well (Figure III-5, 6). The formation of Rad51 foci after IR was also not affected by HDHB depletion. However, the formation of RPA foci after IR was impaired and/or retarded in HDHB-depleted cells. In interpreting this observation, it is important to consider that RPA has at least two roles in HR, first in facilitating the assembly of the Rad51-ssDNA filament prior to the invasion of the donor duplex and later in stabilizing the displaced ssDNA after Rad51-mediated strand invasion (Sugiyama et al., 1997; Sung, 1994; Wang and Haber, 2004). The observation that H2AX and Rad51 foci formed normally in HDHB-depleted cells thus suggests that the processing of double-strand break ends and the loading of Rad51 during homologous recombination are not

dependent on HDHB. In contrast, the slow formation of RPA foci in HDHB-depleted cells suggests a defect in the second role of RPA, the formation or stabilization of the displaced ssDNA during strand exchange, which would be coated by RPA and visible as RPA late-stage foci. The data therefore suggest that HDHB functions in heteroduplex extension after strand invasion.

Consistent with this interpretation, HDHB stimulated the formation of completely exchanged products in a Rad51-mediated 5'-3' strand exchange reaction *in vitro* (Figure III-8-12). The strand exchange in the reverse direction was inhibited by HDHB. Further more, HDHB did not promote the formation of joint molecules, suggesting that only the heteroduplex extension step was stimulated by HDHB. Because HDHB is a 5'-3' DNA helicase (Taneja et al., 2002), our results are consistent with HDHB translocating 5'-3' on either the displaced ssDNA strand or the circular ssDNA, resulting in 5'-3' promotion of heteroduplex extension or 3'-5' inhibition of strand pairing. In T4 bacteriophage, dda and gene 41 were shown to stimulate UvsX-directed heteroduplex DNA extension (Kodadek and Alberts, 1987; Salinas and Kodadek, 1995). In yeast, Mer3 helicase stimulates 3'-5' heteroduplex extension by Rad51 (Mazina et al., 2004). For both yeast Rad51 and human Rad51, the 5'-end of the invading ssDNA is more invasive than the 3'-end, and an ssDNA with a dsDNA tail has even stronger invading activity (Mazin et al., 2000). Considering that 3'-overhanging ssDNA is the invading strand, we speculate that during homologous recombination *in vivo*, the 5'-end of the invading ssDNA, which has a duplex DNA tail, would preferentially invade the homologous duplex. Then with the help of HDHB, the heteroduplex extends 5'-3' with respect to ssDNA (Figure III-13). This extension direction ensures the 3'-end of the invading ssDNA completely pair with the

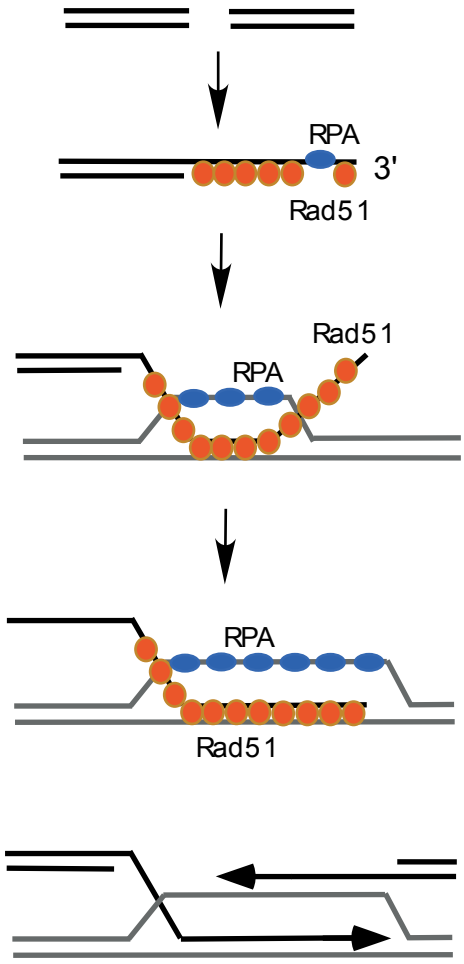

Figure III-13. **A model for the function of HDHB in stimulating heteroduplex extension during homologous recombination.** After Rad51-mediated strand invasion. HDHB is proposed to translocate 5'-3' on the donor DNA to displace the ssDNA ahead of the invading Rad51 filament and promote the heteroduplex extension.

complementary strand, which is critical for the subsequent DNA synthesis from the 3' terminus. So the stimulation of HDHB on 5'-3' heteroduplex extension will likely be biologically important for cells. This is also consistent with the 5'-3' unidirectional heteroduplex extension promoted by RecA in *E. coli* (Cox and Lehman, 1981; West et al., 1981).

We previously showed that HDHB interacts directly with TopBP1 and that HDHB depletion results in reduced TopBP1 foci formation after UV damage (Chapter II). We proposed that HDHB could help DNA polymerase α-primase form primers on RPA-ssDNA that are used to recruit Rad9/Rad1/Hus1 and TopBP1 (Byun et al., 2005). Dpb11, a budding yeast homolog of TopBP1, was shown to bind to the donor DNA during the late stage of HO endonuclease-induced MAT switching (Ogiwara et al., 2006). This binding was dependent on Rad51 (Ogiwara et al., 2006). The function of HDHB in promoting heteroduplex extension could conceivably promote the binding of TopBP1 to the heteroduplex during homologous recombination (Figure III-13), thus facilitating the checkpoint responses initiated by the ssDNA/duplex junction at the heteroduplex DNA and ATR (Bartek and Mailand, 2006). Another potential role of the heteroduplex extension promoted by HDHB would be to facilitate subsequent DNA synthesis from the 3'-end of the invading ssDNA. Interestingly, ATR affects cell viability after irradiation through homologous recombination, but not through NHEJ (Wang et al., 2004). The stimulation of the heteroduplex DNA extension by HDHB would result in a partial DNA duplex on the homologous DNA template, a similar DNA structure as the reaction product of polymerase α-primase promoted by HDHB. Thus, HDHB might display a common activity for the stimulation of partial DNA duplex formation *in vivo*.

CHAPTER IV

CONCLUSIONS AND FUTURE DIRECTIONS

DNA helicase B has been studied for nearly 25 years. *In vitro,* DNA helicase B promotes the primer synthesis by DNA polymerase α-primase on RPA-coated ssDNA (Saitoh et al., 1995; Taneja et al., 2002). Mouse cells with temperature-sensitive DNA helicase B have an impaired initiation of DNA replication when exposed to non-permissive temperature (Seki et al., 1995). The injection of a Walker B mutant HDHB into the nucleus of cells in early G1 blocks the initiation of DNA synthesis (Taneja et al., 2002), suggesting that HDHB may regulate DNA synthesis *in vivo,* possibly by participating in DNA replication initiation. Furthermore, ectopically expressed GFP-HDHB nuclear foci are stimulated by different DNA damaging agents (Gu et al., 2004), indicating that HDHB nuclear foci are associated with DNA damage response.

The research in this dissertation has been focused on unveiling the potential function of HDHB in DNA damage response. In Chapter II, we isolated chromatin from cells and observed the accumulation of HDHB on chromatin after DNA damage. HDHB chromatin accumulation is most prominent in S phase cells exposed to agents that cause replication fork stalling or collapse.

A question that would directly challenge the function of HDHB is how HDHB is recruited to chromatin after DNA damage. PIKK family kinases are the key proteins in DNA damage signaling. However, either the inhibitor of PIKK kinases or siRNA targeting ATM and ATR did not inhibit the damage-induced HDHB accumulation on

chromatin, suggesting that HDHB functions independent of ATR and ATM. We further found that UV-induced TopBP1 foci were diminished in HDHB-depleted cells. In consistent with the role of TopBP1 in stimulating ATR activity, UV-induced ATR-dependent CHK1 phosphorylation is impaired in HDHB-depleted cells.

Taken together, our data demonstrate that HDHB may have roles in the initiation of DNA damage signaling after replication fork arrest. The phosphorylation of CHK1 by ATR after replication fork uncoupling requires the priming on ssDNA by DNA polymerase α-primase (Byun et al., 2005). Because HDHB promotes primer synthesis on ssDNA by DNA polymerase α-primase (Taneja et al., 2002), we speculate that HDHB can facilitate the primer synthesis after the uncoupling of replication forks, thus enhance the activation of ATR by the partial DNA duplex structure.

If this model is correct, HDHB will act at a very early step during UV-induced DNA damage signaling, probably just follow the formation of long stretches of ssDNA at the uncoupled replication forks. The recruitment of HDHB to DNA may be dependent on the direct interaction of HDHB with RPA (Gulfem Guler, unpublished result) on the ssDNA, or may only require the ssDNA-binding activity of HDHB. An HDHB chromatin association experiment conducted with RPA-depleted cells will be able to address this question.

It also needs to be noted that in untreated cells, only a small portion of HDHB binds with chromatin. However, large amount of ssDNA created at stalled replication forks induces significant accumulation of HDHB on chromatin. Ionizing radiation generates double strand breaks, but only induces modest HDHB accumulation on

chromatin. Thus, ssDNA has much stronger effect of promoting HDHB accumulation on chromatin than dsDNA or double strand breaks.

The depletion of HDHB diminished UV-induced TopBP1 foci, thus raised the question of how HDHB regulates TopBP1 localization after UV damage. HDHB can directly interact with TopBP1 (Figure II-8D). This interaction could be important for the loading of TopBP1 to DNA by HDHB. It will be interesting to map the region on TopBP1 that interacts with HDHB and see whether the loading of TopBP1 requires this region. On the other hand, we cannot rule out the possibility that the requirement of HDHB for TopBP1 loading is an indirect result. The current model for activation of the S phase damage response involves two independent pathways that converge to activate ATR kinase activity (Cortez, 2005). In one pathway, Rad17-RFC loads the Rad9-Hus1-Rad1 clamp at recessed 5' primer ends on the RPA-ssDNA (Byun et al., 2005; Michael et al., 2000; Parrilla-Castellar and Karnitz, 2003; You et al., 2002). Loading of the Rad9-Hus1-Rad1 clamp requires that polymerase α-primase first generate these primers on the RPA-ssDNA template (Byun et al., 2005; Michael et al., 2000; Parrilla-Castellar and Karnitz, 2003; You et al., 2002). In *Schizosaccharomyces pombe*, phosphorylated Rad9 loads $Rad4^{TopBP1}$ to $Rad3^{ATR}$ and activates CHK1 (Furuya et al., 2004). We showed GFP-HDHB colocalized partially with Rad9 (Figure II-8). If HDHB promotes the priming of polymerase α-primase on RPA-ssDNA, its function will be required for the loading of Rad9-Hus1-Rad1 clamp and the subsequent TopBP1 recruitment. This could be an indirect effect of HDHB on the loading of TopBP1 onto DNA damage sites.

HDHB shares sequence motifs with *E. coli* RecD and T4 dda helicases (Taneja et al., 2002). Both of these prokaryotic proteins are involved in homologous recombination

(Dudas and Chovanec, 2004; Paques and Haber, 1999). In Chapter III, we further studied the role of HDHB in homologous recombination. Our *in vivo* reporter system indicates that HDHB-depleted cells have less recombination events.

During homologous recombination, the end of a double strand break is processed by nucleases into 3'-overhanging ssDNA. Rad51 promotes the invasion of this ssDNA into a homologous DNA duplex. To learn the detailed function of HDHB in homologous recombination, we first studied ionizing radiation-induced H2AX, Rad51 and RPA foci in HDHB-depleted cells. The observation that H2AX and Rad51 foci formed normally in HDHB-depleted cells suggests the processing of double-strand break ends and the loading of Rad51 during homologous recombination are not dependent on HDHB. In contrast, the slow formation of RPA foci in HDHB-depleted cells suggests a defect in the role of RPA for the formation or stabilization of the displaced ssDNA during strand exchange, which would be coated by RPA and visible as RPA late-stage foci. To further investigate the function of HDHB in homologous recombination, we performed *in vitro* strand exchange assay and showed HDHB can stimulate Rad51-mediated 5'-3' heteroduplex extension during homologous recombination. As reported previously (Mazin et al., 2000), the 5'-end of the invading ssDNA is more invasive than the 3'-end, and an ssDNA with a dsDNA tail has even stronger invading activity. If Rad51 initiates the invasion of the 5' end of the 3'-overhanging ssDNA into the homologous duplex, the rest regions of the long stretch ssDNA will need to be paired with the homologous complimentary DNA before the DNA extension from the 3'-terminus of the ssDNA can be initiated. By now there is no report in eukaryotes stating any enzyme involved in this process. In this dissertation, we propose that the stimulation of HDHB on Rad51-

mediated heteroduplex extension will greatly accelerate this process and ensure the pairing of 3'-terminus of the ssDNA with the complimentary DNA strand.

During heteroduplex extension, the invading ssDNA rapidly pairs with the complimentary strand and is converted to a partial DNA duplex. Since partial DNA duplex are good substrates for the activation of ATR-dependent signaling, the heteroduplex extension and the subsequent DNA extension would also involve the activation of ATR. Dpb 11, a budding yeast homolog of TopBP1, was reported to function with the checkpoint clamp in recombination repair (Ogiwara et al., 2006). In Chapter II, we reported that HDHB is required for TopBP1 focus formation after UV radiation. It will be interesting to see whether the stimulation of heteroduplex extension by HDHB can also facilitate the loading of TopBP1 to the donor strand during homologous recombination.

With our current model of HDHB stimulating 5'-3' heteroduplex extension during homologous recombination, we can imagine that if we deplete or mutate HDHB in cells, the heteroduplex extension will be delayed. Thus the subsequent DNA synthesis initiated from the 3'-terminus of invading ssDNA will be impaired. This prediction can be tested in the future.

APPENDIX

PHOSPHORYLATION OF HDHB AFTER DNA DAMAGE

Many proteins involved in DNA damage responses are phosphorylated after DNA damage treatment. Since HDHB is involved in DNA damage response, we studied the potential modification of HDHB after DNA damage.

Materials and Methods

U2OS cells were synchronized at G1/S by a double thymidine block. Cells were then released into fresh DMEM medium for 3 h. Then cells were treated with 20 Gy IR, 100 J/m^2 UV, or 10 μM camptothecin. About 1×10^7 cells were trypsinized, washed once with PBS, and resuspended in 500 μl solution A with 0.04% Triton X-100. Cells were incubated on ice for 5 min. Cytoplasmic proteins were separated from nuclei by centrifugation at 1300 × *g* for 5 min. Isolated nuclei were washed once with solution A and extracted in 500 μl IP buffer (20 mM Tris-Cl at pH 7.5, 150 mM NaCl, 0.5% NP-40, 1 mM DTT, 10 mM NaF, 1 mM Na_3VO_4, 1 mM PMSF, 10 μg/ml aprotinin, 1 μM leupeptin) for 20 min on ice. After centrifugation at 12500 × rpm, supernatant was collected and incubated with 3 μl polyclonal anti-HDHB antibody at 4 °C. Two h later, 20 μl protein A beads were added and the incubation was continued for 1 h. Protein A beads bound with HDHB were washed 3 times with IP buffer without NaF and Na_3VO_4. Beads were then washed once in 1× λ-phosphatase buffer (New England Biolabs, Beverly, MA) and resuspended in 100 μl 1× λ-phosphatase buffer. $MnCl_2$ was added to a

final concentration of 2 mM. Beads were incubated with 300 U λ-phosphatase for 1 h at 30 °C. Beads were then collected by centrifugation and boiled in 40 µl 2 × SDS buffer for 5 min. Proteins were separated by 7.5% SDS-PAGE. Electrophoresis was stopped when the 84 kDa marker had reached the bottom of the gel.

Results

To test whether HDHB can be phosphorylated after DNA damage, U2OS cells that had been treated during S phase with IR, UV, or camptothecin were used to prepare soluble and chromatin-bound nuclear protein fractions (S2 and P2). HDHB isoforms were separated by prolonged denaturing gel electrophoresis and analyzed by western blotting. HDHB in the soluble nuclear protein fraction from genotoxin-treated cells displayed a slower electrophoretic mobility than that from untreated cells (Figure IV-1). The retarded mobility observed with chromatin-bound HDHB from camptothecin-treated cells was similar to that of soluble nuclear HDHB from the same cells (Figure IV-1B, compare lanes 2, 4). These results suggest that the soluble and chromatin-bound fractions of nuclear HDHB undergo similar modifications after damage.

We next sought to determine whether the slowly migrating HDHB band was phosphorylated. HDHB was immunoprecipitated from nuclear extracts of camptothecin-treated or control S phase cells and then treated with λ-phosphatase. Hydrolysis of the phosphorylated residues should restore the mobility of HDHB to that of HDHB from extracts of undamaged cells. The slowly migrating band of HDHB observed in camptothecin-treated cells (Figure IV-1C, lane 2) was restored to the mobility of nuclear HDHB from undamaged cells after λ-phosphatase treatment (Figure IV-1C, lane 5),

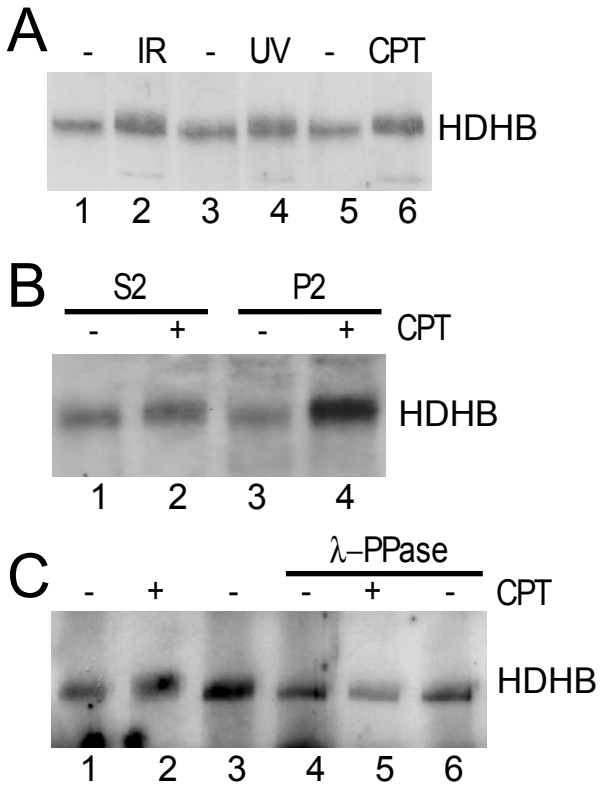

Figure IV-1. **DNA damage induces phosphorylation of HDHB**. A, U2OS cells were synchronized in S phase and treated with 20 Gy IR, 100 J/ m^2 UV, or 10 μM camptothecin (CPT). Two h later, cells were fractionated. S2 fractions were analyzed by 7.5% SDS-PAGE and western blotting with anti-HDHB antibody. B, S phase U2OS cells were treated with 10 μM camptothecin (CPT). Two h later, cells were fractionated. S2 and P2 fractions were analyzed as in A. C, S phase U2OS cells were treated with 10 μM camptothecin (CPT). Two h later, nuclei were isolated and extracted with IP buffer. HDHB was immunoprecipitated using polyclonal anti-HDHB antibody and protein A beads, then treated with λ-phosphatase as indicated, and analyzed as in A.

arguing that nuclear HDHB in camptothecin-treated cells was in fact phosphorylated. More works are required to elucidate the detailed function of this phosphorylation event.

REFERENCES

Abdel-Monem, M., Durwald, H. and Hoffmann-Berling, H. (1976) Enzymic unwinding of DNA. 2. Chain separation by an ATP-dependent DNA unwinding enzyme. *Eur J Biochem*, **65**, 441-449.

Abraham, R.T. (2001) Cell cycle checkpoint signaling through the ATM and ATR kinases. *Genes Dev*, **15**, 2177-2196.

Adachi, N., So, S. and Koyama, H. (2004) Loss of nonhomologous end joining confers camptothecin resistance in DT40 cells. Implications for the repair of topoisomerase I-mediated DNA damage. *J Biol Chem*, **279**, 37343-37348.

Adams, K.E., Medhurst, A.L., Dart, D.A. and Lakin, N.D. (2006) Recruitment of ATR to sites of ionising radiation-induced DNA damage requires ATM and components of the MRN protein complex. *Oncogene*, **25**, 3894-3904.

Ahuja, D., Saenz-Robles, M.T. and Pipas, J.M. (2005) SV40 large T antigen targets multiple cellular pathways to elicit cellular transformation. *Oncogene*, **24**, 7729-7745.

Aladjem, M.I. and Fanning, E. (2004) The replicon revisited: an old model learns new tricks in metazoan chromosomes. *EMBO Rep*, **5**, 686-691.

Anderson, D.G. and Kowalczykowski, S.C. (1997) The recombination hot spot chi is a regulatory element that switches the polarity of DNA degradation by the RecBCD enzyme. *Genes Dev*, **11**, 571-581.

Arai, K. and Kornberg, A. (1979) A general priming system employing only dnaB protein and primase for DNA replication. *Proc Natl Acad Sci U S A*, **76**, 4308-4312.

Araki, H., Leem, S.H., Phongdara, A. and Sugino, A. (1995) Dpb11, which interacts with DNA polymerase II(epsilon) in Saccharomyces cerevisiae, has a dual role in S-phase progression and at a cell cycle checkpoint. *Proc Natl Acad Sci U S A*, **92**, 11791-11795.

Arlt, M.F., Casper, A.M. and Glover, T.W. (2003) Common fragile sites. *Cytogenet Genome Res*, **100**, 92-100.

Arthur, A.K., Hoss, A. and Fanning, E. (1988) Expression of simian virus 40 T antigen in Escherichia coli: localization of T-antigen origin DNA-binding domain to within 129 amino acids. *J Virol*, **62**, 1999-2006.

Baker, T.A., Sekimizu, K., Funnell, B.E. and Kornberg, A. (1986) Extensive unwinding of the plasmid template during staged enzymatic initiation of DNA replication from the origin of the Escherichia coli chromosome. *Cell*, **45**, 53-64.

Bakkenist, C.J. and Kastan, M.B. (2003) DNA damage activates ATM through intermolecular autophosphorylation and dimer dissociation. *Nature*, **421**, 499-506.

Balajee, A.S. and Geard, C.R. (2004) Replication protein A and gamma-H2AX foci assembly is triggered by cellular response to DNA double-strand breaks. *Exp Cell Res*, **300**, 320-334.

Ball, H.L., Ehrhardt, M.R., Mordes, D.A., Glick, G.G., Chazin, W.J. and Cortez, D. (2007) Function of a Conserved Checkpoint Recruitment Domain in ATRIP Proteins. *Mol Cell Biol*, **27**, 3367-3377.

Ball, H.L., Myers, J.S. and Cortez, D. (2005) ATRIP binding to replication protein A-single-stranded DNA promotes ATR-ATRIP localization but is dispensable for Chk1 phosphorylation. *Mol Biol Cell*, **16**, 2372-2381.

Bambara, R.A., Murante, R.S. and Henricksen, L.A. (1997) Enzymes and reactions at the eukaryotic DNA replication fork. *J Biol Chem*, **272**, 4647-4650.

Banin, S., Moyal, L., Shieh, S., Taya, Y., Anderson, C.W., Chessa, L., Smorodinsky, N.I., Prives, C., Reiss, Y., Shiloh, Y. and Ziv, Y. (1998) Enhanced phosphorylation of p53 by ATM in response to DNA damage. *Science*, **281**, 1674-1677.

Bartek, J., Lukas, C. and Lukas, J. (2004) Checking on DNA damage in S phase. *Nat Rev Mol Cell Biol*, **5**, 792-804.

Bartek, J. and Mailand, N. (2006) TOPping up ATR activity. *Cell*, **124**, 888-890.

Bell, S.P. (1995) Eukaryotic replicators and associated protein complexes. *Curr Opin Genet Dev*, **5**, 162-167.

Bell, S.P. and Dutta, A. (2002) DNA replication in eukaryotic cells. *Annu Rev Biochem*, **71**, 333-374.

Bermudez, V.P., Lindsey-Boltz, L.A., Cesare, A.J., Maniwa, Y., Griffith, J.D., Hurwitz, J. and Sancar, A. (2003) Loading of the human 9-1-1 checkpoint complex onto DNA by the checkpoint clamp loader hRad17-replication factor C complex in vitro. *Proc Natl Acad Sci U S A*, **100**, 1633-1638.

Bianco, P.R. and Kowalczykowski, S.C. (1997) The recombination hotspot Chi is recognized by the translocating RecBCD enzyme as the single strand of DNA containing the sequence 5'-GCTGGTGG-3'. *Proc Natl Acad Sci U S A*, **94**, 6706-6711.

Boule, J.B. and Zakian, V.A. (2006) Roles of Pif1-like helicases in the maintenance of genomic stability. *Nucleic Acids Res*, **34**, 4147-4153.

Bramhill, D. and Kornberg, A. (1988) Duplex opening by dnaA protein at novel sequences in initiation of replication at the origin of the E. coli chromosome. *Cell*, **52**, 743-755.

Bravo, R., Frank, R., Blundell, P.A. and Macdonald-Bravo, H. (1987) Cyclin/PCNA is the auxiliary protein of DNA polymerase-delta. *Nature*, **326**, 515-517.

Brown, E.J. and Baltimore, D. (2000) ATR disruption leads to chromosomal fragmentation and early embryonic lethality. *Genes Dev*, **14**, 397-402.

Brown, E.J. and Baltimore, D. (2003) Essential and dispensable roles of ATR in cell cycle arrest and genome maintenance. *Genes Dev*, **17**, 615-628.

Brummelkamp, T.R., Bernards, R. and Agami, R. (2002a) Stable suppression of tumorigenicity by virus-mediated RNA interference. *Cancer Cell*, **2**, 243-247.

Brummelkamp, T.R., Bernards, R. and Agami, R. (2002b) A system for stable expression of short interfering RNAs in mammalian cells. *Science*, **296**, 550-553.

Bugreev, D.V. and Mazin, A.V. (2004) Ca2+ activates human homologous recombination protein Rad51 by modulating its ATPase activity. *Proc Natl Acad Sci U S A*, **101**, 9988-9993.

Bugreev, D.V., Mazina, O.M. and Mazin, A.V. (2006) Rad54 protein promotes branch migration of Holliday junctions. *Nature*, **442**, 590-593.

Bullock, P.A. (1997) The initiation of simian virus 40 DNA replication in vitro. *Crit Rev Biochem Mol Biol*, **32**, 503-568.

Bullock, P.A., Seo, Y.S. and Hurwitz, J. (1991) Initiation of simian virus 40 DNA synthesis in vitro. *Mol Cell Biol*, **11**, 2350-2361.

Byrd, A.K. and Raney, K.D. (2004) Protein displacement by an assembly of helicase molecules aligned along single-stranded DNA. *Nat Struct Mol Biol*, **11**, 531-538.

Byun, T.S., Pacek, M., Yee, M.C., Walter, J.C. and Cimprich, K.A. (2005) Functional uncoupling of MCM helicase and DNA polymerase activities activates the ATR-dependent checkpoint. *Genes Dev*, **19**, 1040-1052.

Campbell, K.S., Mullane, K.P., Aksoy, I.A., Stubdal, H., Zalvide, J., Pipas, J.M., Silver, P.A., Roberts, T.M., Schaffhausen, B.S. and DeCaprio, J.A. (1997) DnaJ/hsp40 chaperone domain of SV40 large T antigen promotes efficient viral DNA replication. *Genes Dev*, **11**, 1098-1110.

Canman, C.E., Lim, D.S., Cimprich, K.A., Taya, Y., Tamai, K., Sakaguchi, K., Appella, E., Kastan, M.B. and Siliciano, J.D. (1998) Activation of the ATM kinase by ionizing radiation and phosphorylation of p53. *Science*, **281**, 1677-1679.

Carney, J.P., Maser, R.S., Olivares, H., Davis, E.M., Le Beau, M., Yates, J.R., 3rd, Hays, L., Morgan, W.F. and Petrini, J.H. (1998) The hMre11/hRad50 protein complex and Nijmegen breakage syndrome: linkage of double-strand break repair to the cellular DNA damage response. *Cell*, **93**, 477-486.

Chaganti, R.S., Schonberg, S. and German, J. (1974) A manyfold increase in sister chromatid exchanges in Bloom's syndrome lymphocytes. *Proc Natl Acad Sci U S A*, **71**, 4508-4512.

Chehab, N.H., Malikzay, A., Stavridi, E.S. and Halazonetis, T.D. (1999) Phosphorylation of Ser-20 mediates stabilization of human p53 in response to DNA damage. *Proc Natl Acad Sci U S A*, **96**, 13777-13782.

Cimprich, K.A., Shin, T.B., Keith, C.T. and Schreiber, S.L. (1996) cDNA cloning and gene mapping of a candidate human cell cycle checkpoint protein. *Proc Natl Acad Sci U S A*, **93**, 2850-2855.

Coleman, T.R., Carpenter, P.B. and Dunphy, W.G. (1996) The Xenopus Cdc6 protein is essential for the initiation of a single round of DNA replication in cell-free extracts. *Cell*, **87**, 53-63.

Collis, S.J., DeWeese, T.L., Jeggo, P.A. and Parker, A.R. (2005) The life and death of DNA-PK. *Oncogene*, **24**, 949-961.

Constantin, N., Dzantiev, L., Kadyrov, F.A. and Modrich, P. (2005) Human mismatch repair: reconstitution of a nick-directed bidirectional reaction. *J Biol Chem*, **280**, 39752-39761.

Constantinesco, F., Forterre, P., Koonin, E.V., Aravind, L. and Elie, C. (2004) A bipolar DNA helicase gene, herA, clusters with rad50, mre11 and nurA genes in thermophilic archaea. *Nucleic Acids Res*, **32**, 1439-1447.

Cortez, D. (2005) Unwind and slow down: checkpoint activation by helicase and polymerase uncoupling. *Genes Dev*, **19**, 1007-1012.

Cortez, D., Guntuku, S., Qin, J. and Elledge, S.J. (2001) ATR and ATRIP: partners in checkpoint signaling. *Science*, **294**, 1713-1716.

Cortez, D., Wang, Y., Qin, J. and Elledge, S.J. (1999) Requirement of ATM-dependent phosphorylation of brca1 in the DNA damage response to double-strand breaks. *Science*, **286**, 1162-1166.

Cox, M.M. and Lehman, I.R. (1981) Directionality and polarity in recA protein-promoted branch migration. *Proc Natl Acad Sci U S A*, **78**, 6018-6022.

Crabbe, L., Verdun, R.E., Haggblom, C.I. and Karlseder, J. (2004) Defective telomere lagging strand synthesis in cells lacking WRN helicase activity. *Science*, **306**, 1951-1953.

D'Amours, D. and Jackson, S.P. (2002) The Mre11 complex: at the crossroads of dna repair and checkpoint signalling. *Nat Rev Mol Cell Biol*, **3**, 317-327.

Daniels, D.S. and Tainer, J.A. (2000) Conserved structural motifs governing the stoichiometric repair of alkylated DNA by O(6)-alkylguanine-DNA alkyltransferase. *Mutat Res*, **460**, 151-163.

DeCaprio, J.A., Ludlow, J.W., Figge, J., Shew, J.Y., Huang, C.M., Lee, W.H., Marsilio, E., Paucha, E. and Livingston, D.M. (1988) SV40 large tumor antigen forms a specific complex with the product of the retinoblastoma susceptibility gene. *Cell*, **54**, 275-283.

Dillingham, M.S., Spies, M. and Kowalczykowski, S.C. (2003) RecBCD enzyme is a bipolar DNA helicase. *Nature*, **423**, 893-897.

Dodson, M., Dean, F.B., Bullock, P., Echols, H. and Hurwitz, J. (1987) Unwinding of duplex DNA from the SV40 origin of replication by T antigen. *Science*, **238**, 964-967.

Dornreiter, I., Copeland, W.C. and Wang, T.S. (1993) Initiation of simian virus 40 DNA replication requires the interaction of a specific domain of human DNA polymerase alpha with large T antigen. *Mol Cell Biol*, **13**, 809-820.

Dornreiter, I., Erdile, L.F., Gilbert, I.U., von Winkler, D., Kelly, T.J. and Fanning, E. (1992) Interaction of DNA polymerase alpha-primase with cellular replication protein A and SV40 T antigen. *Embo J*, **11**, 769-776.

Dornreiter, I., Hoss, A., Arthur, A.K. and Fanning, E. (1990) SV40 T antigen binds directly to the large subunit of purified DNA polymerase alpha. *Embo J*, **9**, 3329-3336.

Drury, L.S., Perkins, G. and Diffley, J.F. (2000) The cyclin-dependent kinase Cdc28p regulates distinct modes of Cdc6p proteolysis during the budding yeast cell cycle. *Curr Biol*, **10**, 231-240.

Dudas, A. and Chovanec, M. (2004) DNA double-strand break repair by homologous recombination. *Mutat Res*, **566**, 131-167.

Ellis, N.A., Groden, J., Ye, T.Z., Straughen, J., Lennon, D.J., Ciocci, S., Proytcheva, M. and German, J. (1995) The Bloom's syndrome gene product is homologous to RecQ helicases. *Cell*, **83**, 655-666.

Ellison, V. and Stillman, B. (2003) Biochemical characterization of DNA damage checkpoint complexes: clamp loader and clamp complexes with specificity for 5' recessed DNA. *PLoS Biol*, **1**, E33.

Fairman, M.P. and Stillman, B. (1988) Cellular factors required for multiple stages of SV40 DNA replication in vitro. *Embo J*, **7**, 1211-1218.

Falck, J., Mailand, N., Syljuasen, R.G., Bartek, J. and Lukas, J. (2001) The ATM-Chk2-Cdc25A checkpoint pathway guards against radioresistant DNA synthesis. *Nature*, **410**, 842-847.

Fanning, E., Klimovich, V. and Nager, A.R. (2006) A dynamic model for replication protein A (RPA) function in DNA processing pathways. *Nucleic Acids Res*, **34**, 4126-4137.

Fanning, E. and Knippers, R. (1992) Structure and function of simian virus 40 large tumor antigen. *Annu Rev Biochem*, **61**, 55-85.

Findeisen, M., El-Denary, M., Kapitza, T., Graf, R. and Strausfeld, U. (1999) Cyclin A-dependent kinase activity affects chromatin binding of ORC, Cdc6, and MCM in egg extracts of Xenopus laevis. *Eur J Biochem*, **264**, 415-426.

Fishman-Lobell, J., Rudin, N. and Haber, J.E. (1992) Two alternative pathways of double-strand break repair that are kinetically separable and independently modulated. *Mol Cell Biol*, **12**, 1292-1303.

Fuller, R.S. and Kornberg, A. (1983) Purified dnaA protein in initiation of replication at the Escherichia coli chromosomal origin of replication. *Proc Natl Acad Sci U S A*, **80**, 5817-5821.

Gangloff, S., Soustelle, C. and Fabre, F. (2000) Homologous recombination is responsible for cell death in the absence of the Sgs1 and Srs2 helicases. *Nat Genet*, **25**, 192-194.

Garcia, V., Furuya, K. and Carr, A.M. (2005) Identification and functional analysis of TopBP1 and its homologs. *DNA Repair (Amst)*, **4**, 1227-1239.

Garg, P. and Burgers, P.M. (2005) DNA polymerases that propagate the eukaryotic DNA replication fork. *Crit Rev Biochem Mol Biol*, **40**, 115-128.

Glover, T.W., Arlt, M.F., Casper, A.M. and Durkin, S.G. (2005) Mechanisms of common fragile site instability. *Hum Mol Genet*, **14 Spec No. 2**, R197-205.

Glover, T.W. and Stein, C.K. (1987) Induction of sister chromatid exchanges at common fragile sites. *Am J Hum Genet*, **41**, 882-890.

Goetz, G.S., Dean, F.B., Hurwitz, J. and Matson, S.W. (1988) The unwinding of duplex regions in DNA by the simian virus 40 large tumor antigen-associated DNA helicase activity. *J Biol Chem*, **263**, 383-392.

Goldberg, M., Stucki, M., Falck, J., D'Amours, D., Rahman, D., Pappin, D., Bartek, J. and Jackson, S.P. (2003) MDC1 is required for the intra-S-phase DNA damage checkpoint. *Nature*, **421**, 952-956.

Greer, D.A., Besley, B.D., Kennedy, K.B. and Davey, S. (2003) hRad9 rapidly binds DNA containing double-strand breaks and is required for damage-dependent topoisomerase II beta binding protein 1 focus formation. *Cancer Res*, **63**, 4829-4835.

Griffith, J.D., Lindsey-Boltz, L.A. and Sancar, A. (2002) Structures of the human Rad17-replication factor C and checkpoint Rad 9-1-1 complexes visualized by glycerol spray/low voltage microscopy. *J Biol Chem*, **277**, 15233-15236.

Gu, J., Xia, X., Yan, P., Liu, H., Podust, V.N., Reynolds, A.B. and Fanning, E. (2004) Cell cycle-dependent regulation of a human DNA helicase that localizes in DNA damage foci. *Mol Biol Cell*, **15**, 3320-3332.

Hashimoto, Y., Tsujimura, T., Sugino, A. and Takisawa, H. (2006) The phosphorylated C-terminal domain of Xenopus Cut5 directly mediates ATR-dependent activation of Chk1. *Genes Cells*, **11**, 993-1007.

Heller, R.C. and Marians, K.J. (2005) The disposition of nascent strands at stalled replication forks dictates the pathway of replisome loading during restart. *Mol Cell*, **17**, 733-743.

Heller, R.C. and Marians, K.J. (2006) Replisome assembly and the direct restart of stalled replication forks. *Nat Rev Mol Cell Biol*, **7**, 932-943.

Henricksen, L.A., Umbricht, C.B. and Wold, M.S. (1994) Recombinant replication protein A: expression, complex formation, and functional characterization. *J Biol Chem*, **269**, 11121-11132.

Hickson, I.D. (2003) RecQ helicases: caretakers of the genome. *Nat Rev Cancer*, **3**, 169-178.

Hotta, Y. and Stern, H. (1978) DNA unwinding protein from meiotic cells of Lilium. *Biochemistry*, **17**, 1872-1880.

Huang, S., Li, B., Gray, M.D., Oshima, J., Mian, I.S. and Campisi, J. (1998) The premature ageing syndrome protein, WRN, is a 3'-->5' exonuclease. *Nat Genet*, **20**, 114-116.

Ishimi, Y. (1997) A DNA helicase activity is associated with an MCM4, -6, and -7 protein complex. *J Biol Chem*, **272**, 24508-24513.

Ishimi, Y., Claude, A., Bullock, P. and Hurwitz, J. (1988) Complete enzymatic synthesis of DNA containing the SV40 origin of replication. *J Biol Chem*, **263**, 19723-19733.

Jazayeri, A., Falck, J., Lukas, C., Bartek, J., Smith, G.C., Lukas, J. and Jackson, S.P. (2006) ATM- and cell cycle-dependent regulation of ATR in response to DNA double-strand breaks. *Nat Cell Biol*, **8**, 37-45.

Johnson, R.D., Liu, N. and Jasin, M. (1999) Mammalian XRCC2 promotes the repair of DNA double-strand breaks by homologous recombination. *Nature*, **401**, 397-399.

Kaguni, J.M. (2006) DnaA: controlling the initiation of bacterial DNA replication and more. *Annu Rev Microbiol*, **60**, 351-375.

Kaplan, D.L. and O'Donnell, M. (2002) DnaB drives DNA branch migration and dislodges proteins while encircling two DNA strands. *Mol Cell*, **10**, 647-657.

Kenny, M.K., Schlegel, U., Furneaux, H. and Hurwitz, J. (1990) The role of human single-stranded DNA binding protein and its individual subunits in simian virus 40 DNA replication. *J Biol Chem*, **265**, 7693-7700.

Khakhar, R.R., Cobb, J.A., Bjergbaek, L., Hickson, I.D. and Gasser, S.M. (2003) RecQ helicases: multiple roles in genome maintenance. *Trends Cell Biol*, **13**, 493-501.

Kim, S.M., Kumagai, A., Lee, J. and Dunphy, W.G. (2005) Phosphorylation of Chk1 by ATM- and Rad3-related (ATR) in Xenopus egg extracts requires binding of ATRIP to ATR but not the stable DNA-binding or coiled-coil domains of ATRIP. *J Biol Chem*, **280**, 38355-38364.

Kim, S.T., Lim, D.S., Canman, C.E. and Kastan, M.B. (1999) Substrate specificities and identification of putative substrates of ATM kinase family members. *J Biol Chem*, **274**, 37538-37543.

Kitao, S., Shimamoto, A., Goto, M., Miller, R.W., Smithson, W.A., Lindor, N.M. and Furuichi, Y. (1999) Mutations in RECQL4 cause a subset of cases of Rothmund-Thomson syndrome. *Nat Genet*, **22**, 82-84.

Klungland, A. and Lindahl, T. (1997) Second pathway for completion of human DNA base excision-repair: reconstitution with purified proteins and requirement for DNase IV (FEN1). *Embo J*, **16**, 3341-3348.

Kodadek, T. and Alberts, B.M. (1987) Stimulation of protein-directed strand exchange by a DNA helicase. *Nature*, **326**, 312-314.

Kremmer, E., Kranz, B.R., Hille, A., Klein, K., Eulitz, M., Hoffmann-Fezer, G., Feiden, W., Herrmann, K., Delecluse, H.J., Delsol, G., Bornkamm, G.W., Mueller-Lantzsch, N. and Grassert, F.A. (1995) Rat monoclonal antibodies differentiating between the Epstein-Barr virus nuclear antigens 2A (EBNA2A) and 2B (EBNA2B). *Virology*, **208**, 336-342.

Kumagai, A., Kim, S.M. and Dunphy, W.G. (2004) Claspin and the activated form of ATR-ATRIP collaborate in the activation of Chk1. *J Biol Chem*, **279**, 49599-49608.

Kumagai, A., Lee, J., Yoo, H.Y. and Dunphy, W.G. (2006) TopBP1 activates the ATR-ATRIP complex. *Cell*, **124**, 943-955.

Kunkel, T.A. and Erie, D.A. (2005) DNA mismatch repair. *Annu Rev Biochem*, **74**, 681-710.

Labib, K., Tercero, J.A. and Diffley, J.F. (2000) Uninterrupted MCM2-7 function required for DNA replication fork progression. *Science*, **288**, 1643-1647.

LeBowitz, J.H. and McMacken, R. (1986) The Escherichia coli dnaB replication protein is a DNA helicase. *J Biol Chem*, **261**, 4738-4748.

Lee, J.H. and Paull, T.T. (2004) Direct activation of the ATM protein kinase by the Mre11/Rad50/Nbs1 complex. *Science*, **304**, 93-96.

Lee, J.H. and Paull, T.T. (2005) ATM activation by DNA double-strand breaks through the Mre11-Rad50-Nbs1 complex. *Science*, **308**, 551-554.

Lee, J.K. and Hurwitz, J. (2000) Isolation and characterization of various complexes of the minichromosome maintenance proteins of Schizosaccharomyces pombe. *J Biol Chem*, **275**, 18871-18878.

Lehmann, A.R. (2005) Replication of damaged DNA by translesion synthesis in human cells. *FEBS Lett*, **579**, 873-876.

Lei, M., Kawasaki, Y. and Tye, B.K. (1996) Physical interactions among Mcm proteins and effects of Mcm dosage on DNA replication in Saccharomyces cerevisiae. *Mol Cell Biol*, **16**, 5081-5090.

Li, D., Zhao, R., Lilyestrom, W., Gai, D., Zhang, R., DeCaprio, J.A., Fanning, E., Jochimiak, A., Szakonyi, G. and Chen, X.S. (2003) Structure of the replicative helicase of the oncoprotein SV40 large tumour antigen. *Nature*, **423**, 512-518.

Lim, D.S., Kim, S.T., Xu, B., Maser, R.S., Lin, J., Petrini, J.H. and Kastan, M.B. (2000) ATM phosphorylates p95/nbs1 in an S-phase checkpoint pathway. *Nature*, **404**, 613-617.

Linzer, D.I. and Levine, A.J. (1979) Characterization of a 54K dalton cellular SV40 tumor antigen present in SV40-transformed cells and uninfected embryonal carcinoma cells. *Cell*, **17**, 43-52.

Liu, J. and Marians, K.J. (1999) PriA-directed assembly of a primosome on D loop DNA. *J Biol Chem*, **274**, 25033-25041.

Liu, K., Paik, J.C., Wang, B., Lin, F.T. and Lin, W.C. (2006) Regulation of TopBP1 oligomerization by Akt/PKB for cell survival. *Embo J*, **25**, 4795-4807.

Liu, Q., Guntuku, S., Cui, X.S., Matsuoka, S., Cortez, D., Tamai, K., Luo, G., Carattini-Rivera, S., DeMayo, F., Bradley, A., Donehower, L.A. and Elledge, S.J. (2000) Chk1 is an essential kinase that is regulated by Atr and required for the G(2)/M DNA damage checkpoint. *Genes Dev*, **14**, 1448-1459.

Liu, Y., Stasiak, A.Z., Masson, J.Y., McIlwraith, M.J., Stasiak, A. and West, S.C. (2004) Conformational changes modulate the activity of human RAD51 protein. *J Mol Biol*, **337**, 817-827.

Lou, Z., Minter-Dykhouse, K., Wu, X. and Chen, J. (2003) MDC1 is coupled to activated CHK2 in mammalian DNA damage response pathways. *Nature*, **421**, 957-961.

Lupardus, P.J., Byun, T., Yee, M.C., Hekmat-Nejad, M. and Cimprich, K.A. (2002) A requirement for replication in activation of the ATR-dependent DNA damage checkpoint. *Genes Dev*, **16**, 2327-2332.

Ma, Y., Lu, H., Tippin, B., Goodman, M.F., Shimazaki, N., Koiwai, O., Hsieh, C.L., Schwarz, K. and Lieber, M.R. (2004) A biochemically defined system for mammalian nonhomologous DNA end joining. *Mol Cell*, **16**, 701-713.

Machwe, A., Xiao, L., Groden, J. and Orren, D.K. (2006) The Werner and Bloom syndrome proteins catalyze regression of a model replication fork. *Biochemistry*, **45**, 13939-13946.

Mackintosh, S.G. and Raney, K.D. (2006) DNA unwinding and protein displacement by superfamily 1 and superfamily 2 helicases. *Nucleic Acids Res*, **34**, 4154-4159.

Majka, J., Niedziela-Majka, A. and Burgers, P.M. (2006) The checkpoint clamp activates Mec1 kinase during initiation of the DNA damage checkpoint. *Mol Cell*, **24**, 891-901.

Maki, S. and Kornberg, A. (1988) DNA polymerase III holoenzyme of Escherichia coli. I. Purification and distinctive functions of subunits tau and gamma, the dnaZX gene products. *J Biol Chem*, **263**, 6547-6554.

Makiniemi, M., Hillukkala, T., Tuusa, J., Reini, K., Vaara, M., Huang, D., Pospiech, H., Majuri, I., Westerling, T., Makela, T.P. and Syvaoja, J.E. (2001) BRCT domain-containing protein TopBP1 functions in DNA replication and damage response. *J Biol Chem*, **276**, 30399-30406.

Masai, H., Matsui, E., You, Z., Ishimi, Y., Tamai, K. and Arai, K. (2000) Human Cdc7-related kinase complex. In vitro phosphorylation of MCM by concerted actions of Cdks and Cdc7 and that of a criticial threonine residue of Cdc7 bY Cdks. *J Biol Chem*, **275**, 29042-29052.

Masai, H., You, Z. and Arai, K. (2005) Control of DNA replication: regulation and activation of eukaryotic replicative helicase, MCM. *IUBMB Life*, **57**, 323-335.

Matsumoto, K., Seki, M., Masutani, C., Tada, S., Enomoto, T. and Ishimi, Y. (1995) Stimulation of DNA synthesis by mouse DNA helicase B in a DNA replication system containing eukaryotic replication origins. *Biochemistry*, **34**, 7913-7922.

Matsumoto, Y. and Kim, K. (1995) Excision of deoxyribose phosphate residues by DNA polymerase beta during DNA repair. *Science*, **269**, 699-702.

Matsuoka, S., Huang, M. and Elledge, S.J. (1998) Linkage of ATM to cell cycle regulation by the Chk2 protein kinase. *Science*, **282**, 1893-1897.

Mazin, A.V., Zaitseva, E., Sung, P. and Kowalczykowski, S.C. (2000) Tailed duplex DNA is the preferred substrate for Rad51 protein-mediated homologous pairing. *Embo J*, **19**, 1148-1156.

Mazina, O.M., Mazin, A.V., Nakagawa, T., Kolodner, R.D. and Kowalczykowski, S.C. (2004) Saccharomyces cerevisiae Mer3 helicase stimulates 3'-5' heteroduplex extension by Rad51; implications for crossover control in meiotic recombination. *Cell*, **117**, 47-56.

McHenry, C.S. (1982) Purification and characterization of DNA polymerase III'. Identification of tau as a subunit of the DNA polymerase III holoenzyme. *J Biol Chem*, **257**, 2657-2663.

McHenry, C.S. and Crow, W. (1979) DNA polymerase III of Escherichia coli. Purification and identification of subunits. *J Biol Chem*, **254**, 1748-1753.

McHugh, P.J., Spanswick, V.J. and Hartley, J.A. (2001) Repair of DNA interstrand crosslinks: molecular mechanisms and clinical relevance. *Lancet Oncol*, **2**, 483-490.

Melo, J. and Toczyski, D. (2002) A unified view of the DNA-damage checkpoint. *Curr Opin Cell Biol*, **14**, 237-245.

Memisoglu, A. and Samson, L. (2000) Base excision repair in yeast and mammals. *Mutat Res*, **451**, 39-51.

Mendez, J. and Stillman, B. (2000) Chromatin association of human origin recognition complex, cdc6, and minichromosome maintenance proteins during the cell cycle: assembly of prereplication complexes in late mitosis. *Mol Cell Biol*, **20**, 8602-8612.

Merchant, A.M., Kawasaki, Y., Chen, Y., Lei, M. and Tye, B.K. (1997) A lesion in the DNA replication initiation factor Mcm10 induces pausing of elongation forks through chromosomal replication origins in Saccharomyces cerevisiae. *Mol Cell Biol*, **17**, 3261-3271.

Michael, W.M., Ott, R., Fanning, E. and Newport, J. (2000) Activation of the DNA replication checkpoint through RNA synthesis by primase. *Science*, **289**, 2133-2137.

Mimura, S. and Takisawa, H. (1998) Xenopus Cdc45-dependent loading of DNA polymerase alpha onto chromatin under the control of S-phase Cdk. *Embo J*, **17**, 5699-5707.

Mirzoeva, O.K. and Petrini, J.H. (2001) DNA damage-dependent nuclear dynamics of the Mre11 complex. *Mol Cell Biol*, **21**, 281-288.

Mohindra, A., Hays, L.E., Phillips, E.N., Preston, B.D., Helleday, T. and Meuth, M. (2002) Defects in homologous recombination repair in mismatch-repair-deficient tumour cell lines. *Hum Mol Genet*, **11**, 2189-2200.

Mu, D., Wakasugi, M., Hsu, D.S. and Sancar, A. (1997) Characterization of reaction intermediates of human excision repair nuclease. *J Biol Chem*, **272**, 28971-28979.

Myers, J.S. and Cortez, D. (2006) Rapid activation of ATR by ionizing radiation requires ATM and Mre11. *J Biol Chem*, **281**, 9346-9350.

Nairz, K. and Klein, F. (1997) mre11S--a yeast mutation that blocks double-strand-break processing and permits nonhomologous synapsis in meiosis. *Genes Dev*, **11**, 2272-2290.

Nakayama, H., Nakayama, K., Nakayama, R., Irino, N., Nakayama, Y. and Hanawalt, P.C. (1984) Isolation and genetic characterization of a thymineless death-resistant mutant of Escherichia coli K12: identification of a new mutation (recQ1) that blocks the RecF recombination pathway. *Mol Gen Genet*, **195**, 474-480.

Namsaraev, E. and Berg, P. (1997) Characterization of strand exchange activity of yeast Rad51 protein. *Mol Cell Biol*, **17**, 5359-5368.

Namsaraev, E.A. and Berg, P. (1998) Branch migration during Rad51-promoted strand exchange proceeds in either direction. *Proc Natl Acad Sci U S A*, **95**, 10477-10481.

Namsaraev, E.A. and Berg, P. (2000) Rad51 uses one mechanism to drive DNA strand exchange in both directions. *J Biol Chem*, **275**, 3970-3976.

Nelms, B.E., Maser, R.S., MacKay, J.F., Lagally, M.G. and Petrini, J.H. (1998) In situ visualization of DNA double-strand break repair in human fibroblasts. *Science*, **280**, 590-592.

New, J.H. and Kowalczykowski, S.C. (2002) Rad52 protein has a second stimulatory role in DNA strand exchange that complements replication protein-A function. *J Biol Chem*, **277**, 26171-26176.

Newlon, C.S. and Theis, J.F. (1993) The structure and function of yeast ARS elements. *Curr Opin Genet Dev*, **3**, 752-758.

Nguyen, V.Q., Co, C. and Li, J.J. (2001) Cyclin-dependent kinases prevent DNA re-replication through multiple mechanisms. *Nature*, **411**, 1068-1073.

Nishitani, H., Lygerou, Z., Nishimoto, T. and Nurse, P. (2000) The Cdt1 protein is required to license DNA for replication in fission yeast. *Nature*, **404**, 625-628.

Nusslein, V., Otto, B., Bonhoeffer, F. and Schaller, H. (1971) Function of DNA polymerase 3 in DNA replication. *Nat New Biol*, **234**, 285-286.

O'Connell, M.J., Raleigh, J.M., Verkade, H.M. and Nurse, P. (1997) Chk1 is a wee1 kinase in the G2 DNA damage checkpoint inhibiting cdc2 by Y15 phosphorylation. *Embo J*, **16**, 545-554.

Ogiwara, H., Ui, A., Onoda, F., Tada, S., Enomoto, T. and Seki, M. (2006) Dpb11, the budding yeast homolog of TopBP1, functions with the checkpoint clamp in recombination repair. *Nucleic Acids Res*, **34**, 3389-3398.

Oka, A., Sugimoto, K., Takanami, M. and Hirota, Y. (1980) Replication origin of the Escherichia coli K-12 chromosome: the size and structure of the minimum DNA segment carrying the information for autonomous replication. *Mol Gen Genet*, **178**, 9-20.

Olive, P.L. (1998) The role of DNA single- and double-strand breaks in cell killing by ionizing radiation. *Radiat Res*, **150**, S42-51.

Paques, F. and Haber, J.E. (1999) Multiple pathways of recombination induced by double-strand breaks in Saccharomyces cerevisiae. *Microbiol Mol Biol Rev*, **63**, 349-404.

Parrilla-Castellar, E.R., Arlander, S.J. and Karnitz, L. (2004) Dial 9-1-1 for DNA damage: the Rad9-Hus1-Rad1 (9-1-1) clamp complex. *DNA Repair (Amst)*, **3**, 1009-1014.

Parrilla-Castellar, E.R. and Karnitz, L.M. (2003) Cut5 is required for the binding of Atr and DNA polymerase alpha to genotoxin-damaged chromatin. *J Biol Chem*, **278**, 45507-45511.

Parsons, R.E., Stenger, J.E., Ray, S., Welker, R., Anderson, M.E. and Tegtmeyer, P. (1991) Cooperative assembly of simian virus 40 T-antigen hexamers on functional halves of the replication origin. *J Virol*, **65**, 2798-2806.

Paull, T.T. and Gellert, M. (1998) The 3' to 5' exonuclease activity of Mre 11 facilitates repair of DNA double-strand breaks. *Mol Cell*, **1**, 969-979.

Paull, T.T. and Gellert, M. (1999) Nbs1 potentiates ATP-driven DNA unwinding and endonuclease cleavage by the Mre11/Rad50 complex. *Genes Dev*, **13**, 1276-1288.

Paull, T.T., Rogakou, E.P., Yamazaki, V., Kirchgessner, C.U., Gellert, M. and Bonner, W.M. (2000) A critical role for histone H2AX in recruitment of repair factors to nuclear foci after DNA damage. *Curr Biol*, **10**, 886-895.

Perry, J. and Kleckner, N. (2003) The ATRs, ATMs, and TORs are giant HEAT repeat proteins. *Cell*, **112**, 151-155.

Petukhova, G., Sung, P. and Klein, H. (2000) Promotion of Rad51-dependent D-loop formation by yeast recombination factor Rdh54/Tid1. *Genes Dev*, **14**, 2206-2215.

Podust, V.N., Chang, L.S., Ott, R., Dianov, G.L. and Fanning, E. (2002) Reconstitution of human DNA polymerase delta using recombinant baculoviruses: the p12 subunit potentiates DNA polymerizing activity of the four-subunit enzyme. *J Biol Chem*, **277**, 3894-3901.

Ramsden, D.A. and Gellert, M. (1998) Ku protein stimulates DNA end joining by mammalian DNA ligases: a direct role for Ku in repair of DNA double-strand breaks. *Embo J*, **17**, 609-614.

Rogakou, E.P., Boon, C., Redon, C. and Bonner, W.M. (1999) Megabase chromatin domains involved in DNA double-strand breaks in vivo. *J Cell Biol*, **146**, 905-916.

Roman, L.J., Dixon, D.A. and Kowalczykowski, S.C. (1991) RecBCD-dependent joint molecule formation promoted by the Escherichia coli RecA and SSB proteins. *Proc Natl Acad Sci U S A*, **88**, 3367-3371.

Romanowski, P., Madine, M.A., Rowles, A., Blow, J.J. and Laskey, R.A. (1996) The Xenopus origin recognition complex is essential for DNA replication and MCM binding to chromatin. *Curr Biol*, **6**, 1416-1425.

Rowles, A., Chong, J.P., Brown, L., Howell, M., Evan, G.I. and Blow, J.J. (1996) Interaction between the origin recognition complex and the replication licensing system in Xenopus. *Cell*, **87**, 287-296.

Rudolf, J., Makrantoni, V., Ingledew, W.J., Stark, M.J. and White, M.F. (2006) The DNA repair helicases XPD and FancJ have essential iron-sulfur domains. *Mol Cell*, **23**, 801-808.

Ryan, K.M., Phillips, A.C. and Vousden, K.H. (2001) Regulation and function of the p53 tumor suppressor protein. *Curr Opin Cell Biol*, **13**, 332-337.

Saintigny, Y., Makienko, K., Swanson, C., Emond, M.J. and Monnat, R.J., Jr. (2002) Homologous recombination resolution defect in werner syndrome. *Mol Cell Biol*, **22**, 6971-6978.

Saitoh, A., Tada, S., Katada, T. and Enomoto, T. (1995) Stimulation of mouse DNA primase-catalyzed oligoribonucleotide synthesis by mouse DNA helicase B. *Nucleic Acids Res*, **23**, 2014-2018.

Salinas, F. and Kodadek, T. (1994) Strand exchange through a DNA-protein complex requires a DNA helicase. *Biochem Biophys Res Commun*, **205**, 1004-1009.

Salinas, F. and Kodadek, T. (1995) Phage T4 homologous strand exchange: a DNA helicase, not the strand transferase, drives polar branch migration. *Cell*, **82**, 111-119.

Sancar, A. (1994) Structure and function of DNA photolyase. *Biochemistry*, **33**, 2-9.

Sancar, A., Lindsey-Boltz, L.A., Unsal-Kacmaz, K. and Linn, S. (2004) Molecular mechanisms of mammalian DNA repair and the DNA damage checkpoints. *Annu Rev Biochem*, **73**, 39-85.

Sarkaria, J.N., Tibbetts, R.S., Busby, E.C., Kennedy, A.P., Hill, D.E. and Abraham, R.T. (1998) Inhibition of phosphoinositide 3-kinase related kinases by the radiosensitizing agent wortmannin. *Cancer Res*, **58**, 4375-4382.

Scheuermann, R.H. and Echols, H. (1984) A separate editing exonuclease for DNA replication: the epsilon subunit of Escherichia coli DNA polymerase III holoenzyme. *Proc Natl Acad Sci U S A*, **81**, 7747-7751.

Schultz, L.B., Chehab, N.H., Malikzay, A. and Halazonetis, T.D. (2000) p53 binding protein 1 (53BP1) is an early participant in the cellular response to DNA double-strand breaks. *J Cell Biol*, **151**, 1381-1390.

Schwartz, M., Zlotorynski, E., Goldberg, M., Ozeri, E., Rahat, A., le Sage, C., Chen, B.P., Chen, D.J., Agami, R. and Kerem, B. (2005) Homologous recombination and nonhomologous end-joining repair pathways regulate fragile site stability. *Genes Dev*, **19**, 2715-2726.

Seki, M., Enomoto, T., Hanaoka, F. and Yamada, M. (1987) DNA-dependent adenosinetriphosphatase B from mouse FM3A cells has DNA helicase activity. *Biochemistry*, **26**, 2924-2928.

Seki, M., Kohda, T., Yano, T., Tada, S., Yanagisawa, J., Eki, T., Ui, M. and Enomoto, T. (1995) Characterization of DNA synthesis and DNA-dependent ATPase activity at a restrictive temperature in temperature-sensitive tsFT848 cells with thermolabile DNA helicase B. *Mol Cell Biol*, **15**, 165-172.

Sharma, S., Stumpo, D.J., Balajee, A.S., Bock, C.B., Lansdorp, P.M., Brosh, R.M., Jr. and Blackshear, P.J. (2006) RECQL, a Member of the RecQ family of DNA Helicases, Suppresses Chromosomal Instability. *Mol Cell Biol*.

Shiloh, Y. (1997) Ataxia-telangiectasia and the Nijmegen breakage syndrome: related disorders but genes apart. *Annu Rev Genet*, **31**, 635-662.

Shim, K.S., Schmutte, C., Yoder, K. and Fishel, R. (2006) Defining the salt effect on human RAD51 activities. *DNA Repair (Amst)*, **5**, 718-730.

Shinohara, A., Shinohara, M., Ohta, T., Matsuda, S. and Ogawa, T. (1998) Rad52 forms ring structures and co-operates with RPA in single-strand DNA annealing. *Genes Cells*, **3**, 145-156.

Sigurdsson, S., Trujillo, K., Song, B., Stratton, S. and Sung, P. (2001) Basis for avid homologous DNA strand exchange by human Rad51 and RPA. *J Biol Chem*, **276**, 8798-8806.

Simmons, D.T., Melendy, T., Usher, D. and Stillman, B. (1996) Simian virus 40 large T antigen binds to topoisomerase I. *Virology*, **222**, 365-374.

Singleton, M.R. and Wigley, D.B. (2002) Modularity and specialization in superfamily 1 and 2 helicases. *J Bacteriol*, **184**, 1819-1826.

Sobeck, A., Stone, S., Costanzo, V., de Graaf, B., Reuter, T., de Winter, J., Wallisch, M., Akkari, Y., Olson, S., Wang, W., Joenje, H., Christian, J.L., Lupardus, P.J., Cimprich, K.A., Gautier, J. and Hoatlin, M.E. (2006) Fanconi anemia proteins are required to prevent accumulation of replication-associated DNA double-strand breaks. *Mol Cell Biol*, **26**, 425-437.

Sonoda, E., Sasaki, M.S., Morrison, C., Yamaguchi-Iwai, Y., Takata, M. and Takeda, S. (1999) Sister chromatid exchanges are mediated by homologous recombination in vertebrate cells. *Mol Cell Biol*, **19**, 5166-5169.

Soultanas, P. and Wigley, D.B. (2001) Unwinding the 'Gordian knot' of helicase action. *Trends Biochem Sci*, **26**, 47-54.

Spanos, A., Sedgwick, S.G., Yarranton, G.T., Hubscher, U. and Banks, G.R. (1981) Detection of the catalytic activities of DNA polymerases and their associated exonucleases following SDS-polyacrylamide gel electrophoresis. *Nucleic Acids Res*, **9**, 1825-1839.

Stahl, H., Droge, P. and Knippers, R. (1986) DNA helicase activity of SV40 large tumor antigen. *Embo J*, **5**, 1939-1944.

Stauffer, M.E. and Chazin, W.J. (2004) Physical interaction between replication protein A and Rad51 promotes exchange on single-stranded DNA. *J Biol Chem*, **279**, 25638-25645.

Stewart, G.S., Maser, R.S., Stankovic, T., Bressan, D.A., Kaplan, M.I., Jaspers, N.G., Raams, A., Byrd, P.J., Petrini, J.H. and Taylor, A.M. (1999) The DNA double-strand break repair gene hMRE11 is mutated in individuals with an ataxia-telangiectasia-like disorder. *Cell*, **99**, 577-587.

Stewart, G.S., Wang, B., Bignell, C.R., Taylor, A.M. and Elledge, S.J. (2003) MDC1 is a mediator of the mammalian DNA damage checkpoint. *Nature*, **421**, 961-966.

Stiff, T., Walker, S.A., Cerosaletti, K., Goodarzi, A.A., Petermann, E., Concannon, P., O'Driscoll, M. and Jeggo, P.A. (2006) ATR-dependent phosphorylation and activation of ATM in response to UV treatment or replication fork stalling. *Embo J*, **25**, 5775-5782.

Sugawara, N. and Haber, J.E. (1992) Characterization of double-strand break-induced recombination: homology requirements and single-stranded DNA formation. *Mol Cell Biol*, **12**, 563-575.

Sugiyama, T., Zaitseva, E.M. and Kowalczykowski, S.C. (1997) A single-stranded DNA-binding protein is needed for efficient presynaptic complex formation by the Saccharomyces cerevisiae Rad51 protein. *J Biol Chem*, **272**, 7940-7945.

Sung, P. (1994) Catalysis of ATP-dependent homologous DNA pairing and strand exchange by yeast RAD51 protein. *Science*, **265**, 1241-1243.

Tada, S., Kobayashi, T., Omori, A., Kusa, Y., Okumura, N., Kodaira, H., Ishimi, Y., Seki, M. and Enomoto, T. (2001) Molecular cloning of a cDNA encoding mouse DNA helicase B, which has homology to Escherichia coli RecD protein, and identification of a mutation in the DNA helicase B from tsFT848 temperature-sensitive DNA replication mutant cells. *Nucleic Acids Res*, **29**, 3835-3840.

Takahashi, T.S., Wigley, D.B. and Walter, J.C. (2005) Pumps, paradoxes and ploughshares: mechanism of the MCM2-7 DNA helicase. *Trends Biochem Sci*, **30**, 437-444.

Taneja, P., Gu, J., Peng, R., Carrick, R., Uchiumi, F., Ott, R.D., Gustafson, E., Podust, V.N. and Fanning, E. (2002) A dominant-negative mutant of human DNA helicase B blocks the onset of chromosomal DNA replication. *J Biol Chem*, **277**, 40853-40861.

Taniguchi, T. and D'Andrea, A.D. (2006) Molecular pathogenesis of Fanconi anemia: recent progress. *Blood*, **107**, 4223-4233.

Tawaragi, Y., Enomoto, T., Watanabe, Y., Hanaoka, F. and Yamada, M. (1984) Multiple deoxyribonucleic acid dependent adenosinetriphosphatases in FM3A cells. Characterization of an adenosinetriphosphatase that prefers poly [d(A-T)] as cofactor. *Biochemistry*, **23**, 529-533.

Taylor, A.F. and Smith, G.R. (2003) RecBCD enzyme is a DNA helicase with fast and slow motors of opposite polarity. *Nature*, **423**, 889-893.

Tsurimoto, T. and Stillman, B. (1991) Replication factors required for SV40 DNA replication in vitro. I. DNA structure-specific recognition of a primer-template

junction by eukaryotic DNA polymerases and their accessory proteins. *J Biol Chem*, **266**, 1950-1960.

Turchi, J.J., Huang, L., Murante, R.S., Kim, Y. and Bambara, R.A. (1994) Enzymatic completion of mammalian lagging-strand DNA replication. *Proc Natl Acad Sci U S A*, **91**, 9803-9807.

Tuteja, N. and Tuteja, R. (2004) Prokaryotic and eukaryotic DNA helicases. Essential molecular motor proteins for cellular machinery. *Eur J Biochem*, **271**, 1835-1848.

Tye, B.K. (1999) MCM proteins in DNA replication. *Annu Rev Biochem*, **68**, 649-686.

Uziel, T., Lerenthal, Y., Moyal, L., Andegeko, Y., Mittelman, L. and Shiloh, Y. (2003) Requirement of the MRN complex for ATM activation by DNA damage. *Embo J*, **22**, 5612-5621.

Van Komen, S., Petukhova, G., Sigurdsson, S., Stratton, S. and Sung, P. (2000) Superhelicity-driven homologous DNA pairing by yeast recombination factors Rad51 and Rad54. *Mol Cell*, **6**, 563-572.

Venkatesan, M., Silver, L.L. and Nossal, N.G. (1982) Bacteriophage T4 gene 41 protein, required for the synthesis of RNA primers, is also a DNA helicase. *J Biol Chem*, **257**, 12426-12434.

Walker, J.E., Saraste, M., Runswick, M.J. and Gay, N.J. (1982) Distantly related sequences in the alpha- and beta-subunits of ATP synthase, myosin, kinases and other ATP-requiring enzymes and a common nucleotide binding fold. *Embo J*, **1**, 945-951.

Wang, B., Matsuoka, S., Carpenter, P.B. and Elledge, S.J. (2002) 53BP1, a mediator of the DNA damage checkpoint. *Science*, **298**, 1435-1438.

Wang, H., Wang, H., Powell, S.N., Iliakis, G. and Wang, Y. (2004) ATR affecting cell radiosensitivity is dependent on homologous recombination repair but independent of nonhomologous end joining. *Cancer Res*, **64**, 7139-7143.

Wang, X. and Haber, J.E. (2004) Role of Saccharomyces single-stranded DNA-binding protein RPA in the strand invasion step of double-strand break repair. *PLoS Biol*, **2**, E21.

Watson, J.D. and Crick, F.H. (1953) Genetical implications of the structure of deoxyribonucleic acid. *Nature*, **171**, 964-967.

Wessel, R., Schweizer, J. and Stahl, H. (1992) Simian virus 40 T-antigen DNA helicase is a hexamer which forms a binary complex during bidirectional unwinding from the viral origin of DNA replication. *J Virol*, **66**, 804-815.

West, S.C., Cassuto, E. and Howard-Flanders, P. (1981) Heteroduplex formation by recA protein: polarity of strand exchanges. *Proc Natl Acad Sci U S A*, **78**, 6149-6153.

Wu, L. and Hickson, I.D. (2003) The Bloom's syndrome helicase suppresses crossing over during homologous recombination. *Nature*, **426**, 870-874.

Wu, L. and Hickson, I.D. (2006) DNA helicases required for homologous recombination and repair of damaged replication forks. *Annu Rev Genet*, **40**, 279-306.

Wu, X., Avni, D., Chiba, T., Yan, F., Zhao, Q., Lin, Y., Heng, H. and Livingston, D. (2004) SV40 T antigen interacts with Nbs1 to disrupt DNA replication control. *Genes Dev*, **18**, 1305-1316.

Xiao, Z., Chen, Z., Gunasekera, A.H., Sowin, T.J., Rosenberg, S.H., Fesik, S. and Zhang, H. (2003) Chk1 mediates S and G2 arrests through Cdc25A degradation in response to DNA-damaging agents. *J Biol Chem*, **278**, 21767-21773.

Yan, S., Lindsay, H.D. and Michael, W.M. (2006) Direct requirement for Xmus101 in ATR-mediated phosphorylation of Claspin bound Chk1 during checkpoint signaling. *J Cell Biol*, **173**, 181-186.

You, Z., Kong, L. and Newport, J. (2002) The role of single-stranded DNA and polymerase alpha in establishing the ATR, Hus1 DNA replication checkpoint. *J Biol Chem*, **277**, 27088-27093.

Yu, C.E., Oshima, J., Fu, Y.H., Wijsman, E.M., Hisama, F., Alisch, R., Matthews, S., Nakura, J., Miki, T., Ouais, S., Martin, G.M., Mulligan, J. and Schellenberg, G.D. (1996) Positional cloning of the Werner's syndrome gene. *Science*, **272**, 258-262.

Zegerman, P. and Diffley, J.F. (2007) Phosphorylation of Sld2 and Sld3 by cyclin-dependent kinases promotes DNA replication in budding yeast. *Nature*, **445**, 281-285.

Zhang, S., Zhou, Y., Trusa, S., Meng, X., Lee, E.Y. and Lee, M.Y. (2007a) A novel DNA damage response: Rapid degradation of the p12 subunit of DNA polymerase delta. *J Biol Chem*.

Zhang, Z., Fan, H.Y., Goldman, J.A. and Kingston, R.E. (2007b) Homology-driven chromatin remodeling by human RAD54. *Nat Struct Mol Biol*, **14**, 397-405.

Zou, L., Cortez, D. and Elledge, S.J. (2002) Regulation of ATR substrate selection by Rad17-dependent loading of Rad9 complexes onto chromatin. *Genes Dev*, **16**, 198-208.

Zou, L. and Elledge, S.J. (2003) Sensing DNA damage through ATRIP recognition of RPA-ssDNA complexes. *Science*, **300**, 1542-1548.

Zyskind, J.W., Cleary, J.M., Brusilow, W.S., Harding, N.E. and Smith, D.W. (1983) Chromosomal replication origin from the marine bacterium Vibrio harveyi functions in Escherichia coli: oriC consensus sequence. *Proc Natl Acad Sci U S A*, **80**, 1164-1168.